Investigating the link between phosphoinositides, endosomal trafficking and ESCRT function

Dukes, Joe

Award date:
2008

Awarding institution:
University of Bath

Investigating the Link Between Phosphoinositides, Endosomal Trafficking and ESCRT Function

Joseph Donaldson Dukes III

A thesis submitted for the degree of Doctor of Philosophy

University of Bath

Department of Biology and Biochemistry

February 2008

Abstract

The maturation of early endosomes into multivesicular bodies (MVBs) and subsequent trafficking to lysosomes is an important event for the control and silencing of endocytosed membrane receptors. The endosomal-sorting complex required for transport (ESCRT) proteins appear to play a key role in this event. Phosphatidylinositol lipids including PtdIns(3,5)P_2 have been implicated in the MVB-lysosomal pathway and an ESCRT-III component CHMP3 binds to this lipid *in vitro*.

The purpose of this thesis was to investigate the link between ESCRT proteins, PtdIns(3,5)P_2 and endo-lysosomal trafficking. Firstly, a protein expressed by *Salmonella*, which is a phosphatase that acts on PtdIns(3,5)P_2, was investigated as a potential tool for manipulating cellular PtdIns(3,5)P_2 levels. Our results suggest that it is potentially a useful tool for this purpose and that expression of SopB perturbs endosome to lysosome trafficking. These findings provide further evidence for a role of PtdIns(3,5)P_2 in endo-lysosomal trafficking.

In order to characterise PIKfyve, the kinase that produces PtdIns(3,5)P_2, polyclonal antibodies were raised against this protein. Purification and characterisation of the antibody suggest that it recognises recombinant and endogenous PIKfyve.

Thirdly, with the aim of characterising the full protein complement needed for MVB formation, a method was developed to isolate a subcellular compartment and associated proteins (including ESCRT proteins) induced by a dominant negative Vps4 protein.

Finally, we discovered a role for functional ESCRT-III in cytokinesis. Mutant ESCRT-III components expressed in mammalian cells impaired cytokinesis suggesting that these proteins are not only necessary for MVB formation but are very important for the completion of cytokinesis.

Acknowledgments

I would firstly like to thank Dr Paul Whitley for allowing me to carry out this research in his laboratory for the past three years. I would also like to thank him for his supervision and patience throughout my time in his lab. I am also very grateful to other members of the Holman/Whitley/Reeves laboratories for their technical and practical help throughout my PhD, in particular Dr Judith Richardson, Dr Scott Lawrence, Dr Françoise Koumanov, Dr Huai-Lo Lee and Dr Barbara Reeves. Much of their advice and time given to help me has been invaluable and much appreciated. I am also very grateful to Professor Geoff Holman for the use of much of his equipment in his laboratory and also Dr Barbara Reeves for the regular use of her fluorescence microscope along with other equipment.

I am grateful to Dr Huai-Lo Lee for the work to produce Figure 3.3 and also to Dr Judith Richardson for Figure 5.7*A*.

I would also like to thank all the members past and present of the Holman/Whitley/Reeves laboratories who have made my PhD a memorable and enjoyable time, namely Dr Scott Lawrence, Dr Judith Richardson, Dr Françoise Koumanov, Dr Jing Yang, Dr Barbara Reeves, Dr Huai-Lo Lee, Dr Amelia Preedy, Dr Bo Jing, Dr Verna Lavender, Dr Adrian Rogers, Daniel Fazakerley, Sunil Patel and Ying Feng. I would further like to thank all the many people in the department who have made my time here an unforgettable experience, of whom there are too many to name.

I would lastly like to thank all the friends and family who have supported me throughout my PhD, in particular my parents and two of my best friends, Terry Robson and Jenny Howes who have helped keep me motivated as well as laughing when I needed it.

Abbreviations

AMSH	Associated Molecule of SH3 domain of STAM
APS	Ammonium Persulphate
ATP	Adenosine 5'-triphosphate
AAA-type	ATPase Associated with various cellular Activities
BCA	Bicinchoninic Acid
BSA	Bovine Serum Albumin
CHMP	Charged MVB Protein
CHO cells	Chinese Hamster Ovary cells
CI-M6PR	Cation-Independent M6PR
CISK	Cytokine-Independent Survival Kinase
Da	Daltons
DAPI	4',6-diamidino-2-phenylindole
ddH_2O	Double Distilled Water
DMEM	Dulbecco's Modified Eagles Medium
DMSO	Dimethyl Sulfoxide
DNA	Deoxyribonucleic Acid
Dox	Doxycycline
DTT	$_{DL}$-Dithiothreitol
DUBs	Deubiquitinating enzymes
ECL	Enhanced Chemiluminescence
EDTA	Diaminoethanetetra-acetic acid disodium salt
EEA1	Early Endosomal Auto-antigen 1
EGF	Epithelial Growth Factor
EGFR	EGF Receptor
ELISA	Enzyme-Linked Immunosorbent Assay
ESCRT	Endosomal Sorting Complex Required for Transport
FCS	Foetal Calf Serum
FPLC	Fast Protein Liquid Chromatography
FYVE	(Domain found in) Fab1, YOTB, Vac1 and EEA-1
g	Gram
GFP	Green Fluorescent Protein

GLUT4	Glucose Transporter 4
HEPES	(N-[2-Hydroxyethyl]piperazine-N'-[2-ethenesulfonic acid])
HIV	Human Immunodeficiency Virus
hr	Hour
HRP	Horseradish peroxidise
HRS	Hepatocyte growth factor Receptor tyrosine kinase Substrate
IF	Immunofluorescence
IP	Immunoprecipitation
IPTG	Isopropyl β-D-1-thiogalactopyranoside
kb	Kilo Base
kDa	Kilo Daltons
LB	Luria Broth
LBPA	Lysobisphosphatidic Acid
M6PR	Mannose-6-Phosphate Receptor
min	Minutes
MIT domain	Microtubule Interacting and Transport domain
MVB	Multivesicular Body
NRK cells	Normal Rat Kidney cells
OD	Optical density
PBS	Phosphate Buffered Saline
PBST	PBS with Tween-20
PCR	Polymerase Chain Reaction
PFA	Paraformaldehyde
PtdIns(3)P	Phosphatidylinositol (3) Phosphate
PtdIns(3,5)P_2	Phosphatidylinositol (3,5) Bis-Phosphate
PtdIns(4,5)P_2	Phosphatidylinositol (4,5) Bis-Phosphate
RFU	Relative Fluorescence Units
RNA	Ribonucleic Acid
rpm	Revolutions Per Minute
SCV	*Salmonella* Containing Vacuole
SDS	Sodium Dodecylsulphate
SDS-PAGE	SDS Polyacrylamide Gel Electrophoresis

siRNA	Short Interfering RNA
SNARE	Soluble NSF Attachment Proteins Receptors
SPI	*Salmonella* Pathogenicity Island
STAM	Signal Transducing Adaptor Molecule
TAE	Tris-acetate EDTA
TBS	Tris-buffered Saline
TBST	TBS with Tween-20
TEMED	N,N,N', N'-tetramethylethylenediamine
TES	Tris-EDTA Sucrose
TESA	TES with ATP
Tet	Tetracycline
TfR	Transferrin Receptor
TGN	Trans-Golgi Network
Tris	Tris(hydroxymethyl)methylamine
TSG101	Tumour Susceptibility Gene 101
TTSS	Type-III Secretion System
Tween-20	Polyoxyethylene sorbitan monolaureate
TX-100	Triton X-100
Ub	Ubiquitin
UBPY	Ubiquitin-specific processing Protease-Y
UIM	Ubiquitin Interacting Motif
UV	Ultra Violet
Vps	Vacuolar Protein Sorting
WB	Western Blotting
WT	Wild-Type

Table of Contents

CHAPTER 1

1 Introduction

1.1 Multivesicular bodies and membrane trafficking

Membrane trafficking is controlled by the addition and removal of proteins from membrane compartments. In the case of the plasma membrane, removal of existing plasma membrane proteins often occurs via the clathrin-mediated process of endocytosis [reviewed in 1]. Once protein-containing vesicles have been formed via endocytosis, the fate of such proteins in the cell is usually coordinated by endosomes [reviewed in 2]. Endosomes can help determine trafficking of proteins between the trans-Golgi network (TGN) to be returned to the plasma membrane, and lytic organelles such as lysosomes in mammalian cells or vacuoles for example in yeast. Such control and direction of vesicle transport is of utmost importance, as different membrane receptors require different fates. For example, many housekeeping receptors such as the transferrin receptor are sometimes recycled back to the plasma membrane [3]. By trafficking through the early endosomal compartments of the cell, such recycling receptors are able to rid themselves of their bound ligands by dissociation as a result of the mildly acidic compartment they have been trafficked to. Once the ligand has been removed in such a manner they are free to be recycled back to the plasma membrane and this process can be repeated upon ligand binding.

Other cellular plasma membrane receptors are not usually recycled back to the plasma membrane as this may be detrimental to the cell or organism due to repetitive signalling events. For example many growth factor receptors signal the cell to proliferate and divide, and if this process is not tightly regulated, the cell can end up uncontrollably proliferating which may be harmful to the cell [4]. In such cases these signalling receptors may be directed to the lytic lysosome to allow initially for cessation of the signal and secondly the destruction of the protein by

proteolysis. The mediator between delivery to the lytic lysosome of such signalling receptors and the early endosomal compartments is the subset of late endosomes known as multivesicular bodies (MVB) [reviewed in 4-11]. MVBs are given their name due to their prominent appearance of vesicles contained within a spherical late endosomal structure. It would appear that MVBs play an initial role in the trafficking of activated signalling receptors by the silencing of their signals. This is achieved by sequestering the cytoplasmic domains of signalling receptors away from the cytoplasm via the delivery of these proteins by inward budding of vesicles into the lumen of the MVB. Once this process has occurred, the trafficking of the MVB can be followed to fusion with the lysosome where the lumenal contents will be delivered to the lytic environment of the lysosome and degradation can occur [12].

1.2 The Endocytic Pathway

Endosomes can be classed typically as either 'early' or 'late' endosomes depending upon their kinetics of organisation and how they sort protein cargo [reviewed in 7, 13]. Morphologically, early endosomes are seen to have a more tubular appearance when compared with late endosomes, which are characteristically much more spherical in appearance. In mammalian cells the localisation of early endosomal compartments is often found near the periphery of the plasma membrane, whereas late endosomes are found more adjacent to the nucleus. MVBs are considered a subset of late endosomes, possessing a unique multi-vesicular appearance, a result of the budding of vesicles containing receptor cargo from the limiting membrane into their lumen.

One of the most studied transmembrane signalling receptors is the epithelial growth factor receptor (EGFR). The ligand that binds EGFR is epithelial growth factor (EGF), which is a small, secreted peptide that signals the target cell to proliferate and divide. Activation of EGFR by

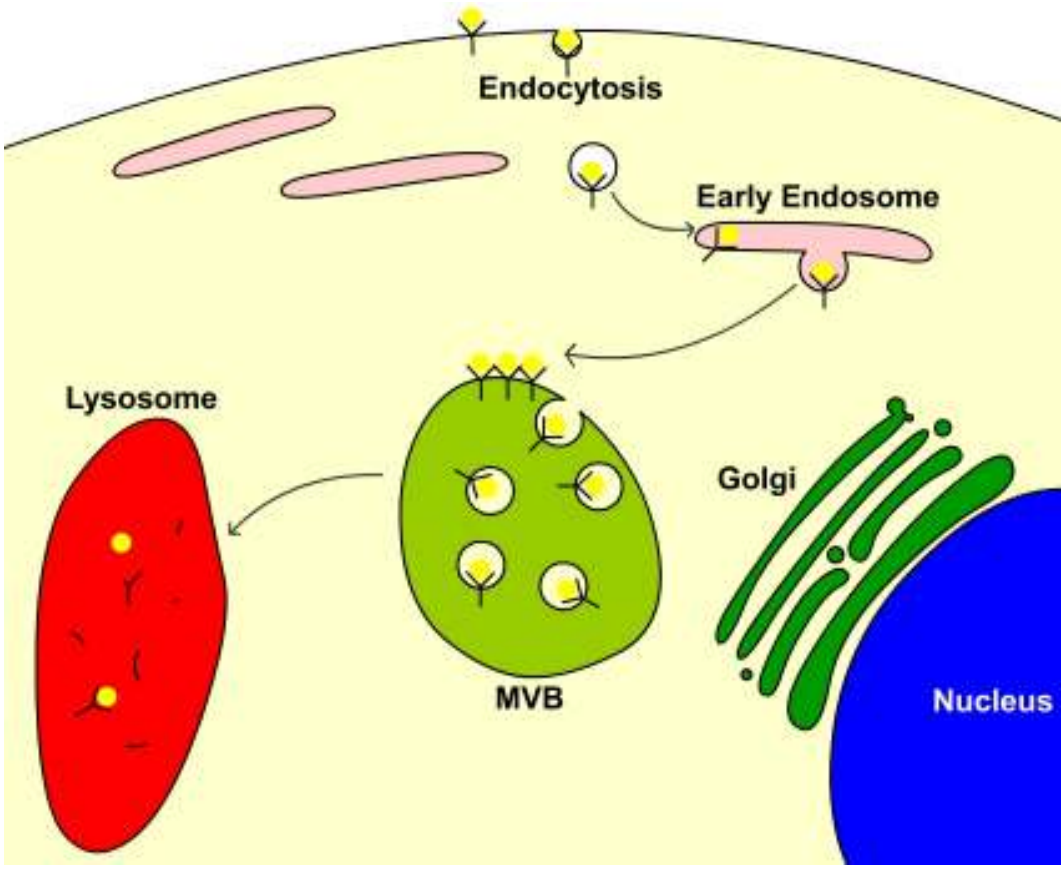

Figure 1.1 – The MVB-lysosomal degradation pathway. A transmembrane receptor, such as EGFR is activated by its ligand (yellow circle) and consequentially endocytosed. After trafficking and sorting through the early endosome, it is directed to the MVB where it is delivered into the lumen as an internal vesicle. The MVB then fuses with the lytic lysosome where degradation can occur. Early endosomes may also be responsible for recycling of membrane receptors as well as trafficking from the Golgi apparatus to the plasma membrane.

binding of EGF at the plasma membrane results in a signalling cascade of events primarily through activation of the tyrosine kinase activity that the intracellular domain of EGFR possesses. Due to the nature of the signal that EGF produces, the cell has to employ measures to make sure that constant stimulation of the tyrosine-kinase activity does not occur, thus the attenuation of EGFR signalling is very important. Using various differently labelled EGF molecules to study this downregulation, it was shown that EGF bound to EGFR was delivered into the lumen of MVBs *en route* to the lysosome where its degradation occurred [14-16]. The

suppression of the tyrosine kinase activity occurs once delivery of the ligand-receptor complex to the MVB lumen has been made, as opposed to its delivery to the lysosome [17]. This highlights the importance of MVBs in the control and cessation of signalling events and that the MVB is an important organelle in the trafficking of such signalling proteins.

The molecular mechanism of delivering cargo into the lumen of MVBs is not one that is well understood. This process differs from classical endocytosis in that the direction of budding is away from the cytoplasm. Studies carried out in *Saccharomyces cerevisiae* initially identified a family of at least 18 conserved proteins known as the class E vacuolar protein sorting (Vps) proteins [reviewed in 4; 18-20]. Disruption of the class E *VPS* genes resulted in a swollen endosomal phenotype (the class E compartment), with protein cargo not being delivered to the yeast vacuole. This swollen endosomal phenotype is a consequence of the addition of membrane to the MVB structure, but due to impaired MVB machinery there is no removal of membrane via the internalisation of vesicles. As a result, the membrane of the MVB increases in size resulting in an enlarged endosomal phenotype (the class E compartment). Thus it seemed apparent that the Vps proteins are involved somehow in the delivery of cargo into the lumen of MVBs. Class E Vps proteins are highly conserved in eukaryotes which emphasises their importance in the cell, and disruption of their protein functions in most cases leads to similar phenotypes as seen in yeast. This suggests that similar mechanisms may occur in mammalian cells as in yeast. It must also be noted that many proteins undergo repeated rounds of internalisation and recycling back to the plasma membrane, thus the process of MVB formation must also be tightly controlled and a fairly selective event [reviewed in 5, 6].

To understand how selectivity of MVB cargo may be achieved, EGFR studies have again given us insight into this matter. Studies were carried out where a point mutation in the kinase domain of EGFR giving a kinase-dead protein resulted in the activated receptor being delivered to the

MVB's limiting membrane, but not internally delivered [17]. Further studies found that the addition of a single ubiquitin molecule onto EGFR (or most other receptors destined for the MVB-lysosomal degradation pathway) was necessary for targeting the cargo for MVB lumenal delivery [21-23]. Removal of residues necessary for ubiquitin addition from membrane receptors results in impaired sorting and degradation of these activated proteins. Likewise, the addition of a mono-ubiquitin molecule to receptors not normally degraded through the MVB pathway causes these receptors to be sorted into MVB lumens [24]. Thus it appears that for cargo to be targeted to the MVB lumen for lysosomal degradation, monoubiquitylation may be the method by which the cell marks a protein for such a fate. This has more recently been further supported by findings that indicate ubiquitin removal proteins are required in the late stages of delivery of cargo to the lumen of the MVB [25-34].

1.3 The ESCRT machinery

The class E Vps proteins can generally be subdivided into four separate endosomal sorting complexes required for transport (ESCRT-0, -I, -II, -III) [reviewed in 4; 9, 35-37]. Much of the initial work that has defined the ESCRT machinery and their roles has been carried out in yeast. Given the high level of conservation between the yeast Vps proteins and mammalian ESCRT proteins, it has been suggested that the mechanisms for MVB formation may also be highly conserved. Indeed many studies have shown that homologues of yeast proteins carry out similar roles in mammalian cells. There are however apparent differences between the roles of yeast Vps proteins and mammalian ESCRT proteins. For example, in mammalian cells it has been demonstrated that the ESCRT-I complex does not directly interact with the ESCRT-III complex [38, 39]. The two complexes do however both interact with ALIX, the homologue of the yeast Vps31 (Bro1) protein [40, 41]. This has been suggested to link the two complexes together, as it has additionally been implied that

ESCRT-II may not be necessary in mammalian cells for proper MVB-lysosomal pathway function, in contrast to yeast [42]. Despite this, in yeast it has been shown that ESCRT-I does interact with ESCRT-III directly and furthermore that the ALIX homologue Vps31 does not associate with the ESCRT-I complex [43]. Thus although it is apparent that similar components of the same machinery are present in yeast and mammalian cells, their functions and mechanisms may differ. It should be noted however that despite one study that suggests the ESCRT-II components are not needed for the degradation of receptors via the MVB-lysosomal route [42], a more recent study contradicts these findings, showing that silencing of certain ESCRT-II components does impair receptor degradation [44]. Thus the exact role of ESCRT-II in mammalian cell has yet to be elucidated.

The Vps proteins that form the ESCRT complexes are recruited from the cell cytosol to the limiting membrane of the endosomal structure where their exact role in delivery of cargo into the MVB lumen and the biogenesis of the MVB itself is not well understood. From studies in yeast a current model has been proposed that involves three main processes occurring on the limiting membrane of endosomes destined to be MVBs (for a schematic representation see Fig 1.3) [reviewed in 4, 9, 45]. In the early stages of MVB biogenesis, cargo recognition occurs, which includes ubiquitin-binding proteins such as Vps27 and Hse1 (Hrs and STAM in mammals; referred to as the ESCRT-0 complex) binding monoubiquitylated protein cargo, and complexing them together. An important point to make here is that the localisation of Vps27 on the endosomal membrane is dependent on its binding of the endosomally localised lipid PtdIns(3)P [46-48]. Secondly, concentration of the cargo occurs. This process involves the recruitment of ESCRT-I machinery (Vps23, 28, 37 in yeast or TSG101, VPS28 and VPS37 in mammals) by Vps27 to assemble at the soon to be MVB membrane [49]. ESCRT-I interacts with monoubiquitylated cargo and in turn recruits the ESCRT-II complex (Vps22, 25, 26 in yeast, EAP30, 25 and 45 in mammals). Assembled ESCRT-II initiates the oligomerisation of at least four small,

coiled-coil CHMP proteins that make up the ESCRT-III complex (Vps2, 20, 24 and Snf7 in yeast, also referred to as CHMP2, 6, 3 and 4 in mammals, respectively) [35]. The exact role of ESCRT-III is not known, however it is thought that the complex recruits additional proteins including Vps31/Bro1 (ALIX in mammals) and the AAA-type (ATPase associated with various cellular activities) ATPase Vps4. Bro1 is thought to recruit the de-ubiquitylating enzyme Doa4 (UBPY in mammals) [50, 51], while Vps4 is responsible for the dissociation of the ESCRT complexes from the MVB membrane to be released back into the cytosol [52, 53]. Dominant negative mutations in Vps4 result in a swollen endosomal (class E compartment) phenotype, implying that the dissociation of the ESCRT machinery is necessary for delivery of cargo into the lumen of the MVB [52], however it is not known if this dissociation is the necessary force to drive inward invagination.

The third step in MVB formation is the actual formation of internal vesicles – that is, the invagination and budding of vesicles containing cargo, into the MVB lumen. This process is poorly understood, and although it is thought that local asymmetry in lipids such as LBPA may play a role in causing membrane deformation and hence curvature, there is currently no comprehensive model for this process [54, 55]. It is thought however that ESCRT-III proteins (CHMPs) are involved in the final stages of MVB formation with regards to inward vesiculation of cargo, however there is conflicting evidence of this anticipated role [56]. Different models have been proposed as to how the ESCRT complexes may facilitate such a process (for an in depth discussion of this see Chapter 7). However these models are based on many different individual experiments including *in vitro* findings, and thus there is not much evidence and these models tend to be rather speculative [4, 57]. Other proteins appear to be necessary for the MVB formation process to occur. These may include deubquitinating enzymes such as Doa4 and Ubp7 (of which UBPY and AMSH are the mammalian homologues, respectively), where in yeast Doa4 has been shown to remove the ubiquitin molecule just prior to cargo delivery into a vacuole [58, 59].

Mammalian protein	Yeast Homologue	Complex	Notes
HRS	Vps27	"ESCRT-0"	FYVE domain, binds Ub (UIM)
STAM	Hse1		Binds Ub (UIM)
TSG101	Vps23	ESCRT-I	Binds Ub, coiled-coil domain
VPS28	Vps28		
VPS37 (A-D)	Vps37		Coiled-coil domain
MVB12 (A-B)	Mvb12	*?? ESCRT-I ??*	
EAP30	Vps22	ESCRT-II	Coiled-coil domain
EAP25	Vps25		
EAP45	Vps36		
CHMP2 (A-B)	Vps2/Did4	ESCRT-III	Coiled-coil domain
CHMP3	Vps24		Coiled-coil, binds $PI(3,5)P_2$
CHMP4 (A-C)	Vps32/Snf7		Coiled-coil
CHMP6	Vps20		Coiled-coil, myristoylated
CHMP1 (A-B)	Fti1/Did2	*??ESCRT-III??*	Coiled-coil domain
CHMP5	Vps60/Mos10	*??ESCRT-III??*	Coiled-coil
CHMP7	?	*??ESCRT-III??*	Snf7 domain, binds CHMP4B
VPS4 (A-B)	Vps4	Vps4 complex	AAA-ATPase, MIT domain
ALIX	Vps31/Bro1		Binds LBPA
UBPY	Doa4		De-ubiquitylating enzyme
AMSH	Ubp7		De-ubiquitylating enzyme
Vta1	LIP5		MIT domain, binds Vps4/CHMPs
PIKfyve	Fab1p	*??*	FYVE domain, PI(3)P to $PI(3,5)P_2$

Table 1.1 – Mammalian and yeast homologues of ESCRT and other proteins involved in MVB formation.

1.4 Phosphoinositides and Endocytosis

It appears that phosphoinositides seem to also play a key role in proper endocytic trafficking events including MVB formation [60-62]. Phosphoinositides are formed by the phosphorylation at various positions of phosphatidylinositol (PtdIns), and their production within the cell can be spatially and temporally regulated [reviewed in 63]. For example, the phosphoinositide lipid $PtdIns(4,5)P_2$ is generally synthesised at the plasma membrane. PtdIns(3)P on the other hand is typically considered to be early endosomally localised. Whereas, $PtdIns(4,5)P_2$ has been implicated in playing a role with clathrin-mediated endocytosis, PtdIns(3)P may play a role in endosomal trafficking and recognition of proteins involved in these pathways. As already mentioned, the ESCRT-0 protein Vps27 (Hrs in mammals) specifically binds to PtdIns(3)P which determines its endosomal localisation. Vps27 possesses a FYVE domain, a domain that is known for binding to the PtdIns(3)P lipid.

Substitution of this FYVE domain in Vps27 impairs its endosomal membrane targeting [4, 48]. As the sub-cellular localisation of proteins can ultimately determine their function within a cell, mis-localised Vps27 proteins as a result of FYVE-domain substitutions hence impair the proper cellular function of Vps27.

The FYVE domain originally was named this due to four proteins this domain was common in: Fab1, YOTB, Vac1 and early endosome antigen-1 (EEA1), although this domain is found in several other proteins, including Vps27/Hrs [64]. FYVE domains bind phosphoinositides with great preference to PtdIns(3)P. The actual domain is a small zinc finger and its binding to PtdIns(3)P results in it being "anchored" to the membrane by both electrostatic and resulting hydrophobic interactions with PtdIns(3)P and surrounding membrane lipids [65]. Hydrophobic residues contained in the FYVE domain actually form what is referred to as an insertion loop. This insertion loops is what enables a tightly bound interaction with the membrane, as hydrophobic residues present on the domain insert into the lipid bilayer of the membrane, forming a loop that sits inside the hydrophobic tail domain region of the membrane lipids. Additionally, there is a specific lipid binding interaction that occurs with the FYVE domain and the inositol head group of PtdIns(3)P [66]. Such specificity is important for a protein given that many different forms of inositol lipids are found throughout the cell at various different membranes, from the Golgi apparatus, to endosomal membranes, to the plasma membrane itself. Thus the cellular localisation of a protein is very important in determining its primary cellular role. For example, a protein containing a domain that recognises PtdIns(4,5)P_2 is likely to be localised to the plasma membrane and its resultant effects will be manifested at this compartment.

One phosphorylated product of the early endosomally localised phosphoinositide PtdIns(3)P is the lipid PtdIns(3,5)P_2. This phosphoinositide has been proposed to be synthesised at endosomal membranes [reviewed in 67]. In yeast, the protein kinase Fab1 is

responsible for the conversion of PtdIns(3)P to PtdIns(3,5)P_2 and mutations in the lipid kinase domain of Fab1 result in decreased levels of PtdIns(3,5)P_2 and altered vacuolar morphology [61, 62]. The yeast strain *Δfab1* is completely devoid of the lipid PtdIns(3,5)P_2 and displays phenotypes that are typified by dramatically enlarged vacuoles, some defects in MVB sorting and various other negative cellular effects that the yeast vacuole helps to control [reviewed in 67; 68]. Conversely, a mutant of Fab1 that results in increased levels of PtdIns(3,5)P_2 results in abnormal decreased vacuolar size suggesting that this lipid is important in the maintenance of vacuolar size with the levels of PtdIns(3,5)P_2 needing to be carefully regulated by Fab1 [69].

The mammalian homologue of Fab1 is PIKfyve, which has also been reported to give swollen vacuolar phenotypes when its normal function is impaired [60, 70]. It should be noted that PIKfyve contains a FYVE domain, as does Fab1. In addition to these studies, the ESCRT-III component Vps24 (CHMP3) has also been identified as a potential PtdIns(3,5)P_2 binding partner [71]. *In vitro*, Vps24 appears to show specificity for PtdIns(3,5)P_2 however the relevance of this *in vitro* binding to *in vivo* function is not yet clear [71]. Dominant negative truncated forms of Vps24 when overexpressed in mammalian cells give a large swollen vacuolar phenotype. Additionally, in the absence of PtdIns(3,5)P_2, membrane protein cargo in yeast found on the limiting membrane of the MVB fails to be delivered to the lumen [62]. Further to Vps24, several other potential effector proteins of PtdIns(3,5)P_2 have been identified *in vitro*, including the cytokine-independent survival kinase (CISK) protein, a soy bean protein termed Ssh1p, and the *S. cerevisiae* protein Gcs1p [72]. Despite the identification of these proteins binding PtdIns(3,5)P_2 *in vitro*, the relevance of their cellular roles and that of PIKfyve/Fab1's apparent function is not obvious. The role of PIKfyve in the endocytic pathway will be discussed in further depth later on in this chapter.

1.5 CHMP proteins

The ESCRT-III complex in mammalian cells is made up of proteins referred to as CHMPs. These are homologues of the yeast Vps proteins; however they all possess similar properties in their structures and actions [reviewed in 4, 9; 73, 74]. CHMP proteins are quite small, being around 200 amino acids in length, and are highly charged molecules, with basic N-terminal and acidic C-terminal domains. They appear to contain coiled-coil domains, predicted by sequence studies [75]. There have been reported to be at least 11 CHMP proteins in mammalian cells, belonging to one of 7 families, CHMP1-7 [76]. It is not clear what the role of each of these 11 CHMPs are, however mutations, gene silencing, and dominant negative overexpression of many of these proteins lead to MVB sorting defects.

CHMP proteins are notable for their distinctly charged N- and C-terminal residues. The basic N-terminus is positively charged compared with the acidic, negatively charged C-terminal domain. It has been proposed that the C-terminus interacts with the N-terminus inhibiting the function of the N-terminal domain [77]. Thus the C-terminus has therefore been called an autoinhibitory domain. For the CHMP to properly function its role in MVB biogenesis, some sort of event (possibly membrane binding) must occur which allows the autoinhibitory C-terminal domain to be removed from binding the N-terminal domain. Truncations that remove the C-terminal inhibitory domain result in impaired CHMP functions and membrane localisation [78]. In the case of ESCRT-III components however, the Vps4 binding site is also found in the C-terminal domain, thus removal of the autoinhibitory C-terminal domain would likely impair the ability of Vps4's AAA-ATPase activity on CHMPs.

The ESCRT-III complex made up in mammalian cells of these CHMPs is thought to play an important role in endosomal invagination and the delivery of cargo to the MVB lumen. Precisely how ESCRT-III is involved

in this invagination process, if at all, is subject to much debate and the exact mechanisms involved are not well known. What is acknowledged however is that recruitment of ESCRT-III components, as already mentioned, is usually the result of ESCRT-II complex formation and endosomal membrane recruitment, at least in yeast. The ESCRT-III complex is thought to be made up of a core of 4 CHMP proteins: CHMP2 (Vps2/Did4), CHMP6 (Vps20), CHMP3 (Vps24) and CHMP4 (Vps32/Snf7) [4, 45]. The other mammalian CHMPs identified (CHMP1, 5 and 7) may be involved in some way such as in having regulatory roles, however these are very poorly understood. The recruitment of ESCRT-III by ESCRT-II complex formation is a process that results in the oligomerisation of these 4 CHMP proteins, giving a concentrated ESCRT-III complex. Yeast two-hybrid studies have identified interactions between these four CHMPs, showing that CHMP3 interacts with both CHMP2 and CHMP4 and CHMP4 interacts with all other members of the complex (CHMP2, 3 and 6) [4]. CHMP2 then interacts with CHMP3 and 4 and CHMP6 only interacts with CHMP4 (see Fig 1.2).

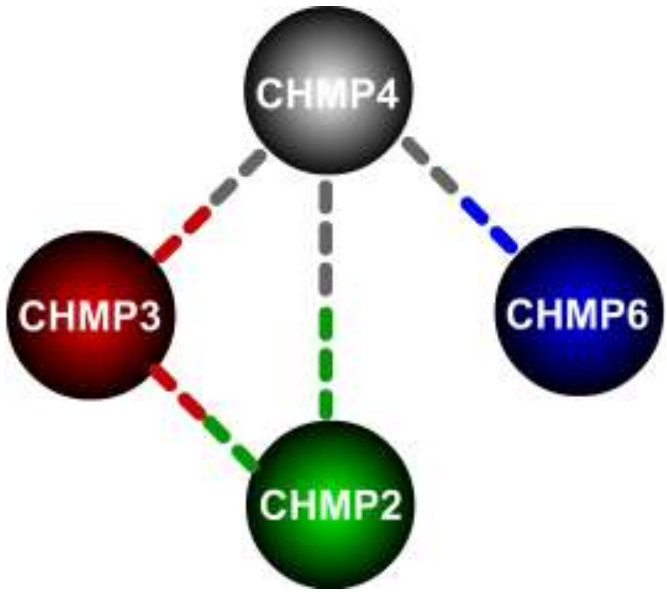

Figure 1.2 – The interactions of the four core mammalian CHMP proteins. The four CHMPs thought to make up the ESCRT-III complex are represented by spheres (CHMP2, 3, 4 and 6). Interactions with other CHMPs are indicated by a dashed line connecting the proteins that interact with each other, as identified by yeast two-hybrid studies [43].

Following the oligomerisation of the four CHMP proteins, the ESCRT-III complex seems to concentrate membrane cargo as well as recruit additional proteins (see Fig. 1.3). The recruitment of Bro1 (ALIX) allows this protein to further recruit Doa4, which appears to have a role in removal of the ubiquitin molecules from the cargo destined for delivery to the MVB lumen. Several other proteins have been implicated in ESCRT-III association at this stage such as Vta1 (which binds Vps4 and is thought to link some CHMPs to Vps4 by direct CHMP binding), but these are more recently described [79]. The ESCRT-III complex then seems to serve as a platform that allows ubiquitylated cargo to be concentrated in a place where ubiquitin molecules are recycled back to the cytosol. This cargo destined for degradation via the lysosome can then be delivered to the lumen of the MVB. The dodecameric AAA-ATPase, Vps4, is responsible for removal of the ESCRT-III machinery complex, which is recycled back to the cytosol after having been removed from the endosomal membrane [35-37, 52, 80] (Fig. 1.3). This removal process carried out by Vps4 seems to be essential for cargo delivery to the lumen. Evidence to support this includes the fact that when a dominant negative Vps4 lacking AAA-ATPase activity is expressed in cells, a swollen vacuolar phenotype is observed and cargo accumulates on the endosomal membrane. This cargo is not delivered into the MVB lumen, and a reduction of internal vesicles is observed [53]. Thus Vps4 acts as a vital component of MVB biogenesis with removal of the ESCRT-III machinery being necessary for proper MVB formation. In addition, the lipid LBPA seems to be highly concentrated and almost found exclusively on internal vesicles of MVBs [54, 55]. The structure of this lipid allows it to perhaps give local asymmetry and membrane curvature, which has hence been suggested to aid in the formation of MVB vesicles [4]. However, it is likely that the presence of LBPA is merely a contributing factor to a much more complex process of invagination and lumenal vesicle formation, and it should be noted that LBPA is not present in yeast.

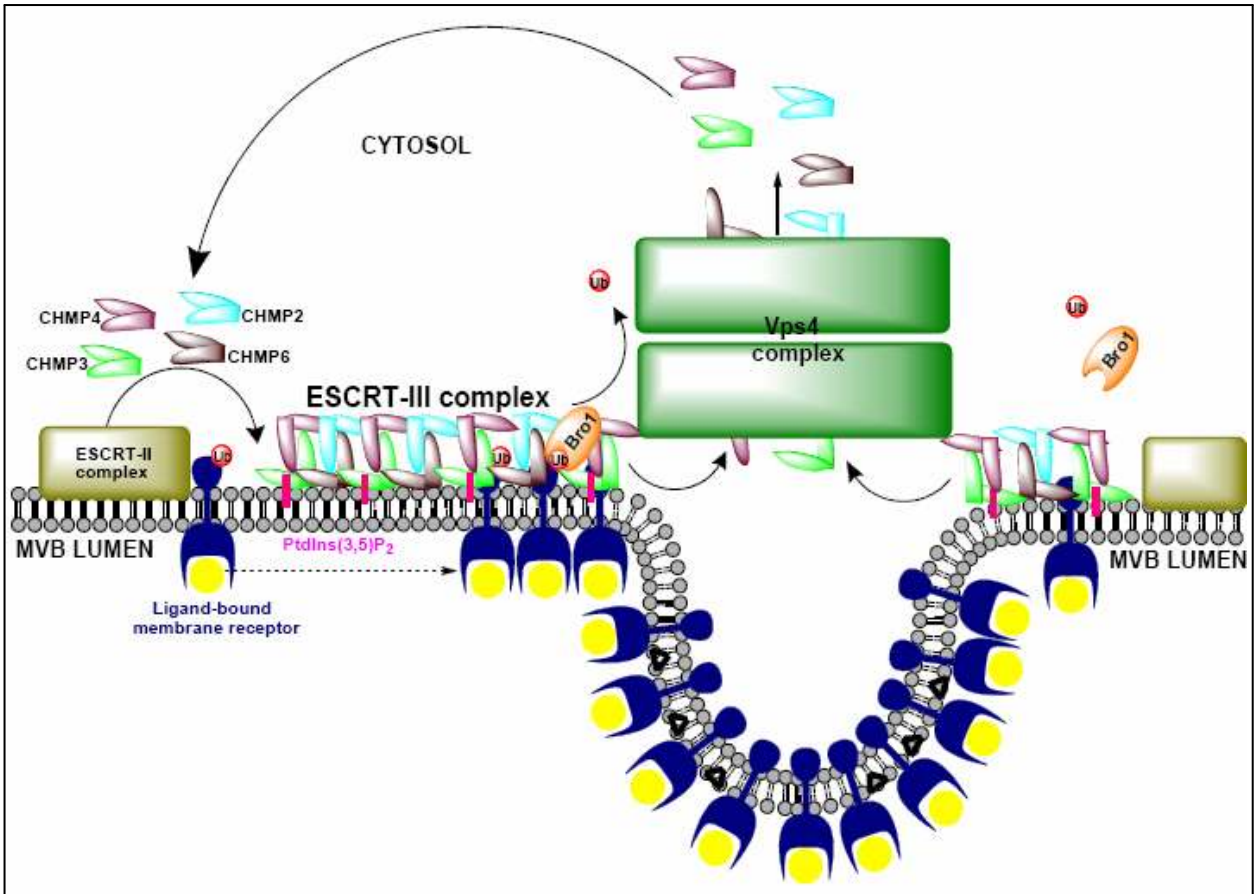

Figure 1.3 – The mammalian ESCRT-III complex and associated proteins in MVB biogenesis. The CHMP proteins (mammalian ESCRT-III components) typically reside in the cytosol. Activation and formation of ESCRT-I, and subsequently ESCRT-II complexes, results in the recruitment and oligomerisation of the ESCRT-III components; CHMP2, 3, 4 and 6. The CHMP proteins reside as a more "closed" conformation, which involves their C-terminus autoinhibiting the N-terminus. Through recruitment and possible binding to PtdIns(3,5)P_2, the CHMPs open up to an active form whereby membrane binding and protein interactions at the N-terminus can occur. Cargo already concentrated by previous ESCRT complexes may also be additionally concentrated by ESCRT-III. Cargo that was initially concentrated by ubiquitin (Ub) recognition is deubiquitylated by enzymes such as Bro1. Interactions of the C-termini of CHMPs with the dodecameric Vps4 complex take place which results in the removal of CHMPs from the membrane possibly causing the membrane to close and pinch off forming an internal vesicle containing concentrated cargo. Local asymmetry may be aided by the presence of the lipid LBPA (represented by black triangles). CHMP proteins are then recycled back to the cytosol where they exist in their autoinhibited form. Note, in the concentric circle theory (reviewed in chapter 7, [57]) important points to make are that it is hypothesised that the ESCRT-II, -I and –0 complexes are found more above and inward to the invaginating vesicle and are removed prior to full invagination and vesicle formation.

One of the ESCRT-III components, CHMP3, has already been mentioned to bind PtdIns(3,5)P_2 *in vitro* [71]. Due to the localisation of ESCRT complexes being thought to be largely determined by Vps27/Hrs membrane binding to PtdIns(3)P, it would be of no surprise if the generation of PtdIns(3,5)P_2 occurred at the same membrane. Indeed, due to the high concentration of PtdIns(3)P found on endosomal membranes, it the generation of PtdIns(3,5)P_2 is thought to occur at endosomal membranes. Given the fact that CHMP3 appears to bind PtdIns(3,5)P_2 specifically *in vitro*, and that this lipid has a strong negative charge, it is possible that PtdIns(3,5)P_2 plays some role in ESCRT-III recruitment and CHMP activation. This may occur as binding of the highly positive N-terminal domain to the membrane is one suggested mechanism by which the CHMP is released of its autoinhibitory C-terminal domain in some fashion. Despite this, there is currently little *in vivo* evidence to support CHMP3 being an effector of PtdIns(3,5)P_2.

1.6 The role of PIKfyve in the endocytic pathway

The enzyme responsible for PtdIns(3,5)P_2 formation, PIKfyve, would appear to play some role in the endo-lysosomal pathway and hence potentially in proper ESCRT function [60, 70, 81, 82]. Certainly, overexpression of a dominant negative mutant PIKfyve lacking kinase activity in mammalian cells has been reported to give a similar swollen endosomal phenotype as seen in mutations of ESCRT proteins [70, 83]. There have been some conflicting studies regarding the localisation of PIKfyve, with it having been reported to be early endosomal as well as late endosomal [84-86]. It is possible that PIKfyve localises to a compartment that contains both early and late endosomal markers. Such a hybrid compartment has been perceived as perhaps what MVB organelles exist as, instead of merely a subset of late endosomes, and has been suggested by others [71]. Also it should be noted that cellular localisation studies are often based on dominant negative and mutant

proteins that perturb proper cellular functions, often resulting in abnormal endosomal structures, which may then not be a true physiological representation of the actual markers found on MVBs within the cell.

PIKfyve, like Vps27, contains a FYVE domain, which as already discussed is a domain specific for the binding of PtdIns(3)P. This domain allows PIKfyve to be localised to the exact lipid which it phosphorylates, to give the product PtdIns(3,5)P_2. Although there is still some debate on the exact role of the product of PIKfyve, PtdIns(3,5)P_2 has been implicated in the endo-lysosomal pathway so it is likely that PIKfyve does play some role in this pathway [62, 71]. In spite of this, PIKfyve is a difficult protein to study and thus the literature on PIKfyve is not as extensive as it is with other MVB proteins.

Despite the lack of extensive studies carried out on PIKfyve, the few that are present in the literature have often provided conflicting reports as to what PIKfyve's role within the mammalian cell is. Regardless of the findings of PIKfyve's involvements with endocytic trafficking and MVB defects, unlike ESCRT-I component mutants, one study found in *Drosophila* that *fab1* mutant cells resulted in the accumulation of endocytosed receptors at endosomal membranes. However this occurred with no accumulation of ubiquitin at these compartments, suggesting cargo was not ubiquitylated or had been deubiquitylated [84]. Furthermore, the *Drosophila fab1* mutant cells resulted in enlarged endosomal structures, which accumulated both receptors and ligands in late endosomal compartments. These compartments contained ESCRT components (Hrs and Tsg101) however despite being enlarged compared with control cells, the cargo was found to be in the lumen of the compartment, suggesting MVB formation was not fully inhibited, although receptor degradation was [84]. Thus one of the conclusions of this study was that Fab1 does not affect silencing of endocytosed receptors but it does however affect their degradation. Interestingly, it has similarly been shown in mammalian cells that CHMP3 depletion perturbs EGFR degradation but not its silencing. This is contrasted by earlier ESCRT

components such as Tsg101 which when silenced by siRNA result in endocytosed receptors still signalling at the endosomal membrane [56]. These results imply a role of PIKfyve (and consequently PtdIns(3,5)P_2) in the trafficking of MVBs to the lysosome as opposed to the actual formation of MVBs. This may also be a potential role for ESCRT-III components given the similar findings, which could link these proteins as being necessary for a common trafficking pathway.

Other recent studies have contradicted these findings suggesting an alternative role for that of PIKfyve in endosomal trafficking. A recent study found that the suppression of endogenous PIKfyve by siRNA appears to result in enlarged early and late endosomal structures, however it does not affect the internalisation and degradation of EGFR nor the internalisation, degradation or recycling of the transferrin receptor (TfR) [86]. However in cells that have suppression of PIKfyve there was found to be abnormal early endosome to TGN retrograde trafficking. The accumulation of membrane resulting in enlarged endosomal structures then was not put down to arresting the inward invagination process that occurs in MVB formation but rather the disruption in trafficking to the TGN due to suppression of endogenous PIKfyve. It should be noted that MVB formation *per se* seemed to be unaffected in that cargo was still delivered to the MVB lumen and more importantly cargo was successfully degraded via the lysosome [86].

Other studies have suggested yet further roles for PIKfyve. It has been stated that in some tumour cells EGFR is transported to the nucleus where it can transmit gene regulation properties. In one study endogenous PIKfyve was apparently identified as a binding partner of endogenous EGFR and transient expression of wild-type PIKfyve resulted in an increase of EGFR found in the nuclei of cells compared with the kinase-dead mutant PIKfyve whose expression inhibited EGFR trafficking to the nucleus [87]. Furthermore, by silencing PIKfyve's endogenous expression it was found that nuclear EGFR was significantly reduced.

Another study using an orthologue of PIKfyve/Fab-1 (PPK-3) found that deletion of this kinase in *C. elegans* is embryonic lethal with partial loss leading to growth retardation [88]. At the cellular level it was found that enlarged vacuoles were observed in many cell types, and that these vacuoles were positive for lysosomal markers such as LAMP-1. From this study then it was concluded that the role of PPK-3 was in one of membrane retrieval from lysosomes and thus due to some mechanism through cellular PtdIns(3,5)P_2 level control, PPK-3 was largely involved in the cellular process of lysosomal maturation [88]. Additionally it should be noted that protein and receptor degradation in the lysosome was unaffected by altering levels of PPK-3.

These studies appear to suggest a rather complicated role of PIKfyve in endosomal trafficking, without distinct cellular functions being clear. Studies however seem to lack consistent findings in simply the localisation of PIKfyve, let alone what parts of the endocytic pathway this kinase helps control. It is significant however that Rusten *et al* demonstrate that PIKfyve is necessary for the degradation of signalling receptors but not the silencing [84], which parallels the findings from Bache *et al*'s study of silencing CHMP3 [56]. As CHMP3 has been implicated as a potential binding partner of PIKfyve's product, PtdIns(3,5)P_2 [71], these two studies then are consistent with the roles of both PIKfyve and CHMP3 as being potential regulators for the trafficking of MVBs to the lysosome. One thing that is certain from the literature however is that much work is needed to be carried out on PIKfyve to better understand its exact function in the mammalian cell and the role of PtdIns(3,5)P_2 in the endo-lysosomal trafficking pathway.

1.7 The AAA-ATPase Vps4

The recruitment and binding to the membrane of CHMPs is only part of the process when it comes to proper ESCRT-III function and MVB

biogenesis. It would appear that as well as binding to the membrane, removal of the ESCRT-III components from the membrane is just as crucial a step in MVB biogenesis. The AAA-ATPase (ATPase associated with various cellular activities) Vps4 is the necessary ESCRT-associated component that allows this process to occur [52, 53, 80]. By mutating the glutamic acid (E) at position 235 in the Vps4B protein to glutamine (Q), a dominant negative Vps4 protein is obtained that is ATPase deficient [89]. Over-expression of this dominant negative $Vps4^{E235Q}$ protein results in large, swollen endosomal structures, which perturb membrane receptor degradation and proper MVB formation. In addition, ESCRT-III components localise to these swollen compartments, co-localising with the $Vps4^{E235Q}$ protein [71]. It would appear that Vps4 interacts with the C-termini of CHMPs via a MIT (microtubule interacting and transport) domain at the N-terminus of Vps4 [89-91]. This interaction seems to be quite specific, with strong binding affinities for a conserved heptad leucine repeat found at the C-terminus of most CHMP proteins. This process may be reliant of the autoinhibitory C-terminal domain being removed from the N-terminus. With the C-terminal removed from inhibiting the N-terminal domain of the CHMP, this allows membrane binding which occurs via the positively charged N-terminus. The C-terminus of the CHMP is now exposed away from the surface of the endosomal membrane. Upon oligomerisation of the ESCRT-III complex, the functional dodecameric Vps4 protein can interact with the C-terminal domains of various CHMP proteins. This will allow for their removal from the membrane through a central pore in the Vps4 oligomer, due to ATP hydrolysis. Without the capacity to effectively hydrolyse ATP, the mutant $Vps4^{E235Q}$ protein would then bind CHMPs via its MIT domain resulting in it becoming permanently bound to the C-terminus of CHMPs. This would result in impaired MVB formation, due to ESCRT-III not being removed from the endosomal membrane, and a swollen endosome arising. One can envisage then that perhaps the actual removal of the ESCRT-III machinery by Vps4 may play a crucial if not central role in the inward invagination and lumenal vesicle formation that occurs during proper MVB biogenesis.

In addition to the dominant negative Vps4^{E235Q} protein, several mutant forms of ESCRT-III and related proteins have been produced and characterised. In particular one protein of significance in this field has been the truncation of the CHMP3 protein. As already discussed, CHMP3 has been reported to contain an autoinhibitory C-terminal domain. Removal of this domain to leave a CHMP3 construct of roughly half its original size (N-terminus only) results in MVB defects and swollen endosomal phenotypes [78]. In addition to this, there have been several reports that merely adding a GFP molecule to the N-terminus of CHMP3 results in impaired MVB formation and typical phenotypes associated with perturbed endosomal trafficking [78]. Constructs that contain a GFP-fusion tag on the C-terminus of CHMP3 however do not exhibit such phenotypes [71, 78]. Additionally, it has been recently shown that varying the length of the truncation of the C-terminus of CHMP3 can alter how strong the phenotype is. Truncations of CHMP3 that remove slightly less than half of the C-terminal domain (50-70 amino acids) give much stronger phenotypes associated with mutant CHMP3 than removal of the whole C-terminal half [78]. The exact reasons for the difference however in the strength of the phenotype are not clear.

Such dominant negative mutants can prove very important for trying to better understand the full and proper function of the ESCRT and related proteins as cellular functions they may be involved with are often perturbed in such cases. In addition, they may help provide us with clues about further interaction partners and other proteins that have not yet been identified but are important in proper MVB formation. As mentioned already, the mechanism by which ESCRT proteins allow for MVB biogenesis and cargo delivery into the MVB lumen is poorly understood. In addition to this, the full complement of proteins involved with ESCRTs and MVB formation may also not be known, and indeed it is possible that there are other proteins involved in this process that have yet to be identified as playing a role in MVB formation. Certainly ubiquitin for example has been shown to play a key role, however the exact recognition process is still under scrutiny. Furthermore, it may be more

complex than simply mono-ubiquitination that determines a protein's fate for lysosomal degradation [92, 93]. Additionally, there have been several deubiquitination proteins identified besides UBPY (Doa4 in yeast) which may also be involved somehow with deubiquitination of cargo when concentrated into ESCRT-containing MVB membranes [reviewed in 94].

As ESCRTs play a key and central role in the formation of MVBs for the proper downregulation of signalling receptors, one can imagine then that dysfunctional ESCRTs may result in signalling events being prolonged. Thus ESCRTs certainly play a key role in the basic control of signalling events which is obviously then important in certain disease states. Further to this however, there are several other disease states and cellular processes that ESCRTs play crucial roles in. This emphasises the importance to more fully understand this class of proteins and their mechanisms.

1.8 ESCRTs and retroviral budding, cytokinesis, other cellular functions and disease states

One major area of research that has been under much scrutiny recently due to ESCRT involvement is that of viral budding, in particular HIV budding [65, 78, 95-103]. HIV spreads by the production of particles that enter uninfected cells and are released in extracellular virons that have bud from infected cells. It would seem that the HIV virus hijacks some of the ESCRT machinery to escape from infected cells (Fig. 1.3*A*) [95]. Certainly, the direction of budding of a virus at the plasma membrane is the same direction as that of vesicle formation into the lumen of the MVB, that is, away from the cytoplasm. Thus it is of little surprise that the HIV virus has adapted to use similar machinery to that of MVB formation. HIV-1 viral protein components (Gag) have been shown to bind to Tsg101, an ESCRT-I component [99, 101, 102]. Furthermore, the expression of dominant negative CHMP proteins including CHMP1-4

results in the blocking of HIV-1 release and reduced infectivity [78]. More specifically, these dominant negative proteins appear to arrest HIV-1 release at a late stage. This leaves the mature viral particles in budding-like structures from the plasma membrane, unable to pinch off from the membrane, staying connected by a thin stalk-like membrane construction. Not only is this the case with dominant negative CHMP proteins but also with a dominant negative ATPase deficient Vps4 protein. This suggests that the ESCRT machinery and some associated proteins are vital for HIV-1 release from an infected cell, thus highlighting the importance of more fully understanding the mechanisms of ESCRT proteins. Furthermore these findings also suggest that the CHMP proteins along with Vps4 may be needed for the final "pinching off" of the membrane from invagination taking place in a direction that is away from the cytoplasm. This may well then be that the specific role of ESCRT-III and Vps4 in MVB biogenesis and lumenal cargo delivery is related to actual vesicle formation instead of other roles such as in cargo recognition, or similar.

As already mentioned, various truncations of CHMP3 that remove the autoinhibitory C-terminal domain have been described [78]. One of the ways in which the potency of these truncations was measured was in fact by measuring its effects on viral budding. The wild type CHMP3 protein is 222 amino acids long, and original truncations of the C-terminus resulted in an N-terminal CHMP3 protein of 113 amino acids in length. The 113 amino acid protein did inhibit HIV-1 viral budding, however much shorter truncations of 200, 179 and 150 amino acids all inhibited HIV-1 viral budding more potently [78]. The 150 amino acid truncation however was reported to be the most potent inhibitor of HIV-1 budding. These results demonstrate not only the importance of the autoinhibitory C-terminal domain but also the key role that CHMP3 plays in the budding and thus infectivity of the HIV-1 virus. Further understanding the exact mechanisms as to how this occurs may be useful for developing therapeutic targets in the treatment of HIV infection.

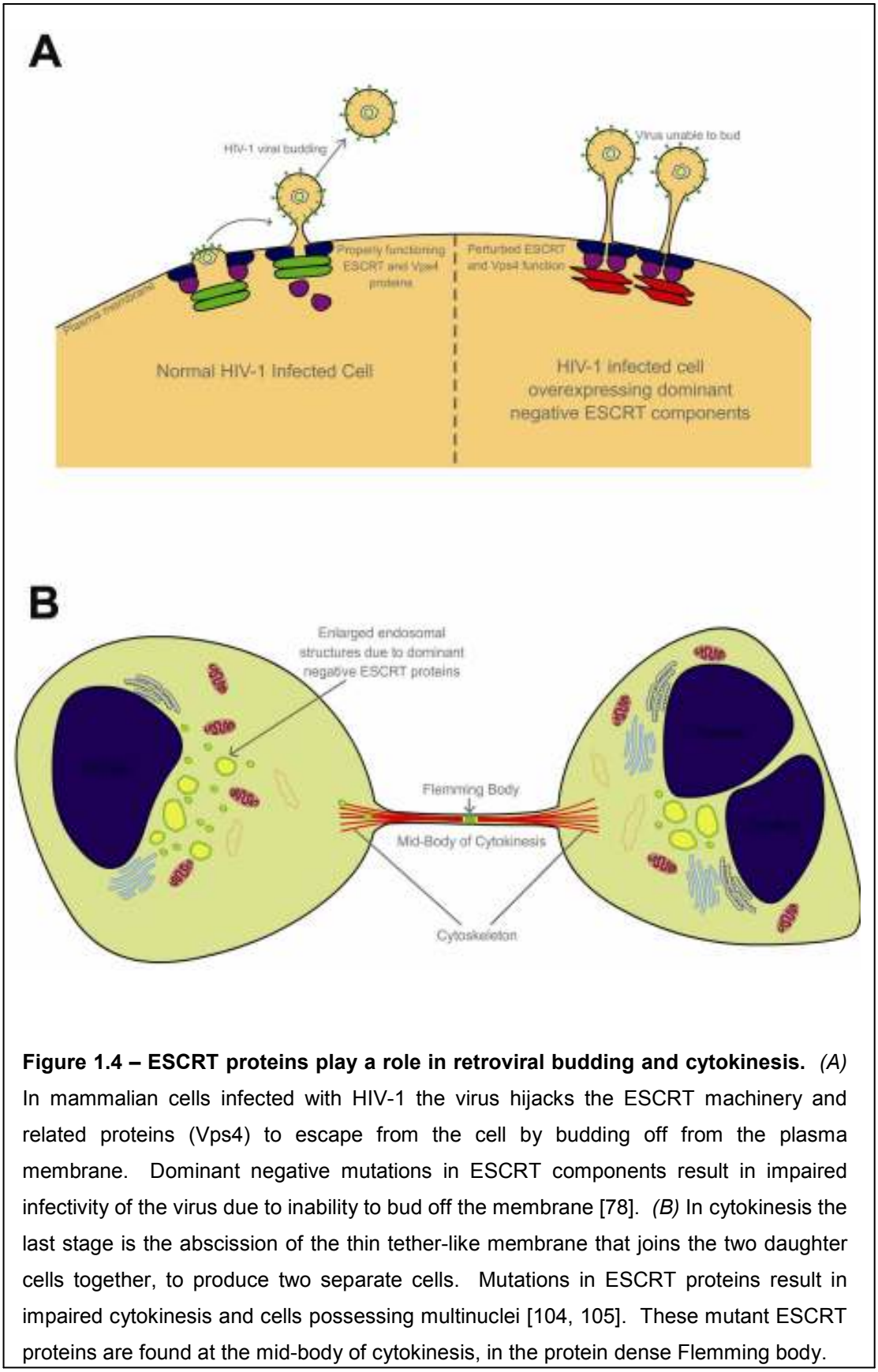

Figure 1.4 – ESCRT proteins play a role in retroviral budding and cytokinesis. *(A)* In mammalian cells infected with HIV-1 the virus hijacks the ESCRT machinery and related proteins (Vps4) to escape from the cell by budding off from the plasma membrane. Dominant negative mutations in ESCRT components result in impaired infectivity of the virus due to inability to bud off the membrane [78]. *(B)* In cytokinesis the last stage is the abscission of the thin tether-like membrane that joins the two daughter cells together, to produce two separate cells. Mutations in ESCRT proteins result in impaired cytokinesis and cells possessing multinuclei [104, 105]. These mutant ESCRT proteins are found at the mid-body of cytokinesis, in the protein dense Flemming body.

It has recently emerged that the ESCRT proteins also play a key role in a vital cellular process, that of cytokinesis [104, 105]. The process of cytokinesis is a highly precise yet complex process necessary for the formation of two daughter cells from a single parent cell. During the final stages of cytokinesis, a mid-body is formed which is a thin tether-like structure connecting the two daughter cells together (Fig 1.3*B*). The end of cytokinesis is typified by the abscission of this structure at the mid-body, which seems to be an event heavily reliant on membrane dynamics [106]. This has been paralleled then to the abscission events that take place in retroviral budding, that is, the pinching off of the membrane stalk formed by viral buds, which seems to involve the ESCRT machinery [105].

There are several theories as to how abscission occurs in cytokinesis to separate the two daughter cells. Perhaps the most attractive theory is the trafficking of membrane vesicles to the mid-body where some apparent fusion event occurs allowing the separation of the two cells and abscission of the plasma membrane at this region [reviewed in 107; 108-109]. It has recently been shown that some ESCRT and related proteins are present at the mid-body and the mutation or silencing of such proteins results in impaired cytokinesis that is paralleled to impaired retroviral budding [105].

In mammalian cells it seems apparent that Rab GTPase proteins are essential for cytokinesis, in particular Rab11 [110]. Rab11 has been shown to be a recycling Rab, involved with the trafficking of endosomes [111-113]. ESCRT proteins have also been found to be involved in cytokinesis, present at the mid-body prior to abscission, similar to Rab11. The area of research involving ESCRT proteins and cytokinesis is very recent, and much of this initial work has focused on the earlier ESCRT and associated proteins, for example ESCRT-I proteins. TSG101 (Vps23) is a component of the mammalian ESCRT-I complex, and this was found to localise to the mid-body in cytokinesis, more specifically a dense structure at the mid-body known as the “Flemming body,” which is

known to contain many other proteins involved in abscission. TSG101 appears to be localised to the mid-body by interactions with the centrosomal protein Cep55, which also localises to the mid-body in cytokinesis, suggesting a role for ESCRT proteins then in the process of cytokinesis [105]. Furthermore, depleting cells of TSG101 resulted in abnormal cytokinesis typified by the presence of multinucleated cells, adding further evidence that TSG101 is important in proper cytokinesis [105].

Further to this, a component of ESCRT-III as well as the AAA-ATPase Vps4 was also investigated for potential roles in cytokinesis [104, 105]. It was found that overexpression of dominant negative versions of CHMP4 and Vps4 both inhibited proper cytokinesis and gave abnormally high levels of multinucleated cells. Note however that ESCRT-II components were not found to have such an effect on cytokinesis when dominant negative constructs or RNA interference was used. Thus these findings highlight the diversity of the ESCRT proteins' role within the cell further than simply MVB biogenesis. It is likely then that the function of ESCRT and related proteins in cytokinesis is very similar to the role that retroviruses such as HIV-1 hijack the machinery for. Indeed in all scenarios there is a requirement for an abscission event to occur, and clearly in both HIV-1 viral budding and cytokinesis, defects in certain ESCRT components result in these events being disrupted. As these events are heavily reliant on membrane dynamics in their late stages, it may be postulated that the ESCRT complexes along with Vps4, in particular ESCRT-III and Vps4 being the last complex on MVBs, are similarly heavily involved in the membrane dynamic events that occur in lumenal vesiculation at the MVB.

Although retroviral infection and budding along with cytokinesis are very important fields of study, ESCRT proteins have further been implicated in several other cellular pathways and disease states as well. Certainly many neurodegenerative diseases have had components of their pathology attributed to aberrant endosomal pathways and dysfunction of

ESCRT proteins. ESCRT-III has been identified to play a role in autophagasome accumulation and neurodegeneration due to loss of expression of certain CHMP proteins [114, 115]. Autophagy is an important process that allows for cellular processes such as the turnover of aggregated proteins as well as organelles and other cytosolic components. Aggregated proteins in neuronal cells are a hallmark of many age-related neurodegenerative diseases, such as Alzheimer and Huntington's diseases. ESCRT proteins then play a key role in autophagy due to their importance in MVB trafficking to the lysosome. Thus loss of function of ESCRT components in neuronal cells can result in such neurodegeneration occurring.

MVB and ESCRT proteins have also been shown to be involved in other events, such as antigen presentation in T-cells, Notch signalling in development, exosome release, cancers, and even in disease states such as cataracts [19, 45, 116]. Thus understanding the exact roles and mechanisms of action for the ESCRT complexes is very important and would certainly enable us to better understand certain disease states and crucial cellular processes, allowing for better therapeutics and approaches to research in these areas.

1.9 Experimental aims of the project described in the thesis

There were three main experimental aims of this thesis:
To more fully understand the role of lipids, in particular PtdIns(3,5)P_2 in MVB biogenesis.
To better characterise proteins in and associated with the ESCRT-III complex, in particular CHMPs, PIKfyve and Vps4.
To further investigate dominant negative mutations in CHMPs and their resultant effects in mammalian cells.

Investigations to better understand the role of PtdIns(3,5)P_2 in MVB formation were undertaken using a protein expressed by *Salmonella* bacteria as a potential tool for manipulating PtdIns(3,5)P_2 levels. The localisation of this protein, SopB, was determined by immunofluorescence studies and its effects on the degradation of the tyrosine-kinase receptor EGFR were also investigated, by utilising a strain of *Salmonella* that had the expression of SopB deleted.

Secondly, investigations were carried out to better characterise PIKfyve, the mammalian enzyme responsible for the production of PtdIns(3,5)P_2 from PtdIns(3)P. As this protein has not been studied for very long, there was no known commercial antibody, so much of this work was focused on the production and characterisation of an antibody that would recognise PIKfyve. Furthermore, to aid in the aim to better understand the ESCRT-III complex and proteins associated with it, an assay was devised and set-up, which would allow a possible mass proteomic approach to the full complement of proteins that are found on MVB membranes. This was achieved using a relatively new tagging and labelling technique, known as Halo®-tag, and involved isolating swollen endosomal compartments that the dominant negative Vps4^{E235Q} was found on when expressed in mammalian cells.

Finally, the effects of truncating and various mutations of CHMP proteins, in particular CHMP3 was looked at more fully. Previously described truncations of CHMP3 and point mutations were investigated to see their effects on endosomal trafficking as well as membrane binding abilities. The effects of such mutant proteins expressed in mammalian cells on cytokinesis were also investigated.

CHAPTER 2

2 Materials and Methods

2.1 Materials

All general laboratory chemicals were of analytical grade and purchased from either Sigma-Aldrich Chemical Company or Fisher Scientific UK Ltd. unless otherwise stated.

2.1.1 Buffers

Phosphate Buffered Saline (PBS):

154 mM NaCl, 12.5 mM Na_2HPO_4.12 H_2O, (pH 7.2).

Tris Buffered Saline - Tween 20 (TBST):

10 mM Tris, (pH 7.4), 154 mM NaCl, 0.1% (v/v) Tween-20.

Sample Buffer:

Protein samples were solubilised in 2% (w/v) SDS, 62.5 mM Tris HCl (pH 6.8), 0.01% (w/v) bromophenol blue, 10% (v/v) glycerol with the reducing agent being 100 mM Dithiothreitol (DTT).

Resolving Gel Buffer:

1.5 M Tris HCl, 0.4% (w/v) SDS, (pH 8.8).

Stacking Gel Buffer:

0.5 M Tris HCl, 0.4% (w/v) SDS, (pH 6.1).

Electrophoresis Running Buffer:

25 mM Tris HCl, (pH 6.3), 0.1% (w/v) SDS, 0.2 M Glycine.

Transfer Buffer:

39 mM Glycine, 48 mM Tris, 0.0375% SDS (w/v), 20% methanol (v/v), (pH 8.8).

Ponceau S Stain:

0.1% (w/v) Ponceau S, 3% (w/v) trichloroacetic acid.

Coupling Buffer:

0.2 M $NaHCO_3$, 0.5 M NaCl

ELISA Plate Coating Buffer:

15 mM Na_2CO_3, 35 mM $NaHCO_3$, 0.01% (v/v) Na Azide, (pH 9.6).

ELISA Plate Blocking Buffer:

PBS, 0.1% (v/v) Tween-20, 1% (w/v) Casein, add casein and dissolve with mixing overnight at 4°C.

Luria Broth (LB):

1% (w/v) Bacto™ Tryptone [BD Biosciences], 0.5% (w/v) Bacto™ Yeast Extract [BD Biosciences], 0.5% NaCl, (pH 7.5; autoclaved).

Agar Plates:

1% (w/v) Bacto™ Tryptone [BD Biosciences], 0.5% (w/v) Bacto™ Yeast Extract [BD Biosciences], 0.5% NaCl, 1.5% (w/v) Agar, (pH 7.5) (autoclaved).

ECL Reagent:

Solution A – 100 mM glycine (pH 10), 0.4 mM luminol, 8 mM 4-iodophenol

Solution B – 0.12% (w/w) hydrogen peroxide in water

TESA Buffer:

255 mM sucrose, 5 mM EDTA, 10 mM Tris-HCl, 2 mM ATP, pH 7.2

2.1.2 Antibodies

Table 2.1 gives a list of antibodies along with their suppliers and dilutions used for different applications. For immunofluorescence studies, primary and fluorescent secondary antibodies were diluted in PBS containing 2%

Antibody	Species	Source	Dilution / Application
α-EGFR (Trans Labs)	mouse, monoclonal	Transduction Laboratories	WB – 1:2000 IF – 1:250
α-GFP	rabbit serum	Molecular Probes	WB – 1:1000
α-GFP$_{IgG2a}$	mouse, monoclonal	Molecular Probes	IP – 2-4μg
α-EEA1	rabbit	Gift, Dr Michael Clague	IF – 1:1000
α-myc $_{4A6}$	mouse, monoclonal	Upstate	IF – 1:300
α-FLAG $_{M2}$	mouse, monoclonal	Sigma	WB – 1:3000 IF – 1:300
α-His$_6$	mouse, monoclonal	Amersham	WB – 1:2000
α-TSG101 $_{4A10}$	mouse, monoclonal	Abcam	WB – 1:500-1000
α-β,tubulin $_{TUB2.1}$	mouse, monoclonal	Sigma	WB – 1:1000
α-Vps4	rabbit	Santa Cruz	WB – 1:1000
α-HA	rat, monoclonal	Roche	IF – 1:300
α-M6PR	rabbit	Gift, Dr Paul Luzio	IF – 1:1200
α-TGN46	sheep	Serotec	IF – 1:300
α-CHMP2	rabbit	In-house	WB – 1:200
α-CHMP3	rabbit	In-house	WB – 1:200
α-CHMP4	rabbit	In-house	WB – 1:200
α-PIKfyve	sheep	**In-house, see chapter 4**	WB - 1:4000
α-CD63	mouse, monoclonal	BD Biosciences	IF – 1:1000
α-Ub $_{FK2}$	mouse, monoclonal	Biomol	WB – 1:1000
α-Rab11$_{IgG2a}$	mouse	BD Transduction Laboratories	IF – 1:50
α–mouse Alexa® Fluor 546	goat	Molecular Probes	IF – 1:100
α–rabbit Alexa® Fluor 546	goat	Molecular Probes	IF – 1:100
α-mouse-HRP	goat	Sigma	1:2000-5000
α-rabbit-HRP	goat	Pierce	1:5000+
α-sheep-HRP	goat	Pierce	1:5000+

Table 2.1 – Various antibodies used experimentally. In-house antibodies (α-CHMP2, 3 and 4) were already made and purified by Dr Paul Whitley. α-PIKfyve production and purification is discussed in Chapter 4. All antibodies are polyclonal unless stated and where known, clone numbers are given. Dilutions are of original supplied stocks. Abbreviations: IF = immunofluorescence, IP = immunoprecipitation, WB = Western blotting.

(v/v) fetal calf serum (FCS). Primary antibodies used for Western blotting were diluted in TBST containing 5% (w/v) Marvel®, whereas secondary horse-radish peroxidase (HRP) conjugated antibodies were diluted in TBST containing 1% (w/v) BSA.

2.2 Methods

2.2.1 Tissue culture

Cos7 (African green monkey kidney), A431 (a human epidermoid carcinoma cell), HeLa (Human cervix carcinoma), NRK cells (normal rat kidney cell line) and CHO-K1 (Chinese hamster ovary) cells were the mammalian cell lines used. Cells (except CHO-K1) were maintained at 37°C, 5% CO_2 (except A431 cells which were maintained at 10% CO_2) in Dulbecco's modified minimal essential medium (DMEM) containing 10% fetal calf serum, 2 mM L-glutamine, 100 units/ml penicillin, and 100 μg/ml streptomycin. CHO-K1 cells were maintained similarly except in Ham's F12 medium supplemented as DMEM. All media and media supplements (including sterile Dulbecco's PBS; DPBS) were purchased from Cambrex, and mammalian cells were originally purchased from ATCC.

2.2.2 General Immunofluorescence studies

Cells were plated onto glass coverslips in 35mm or 16mm wells and grown until ~60-80% confluent prior to transfection using Lipofectamine 2000™ (Invitrogen) or FuGENE 6 transfection reagent (Roche Diagnostics) or *Trans*IT-LT1 (Mirus) according to the manufacturer's instructions. Cells grown on glass cover slips were transfected ~16 hours prior to fixation (unless stated otherwise) and processed for immunofluorescence microscopy as follows.

Media was removed from cells and cells were then rinsed once with PBS and fixed with 4% (w/v) paraformaldehyde (PFA) dissolved in PBS for 20 minutes. Cells were then permeabilised using methanol at -20^{o}C for 5 minutes. Primary antibodies were diluted in PBS containing 2% FCS and incubated with the cells for 2 hours at ~18^{o}C. Appropriate species-specific fluorophore conjugated secondary antibodies were also diluted in PBS containing 2% FCS. Incubations with secondary antibodies were for 1 hour at ~18^{o}C in the dark. Cells were washed 5 times for 5 minutes in PBS containing 2% FCS following all antibody incubations with a further 3 washes in PBS alone. In immunofluorescence studies where nuclear staining was necessary, a 1:500 dilution of DAPI was used during the secondary antibody incubation. Cover slips were mounted in Mowiol (Calbiochem). Cells were examined and images obtained on a Zeiss LSM510 laser scanning confocal microscope unless stated.

Wortmannin treatment:

Transfected cells were treated with 500 nM wortmannin with the media being changed to fresh wortmannin every 1 hour for a period of 3 hours after which they were fixed and processed as necessary.

2.2.2.1 HaloTag® fluorescent labelling

Fluorescent labelling of cells expressing proteins with the HaloTag® were processed according to the manufacturer's instructions (Promega). Briefly, at least 16 hours post-transfection the media covering the cells was removed to leave 100μl in each 16mm well. A further 100μl of the diluted Halo-ligand (diluted 1:500; either diAcFAM or TMR ligands) was added to each well and cells incubated at 37^{o}C, 5% CO_2 in the dark for 15 min. After 15 min incubation, media was removed, cells washed twice with PBS and then fixed in 4% PFA being processed as other immunofluorescence studies.

2.2.2.2 EGF degradation studies

HeLa cells were transfected with appropriate constructs as above and allowed to express for 24 hours until serum-containing medium was removed and replaced with DMEM containing 1% BSA. Cells were serum starved overnight for 16 hours and then incubated with 500ng/ml Alexa-Fluor® 555-conjugated EGF (Invitrogen) for 2 minutes or 60 minutes at 37°C in the dark. Cells were then fixed and viewed under a confocal microscope.

2.2.2.3 Multinucleation counts

HeLa cells were seeded on 13 mm coverslips 24 hours prior to transfections. Cells were then transiently transfected with various constructs. Cells were fixed 24 hours post-transfection and immunostained with anti-ubiquitin followed by Alexa® Fluor 568-conjugated IgG secondary antibodies and DAPI. All transfected cells present on the coverslip were then scored for multinucleation and the results were represented graphically as percentages of multinucleate cells (Graphpad Prism; averaged over 3 experiments).

2.2.3 Salmonella infection studies

Wild type and ΔSopB *Salmonella dublin* strains have been described previously. A431 cells were seeded at ~ 100,000 cells/well into 35mm tissue culture wells (containing a glass cover slip if the cells were later to be used for immunofluorescence studies) and were maintained for 3 days at 37°C in a 10% CO_2 incubator. Cells were infected with log phase *Salmonella* cultures that had been grown overnight in LB medium (supplemented with 30 μg/ml kanamycin when required) and subcultured (1:25 dilution) for ~ 3 hours in fresh medium. Bacteria for inoculation were prepared by pelleting at 10,000 x g for 2 minutes and

resuspending/diluting in PBS. The A431 cells were infected with ~5x10^7 bacterial cells (multiplicity of infection of ~100:1) for 1 hour. Cells were washed with PBS prior to fixation and processing for immunofluorescence or further downstream processing.

2.2.4 EGFR degradation studies of *Salmonella* infected cells

A431 cells were infected with *Salmonella* as described above, with the following modifications. Cells were grown in 35mm tissue culture wells without a cover slip. 16 hours prior to infection, the A431 cells were washed twice with PBS and the medium was changed to a reduced serum medium lacking antibiotics (DMEM containing 1% bovine serum albumin 2mM L-glutamine). Following infection the media was removed, cells were washed twice in PBS and fresh DMEM, 1% BSA 2mM glutamine was added. Cells were immediately stimulated with 500 ng/ml EGF (Calbiochem) for different times (0, 8 and 16 minutes). Following EGF stimulation A431 cells were washed in ice cold PBS and then harvested in 100 μl RIPA buffer (50 mM Tris-HCl, pH 7.5, 150 mM NaCl, 0.5% Na-deoxycholate, 0.1% SDS, 0.1% NP40) containing protease inhibitor cocktail for mammalian cell extracts (Sigma). The protein concentrations of the cell lysates were determined using BCA reagent (Pierce). 40 μg of each sample was separated by SDS PAGE, transferred to nitrocellulose membranes and immunoblotted for the presence of the EGFR and β-tubulin. Signals were detected by ECL and quantified using an Optichem detector with associated software (Ultra Violet Products). For quantification, the amount of EGFR was normalised to the amount of β-tubulin (loading control) in the same sample.

2.2.5 Protein biochemistry techniques

Protein Assay:

The bicinchoninic acid (BCA) protein assay (Pierce) was used to determine protein concentrations. A standard curve of BSA was prepared with a range of 0-10μg total BSA protein from a stock of 2 mg/ml. The BCA working solution was prepared by adding Reagent A and Reagent B together in a ratio of 50:1. 200 μl of this was then added to each of the wells of a 96-well plate containing standard or appropriate samples. The plate was incubated at 37^{o}C for 30 min, and then read on a Spectra Rainbow Thermo microplate spectrophotometer (Tecan) at 565 nm. Results were analysed using Microsoft Excel to determine unknown protein concentration estimations.

Sodiumdodecyl Sulphate – Poly-Acrylamide Gel Electrophoresis (SDS-PAGE):

Electrophoresis was carried out using the Laemmli discontinuous buffer system [117]. Gels were of 1.5 mm thickness and prepared using acrylamide/bis-acrylamide (30% (w/v) acrylamide) and gel buffers already described. Polymerisation of the gels was instigated by the addition of 10% (w/v) ammonium persulphate (APS) and N,N,N,N'-tetramethylethylenediamine (TEMED). The composition of the resolving and stacking gels resulting in different gel percentages is given in Table 2.2. Unless otherwise stated, 50μg of protein samples were solubilised by the addition of sample buffer containing a reducing agent and incubated for 15-20 min at room temperature with occasional vortexing. Samples were loaded onto the gels with different broad range markers as described in Table 2.3. The gels were run at 30 mA per gel for about 45 min until the dye front had just run out of the gel.

Transfer of proteins to nitrocellulose membrane:

Following SDS-PAGE, gels were soaked along with fourteen pieces of filter paper and one nitrocellulose membrane cut to size, in transfer buffer

for ~ 5 min. Seven pieces of the filter paper were then placed on the anode of the electrophoretic apparatus with any air bubbles being removed. The nitrocellulose membrane was then placed on top of the first seven pieces of filter paper with the gel then carefully laid on top of this. Finally, the last seven pieces of filter paper were placed on top of this gel stack and smoothed out to remove any last air bubbles. The cathode was placed on top of this assembly and secured. Transfer of proteins was completed by running the electrophoretic apparatus at 1 mA per square cm of nitrocellulose membrane for 150 min. Typically each gel and nitrocellulose membrane was of dimensions 9 cm wide by 6 cm in length. Following the transfer, nitrocellulose membranes were briefly washed in ddH_2O to remove any transfer buffer or gel remnants, and incubated briefly with Ponceau S stain for confirmation of protein and lane identification.

Stock Solutions	Resolving Gel		Stacking Gel
	6%	12%	
Resolving gel buffer (ml)	2.5	2.5	-
Stacking gel buffer (ml)	-	-	1.25
Acrylamide stock (ml)	1.5	3.0	0.85
Double-distilled water (ml)	3.5	2.0	1.875
Ammonium persulphate (μl)	50	50	20
TEMED (μl)	4	40	5

Table 2.2 – Volumes of stock solutions used for making SDS-PAGE gels. 6% gels were used for separation of higher molecular weight proteins. 12% gels were used for lower molecular weights. Volumes given are for one mini-gel.

Western blotting:

Following transfer of proteins separated by SDS-PAGE onto nitrocellulose membranes, Western blotting techniques were performed. Briefly, membranes were washed in TBST to remove all Ponceau S stain and then blocked using 5% (w/v) Marvel® dissolved in TBST, for at least 30 min. Membranes were then washed twice in TBST to remove any

blocking agent and incubated with the primary antibody for ~ 2 hr at room temperature. Membranes were then washed for a minimum of 5 washes in TBST, each wash lasting a minimum of 5 min. Secondary HRP-conjugated (unless stated) antibodies were incubated with membranes for ~ 1 hr at room temperature. Final washes were carried out similar to washes after primary antibody incubations. Membranes were then incubated for 1 min with equal volumes of Solution A and B of the ECL Reagent or 5 min when using ECL Advanced Reagent (Amersham). Membranes were then developed and images taken using an EPI Chemi II darkroom (UVP) with a Hamamatsu camera attached. Labworks version 4 (UVP) was used for analysis and quantification of bands performed with the Western blots.

Prestained Protein Marker, Broad Range		**Multicoloured Standard**	
Protein	**Mol Weight (kDa)**	**Protein**	**Mol Weight (kDa)**
MBP-b-galactosidase	**175**	Myosin	**250**
MBP-paramyosin	**83**	Phosphorylase B	**148**
Glutamic dehydrogenase	**62**	Glutamic dehydrogenase	**60**
Aldolase	**47.5**	Carbonic anhydrase	**42**
Triosephosphate isomerase	**32.5**	Myoglobin blue	**30**
b-Lactoglobulin A	**25**	Myoglobin red	**22**
Lysozyme	**16.5**	Lysozyme	**17**
Aprotinin	**6.5**	Aprotinin	**6**
		Insulin	**4**

Table 2.3 – Molecular weight markers run on SDS-PAGE gels. The prestained protein broad range markers (New England Biolabs) were primarily used for SDS-PAGE and identification of proteins from Western blotting. The multicoloured markers (Invitrogen) were used when identification of proteins larger than 200kDa was necessary.

2.2.6 Molecular biology techniques

Standard protocols for recombinant DNA manipulations were used. Table 2.4 shows the main specific constructs and plasmids the relevant construct was cloned into. The GFP expression plasmid used to

transform *S. dublin* strains for use in immunofluorescence microscopy was pSU2007.

2.2.6.1 DNA constructs cloned

When cloning desired constructs, the polymerase chain reaction (PCR) was used in conjunction with specifically designed primers for the template DNA. Table 2.5 shows a typical cycle for PCR that was used when cloning constructs throughout the experimental side of this thesis. Note the annealing temperature generally varies based upon the lowest T_m of the primers used, as indicated.

DNA Construct	Plasmid	Manipulations/Notes	Tag on protein
Vps4	pEGFPC1	*Previously constructed, rat*	GFP
	pHM6		HA
	pHT2	**Cloned, see below**	Halo
	pTRE2pur	**Cloned, see below**	Halo
$Vps4^{E235Q}$	pEGFPC1	*Previously constructed, rat*	GFP
	pHM6		HA
	pHT2	**Cloned, see below**	Halo
	pTRE2pur	**Cloned, see below**	Halo
CHMP3	pEGFPC1	*Previously constructed, rat*	GFP
	pFLAG-CMV5c		FLAG
$CHMP3^{1-179}$	pEGFPC1	**Cloned, see below**	GFP
	pFLAG-CMV5c	**Cloned, see below**	FLAG
$CHMP3^{1-150}$	pEGFPC1	**Cloned, see below**	GFP
	pFLAG-CMV5c	**Cloned, see below**	FLAG
$CHMP3^{1-112}$	pEGFPC1	*Previously constructed, rat*	GFP
$CHMP3^{1-179}$M1	pEGFPC1	**Quickchange mutagenesis (Clontech) kit used on $CHMP3^{1-179}$**	GFP
$CHMP3^{1-179}$M2	pEGFPC1	**Quickchange mutagenesis (Clontech) kit used on $CHMP3^{1-179}$**	GFP
PIKfyve	pcdna3-EGFP	**Gift**, Dr Pete Cullen	GFP
PIKfyve MUT	pcdna3-EGFP		GFP
FENS-FYVE	pEGFPC2-iFENS-FYVE-1	**Gift**, Dr Michael Clague	GFP
SopB	pRK5myc	*CMV promoter, previously constructed.*	myc
	pHM6	**Cloned, see below**	HA
$SopB^{C460S}$	pRK5myc	*CMV promoter, previously constructed.*	myc
	pHM6	**Cloned, see below**	HA

Table 2.4 – Mammalian DNA constructs used experimentally in this thesis. Several constructs used were already designed and made prior to the commencement of this work. In the case of DNA constructs that were made during this thesis, the details of these can be found in experimental methods below.

PCR Stage	Temperature	Time	Repeat
1 - Denaturation	95°C	1 min	
2 - Denaturation	94°C	1 min	
3 - Annealing	65°C *	30 sec	
4 - Elongation	72°C	2 min**	Go to step 2 (x 29)
Hold	4°C		

Table 2.5 – A typical PCR cycle used. *Annealing temperature varies depending on the lowest T_m of primers used. Typcially annealing temperature is 5°C lower than the smallest T_m of primers. **The time for elongation depended upon the length of the DNA that was being amplified – 1 min was used for every kb of DNA.

Additionally, the PCR reaction volume included the following components:

- 500 ng of the appropriate DNA template
- 10 x polymerase reaction buffer (usually 5 µl if PCR reaction volume is 50 µl)
- 0.2 mM dNTPs (New England Biolabs)
- 0.4 µM of each oligonucleotide primer
- 0.05 U Pfu polymerase enzyme (Stratagene)

This mixture was usually made up to a total volume of 50 µl by using ddH_2O. MWG Biotech's sequencing service was used to confirm correct DNA sequences of all constructs cloned. For lists of primers used in cloning, see Table 2.6.

SopB-HA and SopB^{C460S}-HA:

The SopB and SopB^{C460S} genes that had been originally cloned into the pRK5myc vector were used as templates to amplify the fragments for isolation. Primers were used that introduced an EcoRI and HindIII restriction sites to either end of the gene (see Table 2.6, *No. 1-2*). Following the PCR cycle, the products were run on a 1% (w/v) agarose gel and identified as 1.6 kb bands, which were subsequently cut out of the gel and purified. Following gel purification, 5 µl of each fragment were end-converted using an end-conversion kit (Novagen) according to the manufacturer's instructions. Fragments were then ligated into a pT7 vector (Novagen) by addition of 50ng of the pT7 vector and 1 µl of T4 DNA ligase, and incubated at 22°C for 15 min. 1.5 µl of the ligation

product was transformed into NovaBlue® supercompetent cells using standard transformation techniques.

DNA isolated from the transformations were digested using EcoR1 and HindIII (Promega), and positive colonies were identified from this digestion by agarose gel electrophoresis, and the correct fragment was gel extracted and purified. 2 µl (200ng) of this fragment was ligated to 2 µl (100ng) of a pHM6 vector already cut with EcoR1 and HindIII using T4 DNA ligase, at 22^{o}C for 1 hr. The resultant ligation was transformed into XL-1 blue cells and colonies were checked for a successful clone by digestion and electrophoresis by use of DNA ladders and comparison with uncut DNA.

Halo-Vps4^{WT} and Halo-Vps4^{E235Q}:

Primers for the Vps4^{WT} and Vps4^{E235Q} Halotag® cloning were designed against the rat sequences with NaeI and NotI sites incorporated (Table 2.6, *3-4*), and the pEGFPC1-Vps4^{WT} and –Vps4^{E235Q} constructs used as templates. Fragments were similarly manipulated as described above (SopB-HA and SopB^{C460S}-HA), being cloned into pT7 blue vectors prior to subcloning into the pHT2 vector. Positive colonies for Halo-Vps4^{E235Q} were identified, so to generate the Halo-Vps4^{WT} construct, site directed mutagenesis of Halo-Vps4^{E235Q} was carried out. Primers were designed according to the Stratagene Quickchange protocol to mutate Q235 of Halo-Vps4^{E235Q} to a glutamic acid (Table 2.6, *5-6*), via a single nucleotide change (c891g). By following the manufacturer's instructions (Stratagene) successful clones of Halo-Vps4^{E235Q} were mutated to give Halo-Vps4^{WT}.

pTRE2pur-Halo-Vps4^{WT} and –Vps4^{E235Q}:

The Halo-Vps4^{WT} and Halo-Vps4^{E235Q} constructs cloned previously were used to obtain a Halo-Vps4^{WT} and Halo-Vps4^{E235Q} fragments. This was achieved by cutting the 2 µg Halo-tagged constructs firstly with NotI enzyme overnight. The cut product was run on an agarose gel and gel purified (Promega kit) to obtain pure NotI cut pHT2-Halo-Vps4^{WT} and

pHT2-Halo-Vps4^{E235Q} DNA fragments. These were then cut as usual for 3 hours with the PvuII restriction enzyme to give the fragments Halo-Vps4^{WT} and Halo-Vps4^{E235Q} with NotI and PvuII cut ends. This was directly cloned by ligation into the pTRE2pur vector, which had also been cut with both NotI and PvuII enzymes. The ligation was checked by cutting with the enzyme NheI, a restriction site not present in the fragments but present in the vector. Transformations into NovaBlue® single competent cells were carried out, and successful clones checked by colony PCR. One successful clone for pTRE2pur-Halo-Vps4^{E235Q} was identified, and using the Stratagene Quickchange mutagenesis technique (primers already made, see Table 2.6, *5-6*) to convert Q at 235 back to E, successful clones of pTRE2pur-Halo-Vps4^{WT} were also obtained.

Truncated CHMP3 constructs and mutants:

Forward oligonucleotide primers for GFP-CHMP3 and FLAG-CHMP3 DNA sequences had been previously used in the lab (Table 2.6, *7, 9, 11, 13*), with a HindIII restriction site present for the FLAG-CHMP3 and a BglII restriction site for GFP-CHMP3. For generation of the truncated FLAG-CHMP3$^{1-150}$ and GFP-CHMP3$^{1-150}$, primers were appropriately designed containing Acc65i restriction sites (Table 2.6, *8* and *10* respectively) just prior to the amino acid at position 150 or 179 of FLAG-CHMP3 appropriately. This was similar for the cloning of FLAG-CHMP3$^{1-179}$ and GFP-CHMP3$^{1-179}$ (Table 2.6, *12* and *14* respectively). Constructs were amplified by PCR and manipulated as already described, cloning into the pT7 vector then followed by sub-cloning into the pFLAG-CMV5c or pEGFPC1 vector for FLAG- and GFP-tagged constructs respectively.

2.2.6.2 DNA Digestions

To check for successful clones from PCR products digestions of the cloned DNA were used, employing restriction enzymes that cleaved the DNA at points within the cloned product and/or outside of the cloned region (in the vector). This technique along with size estimations was

No.	Primer name	Sequence	Use/Notes
1	SopB-EcoR1	5′-ctc**gaattc**tcaagatgtgattaatgaagaaat-3′	FWD primer - SopB- + SopBC460S-HA
2	SopB-HindIII	5′-cac**aagctt**gatgcaaatacagagcttctatcact-3′	REV primer - SopB- + SopBC460S-HA
3	Vps4-NaeI	5'-gag**gccggc**atggcgtccacgaacaccaacctg-3'	FWD primer - Halo-Vps4 + -Vps4EQ
4	Vps4-NotI	5'-gag**gcggccgc**ttagccttcctggccaaaatcttc-3'	REV primer - Halo-Vps4 + -Vps4EQ
5	Vps4QE-FWD	5'-ccatcatcttcatcgatgagattgactctctgtgc-3'	FWD primer for SDM of Vps4EQ
6	Vps4QE-REV	5'-gcacagagagtcaatctcatcgatgaagatgatgg-3'	REV primer for SDM of Vps4EQ
7	CHMP3$^{1-150}$FLAG-HindIII*	5'-gag**aagctt**atggggctgtttggaaaaacccaag-3'	FWD primer - for CHMP3$^{1-150}$ FLAG
8	CHMP3$^{1-150}$FLAG-Acc	5'-ctc**ggtacc**tgctttcaaacgtatcctcta-3'	REV primer - for CHMP3$^{1-150}$ FLAG
9	CHMP3$^{1-150}$GFP-Bgl*	5'-gag**agatct**atggggctgtttggaaaaacc-3'	FWD primer - for CHMP3$^{1-150}$ GFP
10	CHMP3$^{1-150}$GFP-Acc	5'-ctc**ggtacc**atgctttcaaacgtatcctcta-3'	REV primer - for CHMP3$^{1-150}$ GFP
11	CHMP3$^{1-179}$FLAG-HindIII*	*Same as CHMP3$^{1-150}$FLAG-HindIII*	FWD primer - for CHMP3$^{1-179}$ FLAG
12	CHMP3$^{1-179}$FLAG-Acc	5'-ctc**ggtacc**ctttgcccaaggctcctgctg-3'	REV primer - for CHMP3$^{1-179}$ FLAG
13	CHMP3$^{1-179}$GFP-Bgl*	*Same as CHMP3$^{1-150}$GFP-Bgl*	FWD primer - for CHMP3$^{1-179}$ GFP
14	CHMP3$^{1-179}$GFP-Acc	5'-ctc**ggtacc**gctttgcccaaggctcctgctg-3'	REV primer - for CHMP3$^{1-179}$ GFP

Table 2.6 – Primers used for cloning of various constructs. The primers discussed in the methods above are described here and their sequences given. Bold and underlined text indicates restriction sites being introduced into the cloned fragment. SDM represents site directed mutagenesis; FWD is forward; REV is reverse. *These primers were already present in the lab from previous cloning experiments.

useful in identifying positive PCR clones and also necessary for creating linear vector DNA with appropriate restriction enzymes.

For checking of PCR products cloned, 1 U of the appropriate enzymes were incubated with a small volume (10 µl) of the PCR product for 1 hr at 37^{o}C and then analysed by agarose gel electrophoresis. In the case of linearization of vector DNA, more complete digestions were necessary and so 5 U of each restriction enzyme was incubated with the DNA product for 3 hours at 37^{o}C.

2.2.6.3 DNA analysis by agarose gel electrophoresis

PCR products and digested DNA were loaded onto a 1% (w/v) agarose Tris-acetate EDTA (TAE) gel and run in the presence of ethidium bromide for DNA visualisation under UV light at 120 V for 20-40 min depending on size of DNA. Images were examined using an EPI Chemi II darkroom (UVP) with a Hamamatsu camera attached. For the case of DNA isolation from gels, a gel extraction kit (Promega) was followed according to the manufacturer's instructions.

2.2.6.4 Transformations and DNA isolation

For expression and multiplication of DNA constructs, the plasmids were transformed into competent *E. coli* cells. A small amount (1 µl) of the cloned DNA construct was added to 50 µl of competent XL-1 blue cells (unless otherwise stated) on ice and incubated for 5 min. Cells were then heat shocked by incubating at 42^{o}C for 30 seconds exactly, and then placed back on ice for a further 2 min. 250 µl of LB media was added to the heat shocked DNA-cell mixture and this was incubated at 37^{o}C for 1 hr. 50 µl of this mixture was then plated on LB plates that contained the appropriate antibiotic selection that the parental plasmid had resistance to, to ensure selectability, and plates were grown overnight at 37^{o}C.

To obtain a highly concentrated volume of desired DNA, individual colonies were picked and grown in 10 ml cultures (containing relevant antibiotics) overnight, shaking at 37^{o}C. Cultures were pelleted by spinning at 1500 x g for 10 min, and DNA was extracted using mini-prep kits (Promega) or Midi-prep kits (Qiagen) according to the manufacturer's instructions.

2.2.7 Antibody generation

2.2.7.1 Peptide synthesis

A DNA construct was previously cloned into a pET15b vector, of a 118 amino acid hydrophilic rich region of the human PIKfyve protein (including a His_6 tag at the N-terminus of the peptide) aligning from E1083 to D1200 of the sequence, termed His_6-PIK. This peptide was used as the antigen for raising antibodies against in a sheep.

The pET-PIK DNA construct was transformed into E. coli Rosetta® competent cells as previously described. Colonies were picked from ampicilin containing agar plates and grown overnight in 100 ml cultures of LB-Amp. The following morning a 1 in 100 dilution of the culture was made into 1 L flasks of LB-Amp and the new cultures were grown until the optical density (OD) at 600 nm reached 0.6. Cells were induced with 100 mM of IPTG for 3 hr shaking at 37^{o}C. Cells were then pelleted by spinning at 2000 x g for 10 min, and pellets were resuspended in HEPES lysis buffer and sonicated on ice. Large debris was removed by a second pelleting spin and the resulting supernatant was rotated at 4^{o}C with 1 ml of talon resin for 3 hr. The resin was then gently spun down (600 x g) and washed several times with cold HEPES buffer. Resin was resuspended in 10 ml of the lysis buffer, spun down again and then resuspended in a minimal volume of lysis buffer. The purified His_6-PIK protein was then eluted in lysis buffer with 200mM imidazole (pH 8.0) added. Five elutions of 0.5 ml volume were collected and dialysed

against 5 L of PBS overnight to remove all lysis buffer, using a 3,000 kDa cut-off dia-lyser cassette (Pierce). Dialysed His_6-PIK samples were made to 20% (v/v) glycerol and stored at -20^oC until further use. Samples were checked for purity by running on SDS-PAGE gel.

2.2.7.2 ELISA plate assay

ELISA plate coating buffer was made to a 50% (v/v) glycerol stock. 2 ml of this solution was added to 2 mg of the His_6-PIK polypeptide. 100 μl of this was further diluted in 10 ml coating buffer to give a concentration of 10 μg/ml. C8 Maxisorp plates (Nunc) were coated with 100 μl per well of the 10 μg/ml His_6-PIK solution, covered and incubated overnight at 4 ^oC. The following day wells were washed three times with PBST (PBS with 0.1% v/v Tween-20) with rigorous expulsion of liquid out of the wells. The wells were filled with 200 μl ELISA plate blocking buffer and incubated, for 1 hr at room temperature, shaking. The plate was then washed twice with PBST. A 1:100 dilution of pre-immune and first bleed of the antibody was made in PBST. 200 μl of this was placed in the first well. 100 μl was withdrawn and placed into the second well containing 100 μl PBST. This serial dilution was performed 12 times across the plate. The plate was then covered and incubated with gentle shaking for 2 hr at room temperature. Wells were washed three times with PBST and then 100 μl of 1:4000 diluted (PBST) anti-sheep IgG HRP was added to each well and the plate was incubated shaking, for a further 2 hr at room temperature. The plates were then washed three times with PBST and twice with PBS. ELISA sodium acetate/citrate buffer was diluted 1:20 in ddH_2O and 49.5 ml of the solution was added to 0.5 ml Tetramethyl Benzidine (TMB; 10 mg/ml in DMSO) and 10 μl 30% (v/v) H_2O_2. 100 μl of this was added to each of the wells and incubated at room temperature until a blue colour had developed over the range of dilutions. The reaction was stopped by the addition of 50 μl 1.84 M H_2SO_4 per well. The plates were then read in a Spectra Rainbow Thermo microplate spectrophotometer (Tecan) with filter 1 measuring

OD at 450 nm and filter 2 measuring OD at 700 nm (to eliminate background readings).

2.2.7.3 Generation of an affinity column

For coupling of the His_6-PIK antigen to a column, a 1 ml Hi-Trap™ NHS-activated HP column (Amersham) was used according to the manufacturer's instructions. Firstly, a drop of ice-cold 1 mM HCl was added to the column to avoid air bubbles and the column was further washed out three times with 2 ml of ice-cold 1 mM HCl without exceeding a flow rate of 1 ml/min. 1 ml of the antigen (His_6-PIK) was immediately injected onto the column and allowed to stand at room temperature for 30 min. The column was then washed three times with 2 ml Buffer A (0.5 M ethanolamine, 0.5 M NaCl, pH 8.3), three times with 2 ml Buffer B (0.1 M acetate, 0.5 M NaCl, pH 4) and a further three times with Buffer A, then left at room temperature for 30 min. Column was then washed three times with 2 ml Buffer B, three times with 2 ml Buffer A and finally 3 times of 2 ml with Buffer B again. 2 ml of PBS with 0.2% (w/v) sodium azide was then injected into the column and the column was stored at 4^{o}C until needed.

2.2.7.4 Purifying antibodies from serum using FPLC

For purification of the antibody from the serum of the sheep bleeds, the column coupled with the His_6-PIK antigen was attached to an FPLC™ system (Amersham). The column was flushed with 5 ml cold PBS and then 1.5 ml of the serum was mixed with 1.5 ml of PBS and 0.5 ml injected into the column every 30 min. Between each injection the column was closed and incubated standing at room temperature. After full injection of the antibody containing serum into the column, it was

attached to the FPLC™ system and washed with PBS until the absorbance reading at 280 nm levelled off at zero.

The antibody was then eluted into 0.5 ml fractions with 100 mM glycine (pH 2.5) at a flow rate of 0.02 ml/min. Fractions (0.5 ml) were collected in eppendorf tubes that contained 0.2 ml 1M Tris-HCl (pH 8.0) to neutralise, with the absorption at 280 nm monitored and graphed to identify the fractions that contained eluted antibody. Fractions within the range of the peak were pooled and dialysed against 5 L of PBS, overnight at 4^{o}C. The concentration of the purified antibody was then estimated using the extinction coefficient for IgG where at 280 nm, an absorption of 1.0 relates to 0.75 mg/ml IgG. Glycerol was added to the purified antibody to a final concentration of 40% (v/v), and aliquots of 100 µl were made for storage at –20^{o}C until further use.

The purification process was carried out for the first bleed fraction from the immunised sheep and also for the third bleed. When bleeds were received they were dispensed into 20 ml aliquots and stored at –20^{o}C.

2.2.8 Detergent-free cell lysis and immunoprecipitations (IP)

Detergent-free lysis:

Cells transfected with GFP-Vps4^{E235Q} or GFP-Vps4^{WT} were removed from flasks ~ 16 hours post-transfection by incubation with trypsin for 5 min. Complete growth medium was added to neutralise the trypsin and cells were spun at 1000 x g for 3 min to pellet cells. Pellets were washed

once with ice-cold PBS then incubated with 2 ml of TESA buffer (detergent free) containing a mammalian protease inhibitor cocktail (Sigma), and gently pipetted up and down several times. Pellet suspended in TESA buffer were then passed through a 23G needle 10 times followed by passing through a 27G needle a further 10 times. Cells were allowed to sit on ice for a further 15 min to aid in lysis. Cells were then passed through a ball-bearing syringe homogenizer at least 7 x at a clearance of 12 μm to shear cells, then a further 7 passes through a clearance of 4 μm to ensure a full lysis of cells as possible. Lysed cells were then spun at 14,000 x g for 30 min to remove any large and nuclear debris.

GFP IP:

50μl of Protein G beads were washed twice with ice-cold PBS by spinning for 1 min at 6000 x g. Following washes, 4μg of the mouse α-GFP_{IgG2a} antibody was added to beads and allowed to mix at 4°C rotating for 3 hours. Beads were then spun down and the supernatant (any unbound antibody) was removed. Beads were further washed a minimum of three times using ice-cold TESA buffer. Cell lysis homogenate was then added to the beads and allowed to mix overnight at 4°C. The following morning, beads were spun down and the supernatant stored at –20°C to be later run on SDS-PAGE. Beads were washed twice with cold TESA buffer and a further three times with cold PBS by spinning. After the last spin the supernatant was carefully aspirated off and the remaining beads were incubated with 1x sample buffer and boiled for 5 min, with lengthy vortexing before and after boiling. Beads were then run on three lanes of a SDS-PAGE gel along with samples of the cell lysate and the supernatant of the IP (that is, unbound fraction of lysate). Western blotting techniques were used to blot for GFP (using rabbit antibody) and other proteins of interest.

HaloTag® precipitations:

HaloLink® methods of isolating HaloTag® proteins were followed similarly to the manufacturer's instructions being optimised for specific experimental demands. Cells transfected with proteins expressing the HaloTag® (Halo-Vps4^{WT} or Halo-Vps4^{E235Q}) were processed for cell lysis as described above. Following cell lysis, 50 µl of the HaloLink® resin (which allows covalent binding of the HaloTag® to the HaloLink® resin) was washed three times with ice-cold TESA buffer to remove any ethanol and equilibrate the resin with the TESA buffer. 500-750 µl of the prepared cell lysates was then added to the beads, and rotated at 4^{o}C overnight. The following morning the resin was spun down (800 x g for 1 min) and the supernatant (unbound cell lysate) was removed and stored at –20^{o}C until needed for SDS-PAGE. The resin was washed three times using TBS buffer with 10 mg/ml BSA and a further five times using TBS buffer with no BSA, to remove the BSA thus allowing for a cleaner Western blot. After the last wash the resin was spun down for 2 min and 100 µl of sample buffer was added. Samples were vortexed and boiled for 5 min and allowed to sit at room temperature for 15-20 min before loading onto an SDS gel along with a sample of the total cell lysate and the unbound cell lysate fraction. Gels were transferred to nitrocellulose and Western blotting techniques were used to identify various proteins of interest.

Dextran-red uptake assay:

Cells transfected with Halo-Vps4^{WT}, Halo-Vps4^{E235Q} or untransfected were incubated with Texas-Red Dextran (Invitrogen; 1:10,000 dilution) and incubated at 37^{o}C, 5% CO_2 overnight. Cells were then lysed in detergent-free lysis buffer as already described, and incubated with the HaloLink® resin as above. Following final washes of lysate-resin complexes, resins were incubated with 1% (v/v) TritonX-100 for 30 min at room temperature. Fractions were then read on a Fluoro-scan plate reader with excitation of 545 nm and emission read at 612 nm. Values were normalised per mg of protein (using BCA protein assay to

determine protein concentrations) and the relative fluorescent units (RFU) of TritonX-100 measured alone was subtracted as background. RFU values of transfected cell lysates were normalised to untransfected cells treated with Dextran with this RFU value being taken as zero.

2.2.9 Production of stable cells expressing Halo-Vps4^{WT} or Halo-Vps4^{E235Q}

For producing stable cell lines the Tet-Off™ system (Clontech) was used. Briefly, the Tet-Off/On™ systems allows for the expression of a stably expressed construct to be turned on or off via the addition or removal of the antibiotic tetracycline. In the case of Tet-Off™ cell lines, the addition of tetracycline (or doxycycline) results in the expression of the stable construct to be silenced and turned off. Removal of tetracycline/doxycycline allows for the expression of the gene of interest to resume. Doxycycline may also be used as the repression agent for Tet-Off™ systems and is often favoured due to much lower concentrations needed as well as its superior half-life compared to tetracycline. For these experiments, doxycycline was the preferred choice of inducibility agent.

For the Tet-Off™ system to properly function, the gene of interest needs to be cloned into a vector containing the tetracycline repressor element, a pTRE vector. Furthermore, to allow the selectability of stably expressing cells, a second antibiotic marker may be used that is additionally added to certain pTRE vectors for this selection purpose. In this case, a pTRE2pur vector was used, which allows for selection of stably-expressing cells to be isolated via puramycin resistance. Finally, cells already possessing the Tet-Off™ system have a third selectable antibiotic marker of G418, which ensures that the cells that proliferate in the culture are Tet-Off™ cells. The cells used for production of stable cells expressing Halo-Vps4^{WT} or Halo-Vps4^{E235Q} were HeLa Tet-Off™

cells, which were a kind gift from Prof George Banting. For more details on the cloning of Halo-Vps4^{WT} and -Vps4^{E235Q} constructs into the pTRE2pur vectors please refer to section 2.2.6.1.

HeLa Tet-Off™ cells were revived from liquid nitrogen stores and grown in flasks for the first few days under standard conditions (complete DMEM growth medium, 37^{o}C, 5% CO_2). After the first passage of cells, 400 µg/ml G418 was added to the medium to ensure all cells that grew were HeLa Tet-Off™ cells. G418 was always present in the media used for these cells from this point on, at a concentration of 200-400 µg/ml. After the second passage, cells were seeded onto 10 cm plates and grown to ~80% confluency, when they were then transfected with pTRE2pur-Halo-Vps4^{WT} or pTRE2pur-Halo-Vps4^{E235Q} using Lipofectamine 2000™ or FuGene 6™ transfection reagents, according to manufacturer's instructions. Following transfections, puromycin and doxycycline were both added to the media at concentrations of 1 µg/ml. The media was ensured to be changed every 2 days with fresh antibiotics. Transiently transfected cells seeded on 13 mm coverslips were also transfected similarly with wells containing doxycycline and those without doxycycline, and viewed under a fluorescence microscope to demonstrate and ensure doxycycline inducibility.

After at least 10-14 days of transfected cells having been incubated in the presence of puramycin and doxycycline, small individual colonies of clonal cells were isolated and removed from the 10 cm dish to a 96-well tissue culture plate. Each colony of cells were allowed to grow to confluency in a 96-well and then were passaged into a maintenance 35 mm dish as well as coverslips for both +dox and –dox conditions for detection of inducible expression. Cells were incubated on coverslips in the presence of doxycycline or without for 24 hr and then incubated with Halo-ligands and fixed as previously described, being then examined under a fluorescence microscope to confirm expression, doxycycline inducibility and appropriate phenotypes. Cell colonies that lacked any visible expression of the Halo-tagged constructs were discarded. Some

colonies were also assayed for expression of Halo-Vps4^{WT} or -Vps4^{E235Q} constructs via Western blotting techniques to determine if over-expression of the constructs was occurring in an inducible manner.

CHAPTER 3

3 The effects of the *Salmonella* phosphoinositide phosphatase SopB on ESCRT and MVB function*

3.1 Introduction

Salmonella enterica serovars are facultative intracellular bacteria that can target a variety of eukaryotic hosts and are the causative agents of diseases such as food-borne gastroenteritis in humans [reviewed in 118]. These bacteria have developed complicated strategies to regulate host cell responses, which allow them to be internalised, survive and replicate in membrane bound compartments, known as *Salmonella*-containing vacuoles (SCVs) [reviewed in 119]. Upon bacterial invasion of the host, SCVs undergo a remodelling, resembling that of the host cell's endocytic pathway, but their progression down the endocytic pathway is arrested prior to fusion with degradative lysosomes thus aiding bacterial survival [120].

The formation and remodelling of SCVs is dependent upon the secretion, during and immediately after internalisation, of bacterial effector proteins into the host cell cytoplasm. This secretion occurs via a Type III secretion system (TTSS) encoded within pathogenicity island 1 (SPI-1) of the *Salmonella* genome [119, 121]. Among these SPI-1 effectors is SopE, which is a RhoGEF that initiates actin rearrangement in the host cell, leading to plasma membrane ruffling and nascent SCV formation [122, 123]. Another protein secreted by the SPI-I TTSS is SopB (also referred to as SigD), which is a phosphoinositide phosphatase [124-127].

SopB has been shown to possess 5'-phosphatase activity specifically towards PtdIns(3,5)P_2 [128]. Recent evidence suggests that SopB may contribute to the arrest of progression of the SCV down the endosomal trafficking pathway leading to fusion with lysosomes through this phosphatase mechanism [128]. This activity is responsible for the

conversion of PtdIns(3,5)P_2 to PtdIns(3)P by removal of phosphate from the 5' position of the inositol lipid head-group. SopB has additional phosphoinositide and inositol phosphate substrates *in vitro*, and *in vivo* has been implicated in a variety of other host cell manipulations such as Akt activation and modulation of chloride secretory responses [125, 129, 130]. As SopB acts on various phosphoinositide substrates *in vitro*, its localisation within the cell would most likely determine its natural physiological substrate, and indeed different phosphoinositides are considered to be quite specific in their spatial distribution on membranes in mammalian cells. Furthermore, the localisation of phosphoinositides is considered to be temporal given the fact that their generation can often occur due to activation or expression of enzymes that produce specific phosphoinositides from one form to another.

Some studies have already been carried out that suggest the generation of PtdIns(3,5)P_2 may play some role in endosomal trafficking [61, 71, 131]. The aim of this work was then to investigate the localisation and action of SopB, and consequently whether it may be a useful tool to manipulate levels of PtdIns(3,5)P_2 in cells. In doing so, the role of this lipid in endosomal trafficking may be further investigated.

*The work described in this chapter was submitted to the Biochemistry Journal and accepted for publication on 6 January, 2006:

Dukes JD, Lee H, Hagen R, Reaves BJ, Layton AN, Galyov EE, Whitley P. *The secreted Salmonella dublin phosphoinositide phosphatase, SopB, localizes to PtdIns(3)P-containing endosomes and perturbs normal endosome to lysosome trafficking.* Biochem J, 2006. Apr 15;**395**(2):239-47

3.2 Results

3.2.1 SopB localises to early endosomal membranes that contain PtdIns(3)P

Although SopB expressed heterologously in mammalian cells has previously been shown to be present on *Salmonella* containing vacuoles (SCVs) and cell membranes in *Salmonella* infected cells [132], a more detailed characterisation of the subcellular localisation of SopB had not yet been performed. By staining with antibodies against SopB, Marcus *et al* were able to demonstrate that the expression of SopB in *Salmonella* infected cells led to localisation of SopB to the membranes of SCVs. Subcellular fractionation also revealed that SopB was absent from the cytoplasm but present in the host-cell membrane fraction [132].

To further investigate the subcellular location of SopB, we transiently transfected COS-7 cells with pRK5myc SopB or pRK5myc SopB^{C460S} (see 2.2.6.1). These plasmids encode a myc-tagged SopB wild type protein (SopB-wt) and a phosphatase dead myc-tagged SopB protein (SopB^{C460S}) respectively. SopB^{C460S} is a mutant form of SopB, which lacks phosphatase activity. Given that the localisation of SopB has been reported to be independent of its phosphatase activity [132], it was reasoned that this mutant form although lacking phosphatase activity would still localise to the same sub-cellular compartment as the active SopB protein.

Expression of SopB-wt from pRK5myc SopB was highly toxic to the cells and appeared to result in rounded up cells that were dying (Fig. 3.1*b*). The transfection efficiency for SopB-wt was extremely low (>0.01%) and we suspect that this was due to most transfected cells rounding up and detaching from the coverslips prior to fixation, although this was not directly shown. In transfected cells not observed to be rounded up,

SopB-wt was observed to be associated with the membranes of dramatically swollen organelles presumably at a stage prior to the cells rounding up and detaching from the coverslips (Fig. 3.1*a*). The phosphatase dead mutant, SopB^{C460S} was not found to be so toxic to the cells, and showed a punctate localisation throughout the cytoplasm of COS-7 cells (Fig. 3.1*c*). This staining observed resembled such a staining seen of early endosomes, such as with EEA1 (Fig. 3.1*d*). It had no apparent dramatic effect on the morphology of the membranes it was apparently associated with, unlike SopB-wt. Due to the toxicity and low transfection efficiency of SopB-wt, the remainder of the localisation studies were performed with the SopB^{C460S} phosphatase dead protein.

To determine whether the observed SopB^{C460S} containing punctae were associated with specific cellular organelles, double immunostaining with markers for different organelles was performed (Fig. 3.2). These studies revealed that SopB^{C460S} localised primarily to early endosomes, as there was a high degree of co-localisation with early endosomal autoantigen-1 (EEA1; Fig. 3.2*a*-*c*). There was no evidence that SopB associated with other internal membranes such as late endosomes or the trans-Golgi network (TGN) as there was only very limited co-localisation of SopB^{C460S} with CI-M6PR or TGN46 respectively (Fig. 3.2*d*-*i*). The co-localisation with EEA1, which is directed to early endosomes via an interaction with Rab5 and PtdIns(3)P, gives an indication that SopB is targeted primarily to membranes containing PtdIns(3)P.

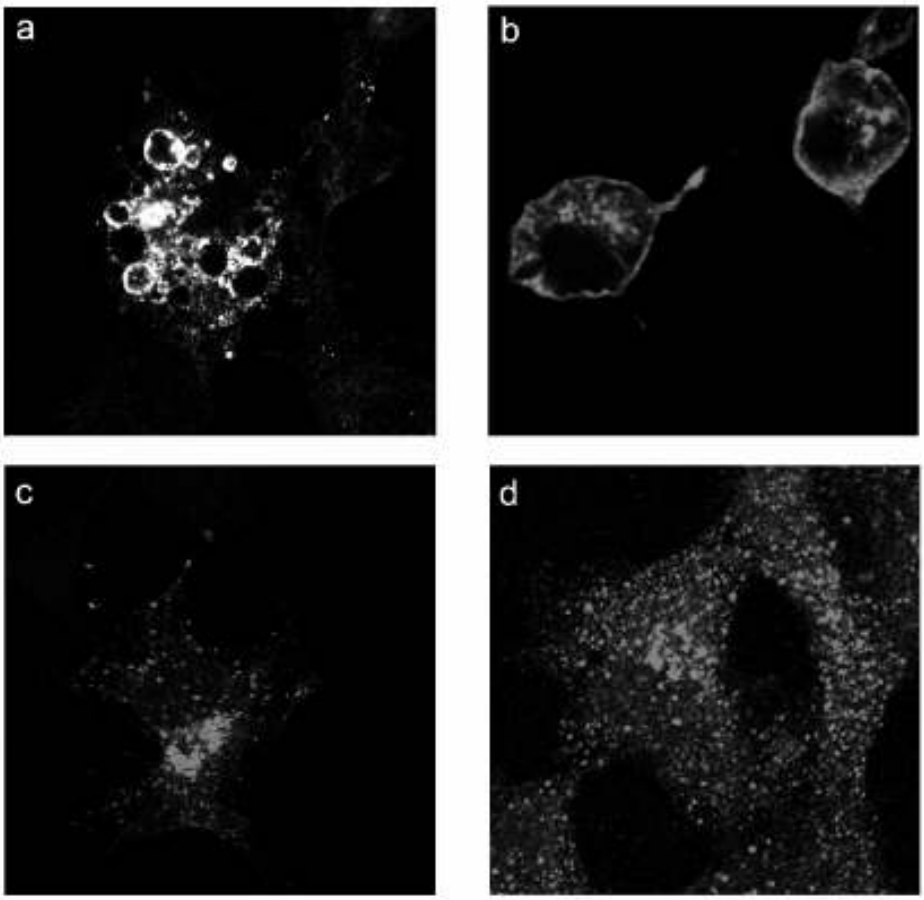

Figure 3.1 – Transient expression of SopB-wt and SopB^{C460S} in Cos-7 cells. COS-7 cells were transfected with (*a* and *b*) pRK5myc SopB or (*c*) pRK5myc SopB^{C460S}. Cells were fixed after 16 hours and immunostained with anti-myc antibodies, followed by Alexa® Fluor 568-conjugated anti-mouse IgG secondary antibodies. Untransfected cells (*d*) were immunostained with anti-EEA1 antibodies followed by Alexa® Fluor 568-conjugated anti-rabbit IgG secondary antibodies.

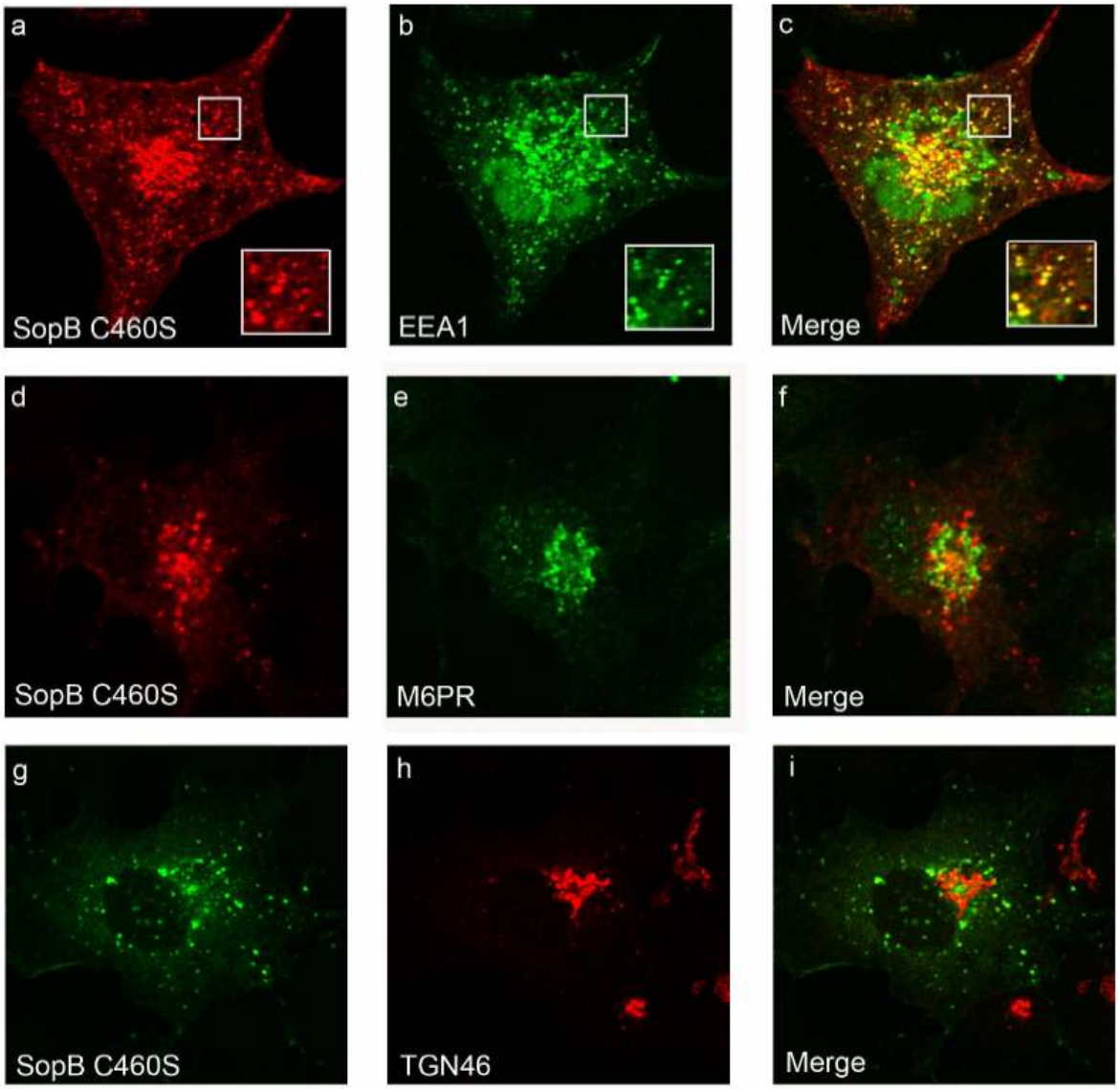

Figure 3.2 – SopB^{C460S} localises to early endosomes. Cos-7 cells were transfected (*a-i*) with pRK5mycSopB^{C460S}. Cells were fixed after 16 hours and immunostained with anti-myc antibodies, followed by (*a-f*) Alexa® Fluor 568-conjugated anti-mouse IgG secondary antibodies or (*g-i*) Alexa® Fluor 488-conjugated anti-mouse IgG secondary antibodies. Cells were co-immunostained with (*a-c*) anti-EEA1, (*d-f*) anti-CI-M6PR or (*g-i*) anti-TGN46 antibodies followed by (*a-f*) Alexa® Fluor 488 conjugated anti-rabbit IgG or (*g-i*) Alexa® Fluor 568 conjugated anti-sheep IgG antibodies. Fluorescence corresponding to (myc) SopB C460S is shown in *a, d* (red) and *g* (green). Fluorescence corresponding to EEA1, CI-M6PR and TGN46 is shown in *b, e* (green) and *h* (red) respectively. Images of merged fluorescence are shown in *c, f* and *i* (yellow fluorescence indicates co-localisation). Insets (*a-c*) are magnifications of boxed areas.

3.2.2 Membrane association of SopB is independent of any interaction with PtdIns(3)P

To address more directly whether SopB localises primarily to PtdIns(3)P containing cellular compartments we co-expressed SopB^{C460S} together with GFP-iFYVE-FENS-1 which is a probe for PtdIns(3)P (Fig. 3.3). As has been shown previously [133], exogenous expression of GFP-iFYVE-FENS-1 causes swelling and vacuolation of early endosomal compartments. SopB^{C460S} showed substantial co-localisation with GFP-iFYVE-FENS-1 on these swollen early endosomes, clearly demonstrating that SopB localises to PtdIns(3)P containing membranes (Fig. 3.3*a*-*c*). To test whether SopB localises to PtdIns(3)P containing endosomes via a direct interaction with PtdIns(3)P, SopB^{C460S} transfected Cos-7 cells were treated with the PI3-kinase inhibitor, wortmannin. This treatment did not result in dissociation of SopB^{C460S} from membranes whereas GFP-iFYVE FENS-1 expressed in the same cells did not remain membrane associated, indicating that PtdIns(3)P levels had been depleted as a result of wortmannin treatment (Fig. 3.3*d*-*f*).

These results provide further evidence that the physiological substrate of SopB-wt may in fact be PtdIns(3,5)P_2 as SopB^{C460S} localises to a compartment where PtdIns(3)P is found. The mammalian kinase that converts PtdIns(3)P to PtdIns(3,5)P_2 is PIKfyve, thus these results indicate that SopB is in a location to antagonise the effects of PIKfyve's conversion of PtdIns(3)P to PtdIns(3,5)P_2. It should further be noted that some reports have indicated a plasma membrane localisation of SopB [134]. However in most of the SopB^{C460S} transfected cells observed, no staining was detected at the plasma membrane. However at higher expression levels of the SopB-wt protein, there may have been some localisation to the plasma membrane in rounded up cells (Fig. 3.1*b*), although these cells appeared to be expressing large amounts of the SopB-wt protein. This indicates that although SopB may possess a

broad range of phosphorylated substrates *in vitro*, including PtdIns(4,5)P_2 which is found at the plasma membrane, its sub-cellular localisation to PtdIns(3)P containing compartments suggest its primary physiological substrate is more likely to be an endosomal phosphoinositide such as PtdIns(3,5)P_2 rather than a plasma membrane phosphoinositide similar to PtdIns(4,5)P_2.

3.2.3 SopB localises to ESCRT-containing compartments

It has previously been shown that an ESCRT-III component, CHMP3, binds to PtdIns(3,5)P_2 *in vitro* and therefore may act as an effector of this phosphoinositide [71]. Thus the action of SopB (by preventing accumulation of PtdIns(3,5)P_2 on ESCRT containing membranes) may manifest itself by compromising ESCRT function or localisation. However there is a lack of *in vivo* evidence to support this hypothesis. As a result of this, SopB^{C460S} was co-expressed together with the dominant negative ESCRT components CHMP3$^{1-112}$-GFP or GFP-Vps4^{E235Q} (Fig. 3.4). CHMP3$^{1-112}$-GFP associates with intracellular membranes of endocytic origin and induces their vacuolation [71].

Vps4 is not strictly a component of ESCRT-I, II or III but catalyses the disassembly and release of ESCRT components from membranes. The dominant negative GFP-Vps4^{E235Q} is ATPase defective, associates with intracellular membranes and is not able to catalyse ESCRT disassembly, also resulting in vacuolation [135]. Co-localisation of SopB^{C460S} with CHMP3$^{1-112}$-GFP (Fig. 3.4*a*- *c*) and GFP-Vps4^{E235Q} (Fig. 3.4*d*-*f*) was observed. This co-localisation is entirely consistent with the action of SopB having an effect on ESCRT function. Thus the co-localisation of the SopB phosphatase that is proposed to manipulate PtdIns(3,5)P_2 levels with ESCRT proteins (CHMP3) put these ESCRT proteins in a location where they could potentially be PtdIns(3,5)P_2 effectors. Despite these findings, there is still a lack of evidence to support any direct

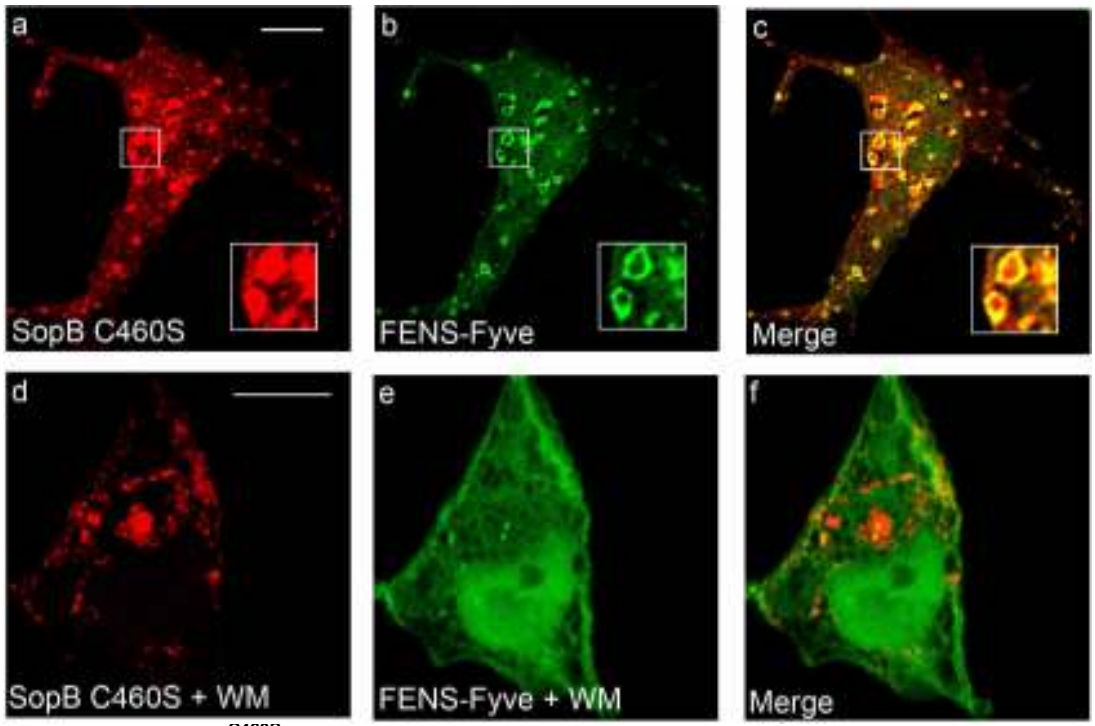

Figure 3.3 – SopB^{C460S} associates with membranes independent of any interaction with PtdIns(3)P. Cos-7 cells were co-transfected (*a-f*) with pRK5mycSopB^{C460S} and GFP-iFYVE FENS-1. Cells in panels *a-c* were mock treated and in panels *d-f* were treated for 3 hr with 100 nM wortmannin (WM) in serum free medium. Cells were fixed and immunostained with (*a-f*) anti-myc antibodies followed by Alexa® Fluor 568-conjugated anti-mouse IgG secondary antibodies. Fluorescence corresponding to (myc) SopB^{C460S} is shown in *a* and *d* (red). Fluorescence corresponding to GFP-iFYVE FENS-1 is shown in *b* and *e* (green). Images of merged fluorescence are shown in *c* and *f* (yellow indicates co-localisation). Scale bar on panels *a* and *d* represent 10 µm.

effector properties of ESCRT proteins with PtdIns(3,5)P_2.

To more fully examine the localisation of SopB with PIKfyve, the kinase that synthesises PtdIns(3,5)P_2, experiments to co-transfect SopB^{C460S} and GFP-PIKfyve into Cos-7 cells were attempted but were not successful as GFP-PIKfyve expression could not be detected in these cells. GFP-PIKfyve could, however, be expressed in CHO-K1 cells, in which co-expressed SopB^{C460S} showed significant punctate co-localisation with GFP-PIKfyve (Fig. 3.4*g-i*). These results again indicate that SopB^{C460S} can localise to a compartment that may allow it to have a quick turnover in antagonising the effects of PIKfyve's actions on PtdIns(3,5)P_2 synthesis.

It must be noted however that regardless of these findings, these experiments were performed with the phosphatase dead mutant $SopB^{C460S}$. It would have been desirable however for such experiments to be carried out using the wild-type SopB protein. These may have given better clues as to the effect of depleting PtdIns(3,5)P_2 levels on ESCRT localisation. However, given the highly toxic nature of SopB-wt expression to cells, such studies were not possible.

3.2.4 Cells infected with Salmonella expressing SopB contain SCVs with enriched EEA1 on membranes

It has been observed that PtdIns(3)P accumulates on SCVs of Henle-407 cells infected with wt *Salmonella* but not a *Salmonella* deletion mutant lacking SopB [128]. To see if this is a general phenomena for other mammalian cell types, A431 cells were infected with wild type *Salmonella* (wt *S. dublin*) or an isogenic deletion mutant lacking SopB (ΔSopB *S. dublin*). In order to visualise the intracellular bacteria the wt *S. dublin* and ΔSopB *S. dublin* were transformed with a GFP expressing plasmid pSU2007 (gift from Dr David Clarke). The presence or absence of PtdIns(3)P on SCVs was monitored by immunostaining fixed cells for endogenous EEA1. Observation of a large number of cells clearly showed that SCVs from wt *S. dublin* infected cells had large amounts of EEA1 associated with them (Fig. 3.5a-c), whereas those from ΔSopB *S. dublin* infected cells had much reduced levels of EEA1 associated with them (Fig. 3.5d-f). We hypothesise that the wt *S. dublin* have increased levels of PtdIns(3)P because of the phosphatase activity of SopB being expressed by the bacterium. This is in agreement with Hernandez *et al* who demonstrated that SopB maintains high levels of PtdIns(3)P levels in infected cells [128].

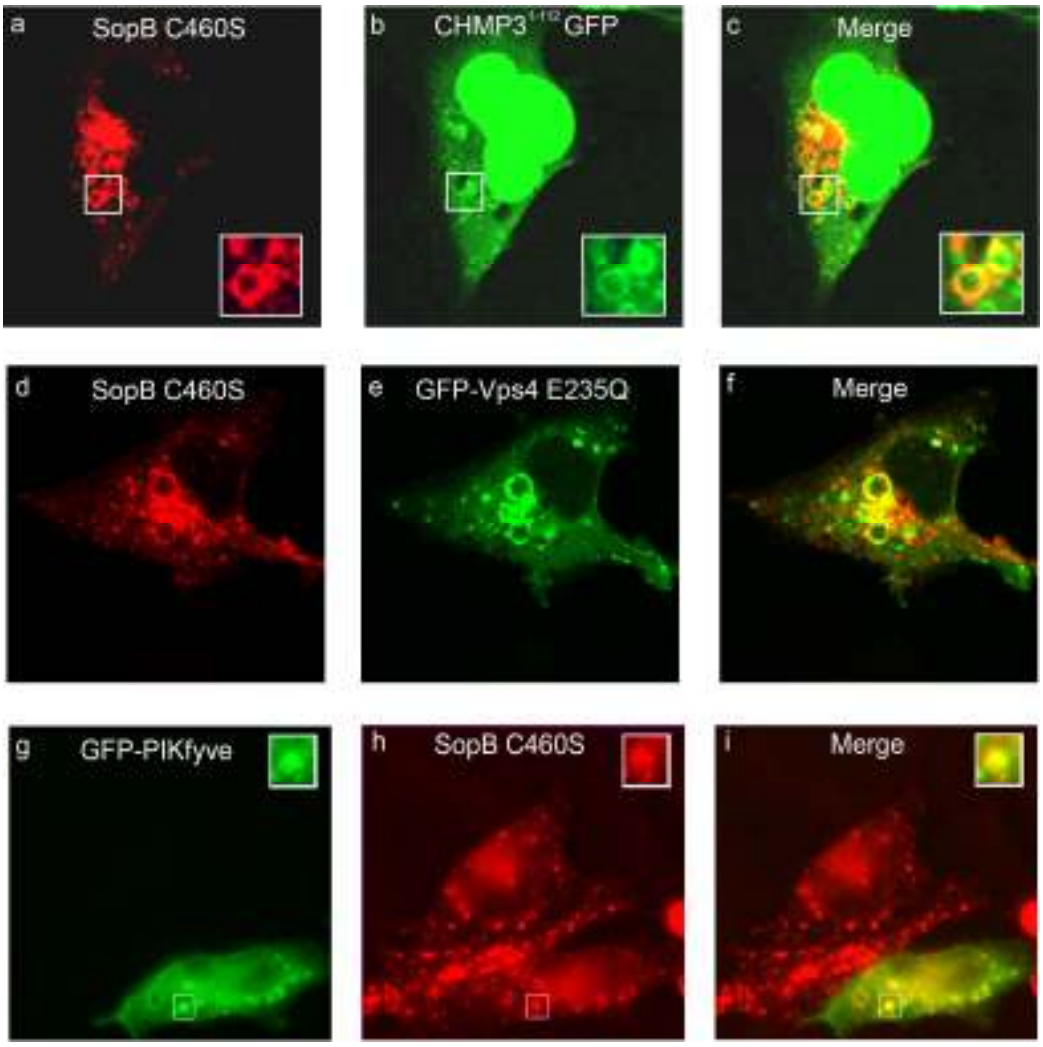

Figure 3.4 – Dominant negative ESCRT components assemble on SopB containing membranes. Cos-7 cells were co-transfected with (*a-f*) pRK5mycSopB^{C460S} and either a construct for the expression of (*a-c*) CHMP3$^{1-112}$GFP or (*d-f*) GFP-Vps4^{E235Q}. CHO-K1 cells were co-transfected with GFP-PIKfyve (*g-i*). Cells were fixed and immunostained with anti-myc antibodies followed by Alexa® Fluor 568-conjugated anti-mouse IgG antibodies. Fluorescence corresponding to (myc) SopB^{C460S} is shown in *a, d* and *h* (red). Fluorescence corresponding to CHMP3$^{1-112}$-GFP, GFP-Vps4^{E235Q} and GFP-PIKfyve are shown in *b*, *e* and *g* respectively (green). Images of merged fluorescence are shown in *c, f* and *i* (yellow fluorescence indicates co-localisation). Inset panels (*a-c, g-i*) are magnifications of boxed areas.

3.2.5 Cells infected with *Salmonella* expressing SopB have defective receptor degradation kinetics

The accumulation of PtdIns(3)P, due to SopB antagonising its transition to PtdIns(3,5)P_2 on SCVs has been proposed to divert SCVs away from the endocytic pathway preventing fusion with destructive lysosomes [128]. In order to test whether SopB could divert endocytic trafficking to lysosomes, an EGFR degradation assay was used. By serum starving cells that express EGFR, the receptor is upregulated to the plasma membrane. Stimulation with EGF causes the internalisation of EGFR and it is well established that stimulated EGFR is endocytosed and trafficked through the endo-MVB-lysosomal pathway where it is degraded via the lysosome. A431 cells were serum starved overnight to allow for upregulation and expression of EGFR at the plasma membrane. Following EGF stimulation of uninfected A431 cells, EGFR was rapidly internalised from the plasma membrane and degraded with a half-life of approximately 8 minutes (Fig. 3.6). If, however the A431 cells were infected with wt *S. dublin* 60 minutes prior to EGF stimulation, the kinetics of EGFR degradation were much reduced. Even 16 minutes after EGF stimulation 87% of the EGFR remained, *ie* was not degraded. The kinetics of degradation of EGFR in cells pre-infected with ΔSopB *S. dublin* 60 min prior to EGF stimulation was virtually identical to that in uninfected cells. This was supported by immunofluorescence studies which showed the accumulation of EGFR in A431 cells infected with wt *S. dublin* for 60 min (Fig. 3.6*c*).

Thus these studies imply that *Salmonella* maintains high levels of PtdIns(3)P via expression of SopB in order to arrest its progression to the lytic lysosome aiding its survival in the infected host cell. The increased levels of EGFR detected in cells infected with SopB expressing *S. dublin* suggests that SopB perturbs the degradation of EGFR by preventing the maturation of compartments containing EGFR towards fusing with the lysosome. However whether the exact actions of

SopB via inhibition of PtdIns(3,5)P_2 production occur at the MVB biogenesis stage or the MVB-lysosomal fusion stage are not clear from this study, if indeed SopB's actions are in fact via directly inhibiting levels of PtdIns(3,5)P_2. However evidence from this and other studies would suggest that this is likely to be the case.

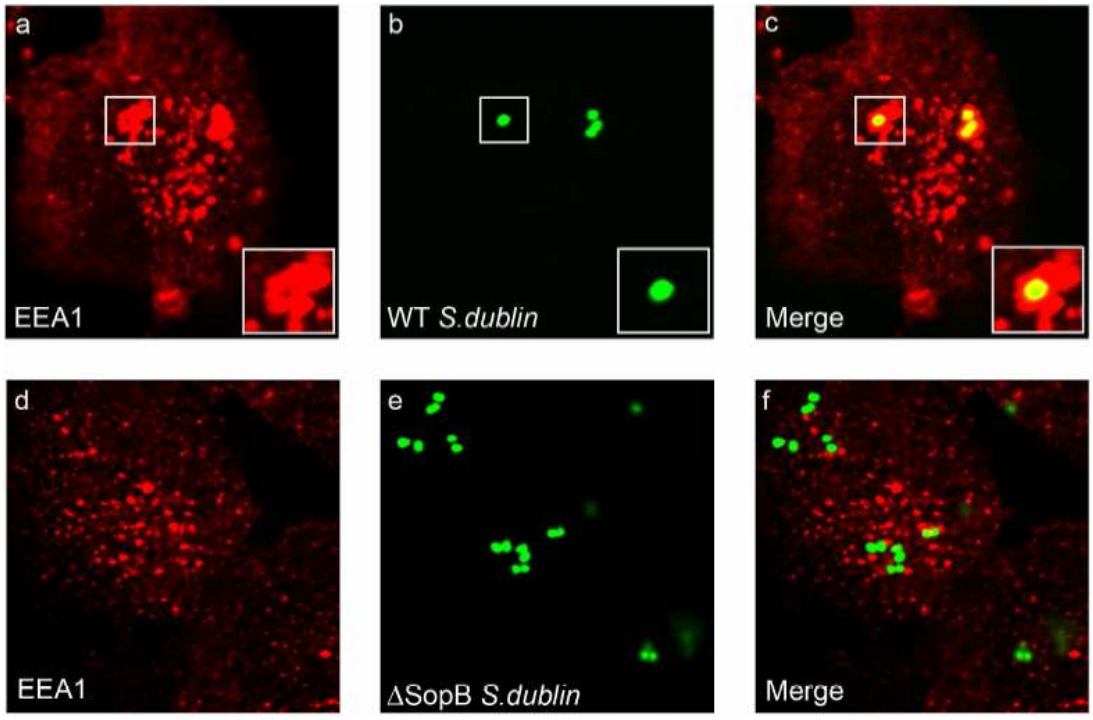

Figure 3.5 – A431 cells infected with wt *S. dublin* have EEA1 enriched SCVs. A431 cells were infected with (*a*-*c*) wt *S. dublin* or (*d*-*f*) ΔSopB *S.dublin,* both transformed with the GFP expression plasmid, pSU2007, for visualisation purposes. Following infection, cells were washed, fixed and immunostained with anti-EEA1 antibodies followed by Alexa® Fluor 568-conjugated anti-rabbit IgG secondary antibody. GFP expressing (*b*) wt *S. dublin* and (*e*) ΔSopB *S. dublin* and (*c*) and (*f*) represent merged images. Inset panels in (*a*-*c*) are magnifications of boxed areas. Fluorescence corresponding to EEA1 is shown in *a* and *d* (red). Fluorescence corresponding to wt *S. dublin* and ΔSopB *S.dublin* are shown in *b* and *e* respectively (green). Images of merged fluorescence are shown in *c* and *f.* Inset panels (*a*-*c*) are magnifications of boxed areas.

Figure 6

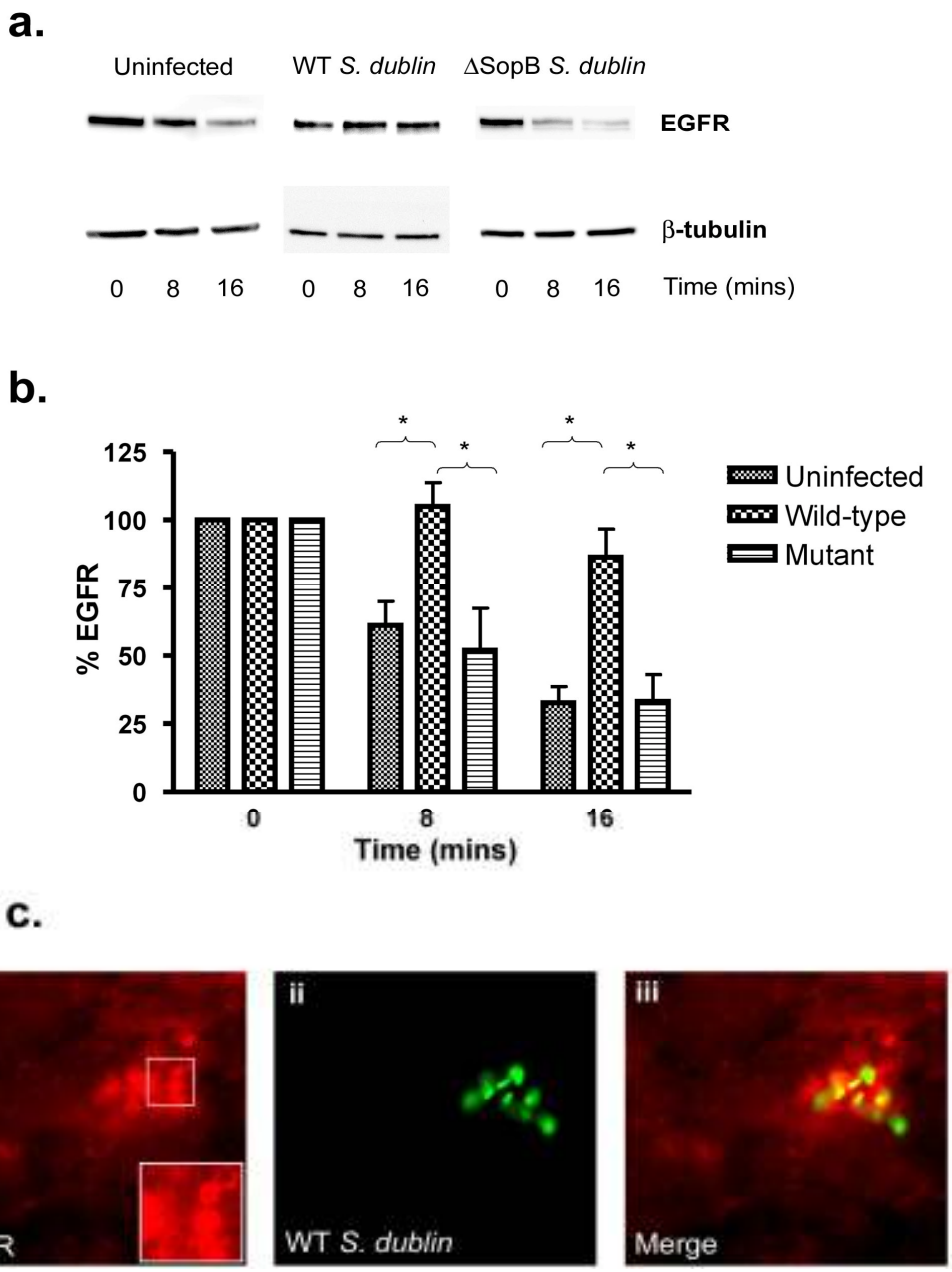

Figure 3.6 – Cells infected with wt-*S.dublin* have impaired EGFR trafficking to the lysosome. A431 cells were infected with wt *S. dublin*, ΔSopB *S.dublin* or mock treated. Following infection, cells were washed and incubated in fresh media containing 500 ng/ml EGF. Cell were harvested at the times indicated, protein extracts were made and analysed by Western blotting for EGFR and β-tubulin. (*a*) Immunoblots from a representative experiment are shown. (*b*) Shows a graphical representation of quantifications of immunoblots from 3 separate experiments. Significant differences * (t-test; $p < 0.05$) are indicated. (*c*) A431 cells infected with wt *S. dublin* were incubated with EGF as described above. After 1 hr the cells were washed, fixed and immunostained with anti-EGFR antibodies followed by Alexa Fluor 568-conjugated anti-mouse IgG secondary antibody. Panels i) ii) and iii) show GFP labelled wt *S. dublin*, EGFR staining and merged images respectively. Note: neighbouring cells not infected with bacteria do not accumulate an intracellular pool of EGFR.

3.3 Discussion

This study sought to more fully characterise the subcellular localisation of SopB and thus whether it may be a useful tool for the manipulation of PtdIns(3,5)P_2. The subcellular localisation of SopB should be relevant to its site of action. SopB has been shown to possess phosphoinositide phosphatase activity, with PtdIns(3,5)P_2 being a preferred substrate, although *in vitro* SopB has been shown to possess a broad specificity as a lipid phosphatase [125, 126]. Different phosphoinositides seem to be spatially restricted on various compartments in eukaryotic cells, thus although SopB may act on other lipid substrates *in vitro* (such as PtdIns(4,5)P_2 which is found in high concentrations at the plasma membrane), its localisation within the cell will determine which substrate it will dephosphorylate. These results indicate that SopB has a subcellular localisation that puts it in the correct compartment to maintain high levels of PtdIns(3)P by antagonising the effects of PIKfyve's production of PtdIns(3,5)P_2 as the two proteins appear to be found on the same compartment. Furthermore, infection of cells with *Salmonella* bacteria expressing active SopB impairs the normal degradation kinetics of EGFR, which is known to progress through the MVB-lysosomal pathway. These results then indicate that SopB may prevent the SCV from fusion with the lysosome by keeping PtdIns(3,5)P_2 levels at a minimum, suggesting that PtdIns(3,5)P_2 plays a role in the endo-lysosomal trafficking pathway.

It has been proposed that by antagonising the effects of PIKfyve, SopB allows the bacteria to survive and replicate in its host. This hypothesis was further strengthened by the findings that SopB localises to PtdIns(3)P containing membranes in addition to compartments that contain PIKfyve. The membrane association of SopB appears to be independent of its phosphatase domain, so there is no reason to assume that the localisation of SopB^{C460S} should differ any from that of SopB-wt [132]. To confirm this, a second tagged form of SopB was cloned into a

pHM6 vector, to give HA-SopB and HA-SopB^{C460S}. HA-tagged SopB was transiently transfected on several occasions with the aim to co-transfect with myc-SopB^{C460S} in order to demonstrate similar localisation upon overexpression within the cell; however there were various technical problems with the HA-tagged SopB which resulted in no visual detection of an immunofluorescent signal. As this was seen to be a minor issue with the localisation of SopB having been reported elsewhere to be independent of its phosphatase activity [132], this approach was not further pursued after several attempts to overexpress HA-SopB.

SopB^{C460S} localised to membrane compartments that contained EEA1, however no obvious colocalisation was seen with the late endosomal marker CI-M6PR or the trans-Golgi network marker TGN46. Some studies have suggested that SopB also localises to the plasma membrane [134], however these results show little if any localisation to the plasma membrane, but rather punctae that are typical of an early endosomal staining. At very high levels of expression, SopB-wt may have appeared to localise partially to the plasma membrane, however such localisation was not observed in cells expressing moderate amounts of protein or in any cells expressing the phosphatase dead mutant SopB^{C460S}. When co-expressed with the PtdIns(3)P reporter FENS-FYVE, SopB^{C460S} colocalised on the FENS-FYVE containing membranes. The EEA1 and FENS-FYVE colocalisation data all indicate that SopB associates with PtdIns(3)P containing membranes. As EEA1 associates with PtdIns(3)P these results are in agreement with previous findings that implicate SopB as being responsible for maintaining high levels of PtdIns(3)P on the SCV. Thus SopB's localisation seems consistent with its suggested role as a phosphoinositide phosphatase with activity for PtdIns(3,5)P_2.

In order to establish whether SopB associates with membranes via an interaction with PtdIns(3)P, production of this lipid was inhibited with the PI-3 kinase inhibitor, wortmannin. SopB does not appear to associate

with PtdIns(3)P directly, as upon wortmannin treatment of Cos-7 cells co-expressing SopB^{C460S} and FENS-FYVE, the FENS-FYVE dissociated from the membranes whereas the SopB^{C460S} remained membrane associated. The basis for the association of SopB with endosomal membranes remains to be established although a predicted coiled-coil domain in SopB appears necessary for membrane targeting [132].

It has previously been demonstrated that one of the ESCRT-III proteins, CHMP3, binds *in vitro* to PtdIns(3,5)P_2 and that this lipid may be necessary for correct ESCRT-III assembly and function [71]. It is reasonable to assume then that if SopB acts on PtdIns(3,5)P_2 that it may localise with CHMP3. CHMP3 typically resides in the cytoplasm, however the dominant negative N-terminal construct of CHMP3 (CHMP3$^{1-112}$) binds to endosomal membranes, resulting in swollen endosomal class E-like phenotypes. We expressed SopB^{C460S} in Cos-7 cells along with CHMP3$^{1-112}$-GFP, and found a substantial degree of colocalisation. In addition, the dominant negative ATP-ase defective GFP-Vps4^{E235Q} was co-expressed with SopB^{C460S} and clear colocalisation was observed. As Vps4^{E235Q} is unable to catalyse the removal of the ESCRT machinery from the limiting membranes of endosomes, a swollen endosomal phenotype is again observed. In both cases SopB^{C460S} was found on compartments that contain ESCRT machinery. It would indeed be very interesting to observe the localisation of ESCRT machinery in SopB-wt expressing cells. One might speculate that with an active phosphatase activity, SopB-wt may prevent components such as CHMP3 from binding to those membranes where SopB-wt is localised. Such experiments were unable to be performed however due to the toxicity of SopB-wt when overexpressed in mammalian cells. Despite this it must be again noted that the role of PtdIns(3,5)P_2 in endo-lysosomal trafficking is uncertain and these studies do not provide conclusive findings about such a role.

The effects of SopB on the cell would appear then as suggested, to be antagonistic to the actions of PIKfyve, the mammalian kinase that

catalyses the conversion of PtdIns(3)P to PtdIns(3,5)P_2. PIKfyve localises to membranes containing PtdIns(3)P via its FYVE domain which binds PtdIns(3)P. It may be expected then that SopB would be found in a similar compartment to PIKfyve, as this would allow for a very quick turnaround of ensuring that PtdIns(3,5)P_2 levels are kept as low as possible thus aiding in the avoidance of lysosomal fusion with the SCV. When GFP-PIKfyve was co-expressed with SopB^{C460S} it was unsurprisingly found to have a considerable degree of colocalisation. This is entirely consistent with SopB having an antagonistic effect on the role of PIKfyve within an infected mammalian cell via manipulation of PtdIns(3)P levels.

SopB appears to have a role of maintaining high levels of PtdIns(3)P in relation to the PIKfyve product PtdIns(3,5)P_2. This is an important mechanism for *Salmonella's* survival within the host cell as the SCV needs to be diverted away from being trafficked to the lysosome. EEA1 specifically binds to PtdIns(3)P enriched membranes, and it was shown that the membranes surrounding the GFP-tagged wt-*S. dublin* are enriched with EEA1. These results are consistent with SopB-producing *Salmonella* maintaining high levels of PtdIns(3)P on the SCV membrane, which is suggested to prevent its trafficking to and fusion with the lytic lysosome [128]. These results then suggest that SopB is antagonising PIKfyve in the production of PtdIns(3,5)P_2, and that this lipid may play a role in endo-lysosomal trafficking.

EGFR is a well-studied receptor in downregulation and receptor degradation experiments. It is also well established that EGFR is degraded via the ESCRT-mediated MVB formation process and fusion with the lytic lysosome. Thus to further investigate the action of SopB and thus PtdIns(3,5)P_2 on receptor degradation, a combined use of an EGFR degradation assay and infection of mammalian cells with the *Salmonella dublin* strain of bacteria was used. The wild-type strain of *S. dublin* contains the gene for a functional SopB protein, however the ΔSopB *S. dublin* does not express SopB. An EGFR downregulation

assay was carried out in A431 cells, and it was found that wt-*S. dublin* infected cells maintained high levels of EGFR compared with ΔSopB-*S. dublin*, which exhibited very similar degradation kinetics to the uninfected cells. There is no statistically significant difference between the ΔSopB-*S. dublin* and uninfected A431 cells, however there is a significant difference ($p<0.05$) between the wt-*S. dublin* and both ΔSopB-*S. dublin* and uninfected cells after 8 and 16 minutes of EGF stimulation. Following 16 minutes of EGF stimulation, wt-*S. dublin* infected cells maintained on average 87% of the EGFR present at t = 0, which is over three times more than the ΔSopB-*S. dublin* and uninfected cells. These findings suggest that SopB is specifically responsible for delaying the degradation of EGFR as well as delaying processes that would be detrimental to the bacteria.

These results would suggest that the action of antagonising PtdIns(3,5)P_2 production in the cell by SopB may be what is responsible for delaying EGFR degradation. There is however some inconsistency in the literature regarding the relationship between PtdIns(3,5)P_2 levels and EGFR degradation. Ikonomov *et al* expressed a mutant form of PIKfyve that lacks its lipid kinase activity (and hence is unable to convert PtdIns(3)P to PtdIns(3,5)P_2) in mammalian cells, and determined the levels of EGFR present following stimulation with EGF using Western blotting techniques. They found that there was no significant difference in the degradation of EGFR when expression of the kinase-dead PIKfyve protein was compared with expression of wild-type PIKfyve [136]. In contrast to this study however, overexpression of myotubularin (a phosphoinositide 3-phosphatase shown to bind to and thought to dephosphorylate PtdIns(3,5)P_2 to PtdIns(5)P), was shown to delay the degradation of EGFR in Cos-7 cells compared with untransfected cells [137]. As PIKfyve has been demonstrated to be necessary for PtdIns(3,5)P_2 production and myotubularin is suggested to dephosphorylate PtdIns(3,5)P_2, these studies seem to be conflicting and

suggest that more work into fully understanding PIKfyve and its role(s) within the mammalian cell are necessary.

Due to SopB's localisation with respect to the SCV, it is reasonable to assume that the undegraded EGFR would be found in higher concentrations on the SCV in wt-*S. dublin* when compared to ΔSopB-*S. dublin* infected cells. When infected cells were fixed after 16 min of EGF stimulation and EGFR stained for, this was in fact supported by immunofluorescence. An accumulation of undegraded EGFR around the area where the bacteria is present is clearly seen, thus supporting the biochemical data from Western blots. Such an accumulation is not seen in uninfected cells (see neighbouring cells in Fig. 3.6*c*) nor in ΔSopB-*S. dublin* infected cells (not shown). These results are hence consistent with PtdIns(3,5)P_2 being a lipid that is necessary for normal receptor degradation kinetics, as evidence suggests PtdIns(3,5)P_2 is a substrate for SopB. The finding that EEA1 is present in high concentrations on the SCV of wt-*S. dublin* infected cells adds further support to this theory.

3.4 Conclusion

This study demonstrates that the lipid PtdIns(3,5)P_2 may play a role in receptor degradation and further support the role of SopB as a phosphoinositide phosphatase with PtdIns(3,5)P_2 as a substrate. It is hypothesised that SopB diverts the SCV away from being targeted to the lytic lysosome via its phosphatase activity specifically on PtdIns(3,5)P_2. The localisation of transiently transfected SopB within the cell also is in agreement with this hypothesis. PtdIns(3,5)P_2 may then play an important role in receptor degradation and MVB formation however its exact role is uncertain. Studies on PIKfyve and its yeast homologue Fab1 have also suggested that PtdIns(3,5)P_2 plays a role in endo-lysosomal trafficking and possibly MVB formation, however little work has been done on PIKfyve [60-62, 70, 84, 88, 138]. As so little is known

about the exact role of PtdIns(3,5)P_2 in the endocytic pathway, this study has further characterised SopB as a potentially useful tool for manipulation of PtdIns(3,5)P_2. Unfortunately high levels of wild-type SopB have been found to be highly toxic to mammalian cells. As the myc-tagged SopB in these experiments was under the control of a CMV promoter which would result in high levels of expression, an expression system that has more controlled and lower levels of SopB would be an ideal approach for better manipulation of PtdIns(3,5)P_2 levels.

CHAPTER 4

4 Generation of an antibody against the mammalian phosphoinositide kinase PIKfyve

4.1 Introduction

The generation of PtdIns(3,5)P_2 from its precursor PtdIns(3)P appears to be an important event in the proper function of the endo-lysosomal pathway [60, 70, 82, 131]. The early endosomally localised lipid PtdIns(3)P is an important lipid itself in the recruitment and hence localisation of cellular proteins to the early endosomal membrane [47, 48]. In yeast it has been shown that the enzyme responsible for PtdIns(3)P conversion to PtdIns(3,5)P_2 is Fab1, and the Δ*fab1* mutant displays various growth defects along with a distinctly enlarged vacuole [139]. The mammalian homologue of Fab1 has been shown to be PIKfyve [140]. Like Fab1, PIKfyve also contains a FYVE domain, a domain known for interaction and binding to PtdIns(3)P at the endosomal membrane. Additionally, a kinase-dead dominant negative form of PIKfyve when expressed in mammalian cells has been reported to give an enlarged vacuolar phenotype [70]. These swollen vacuoles appear to be endosomally derived, and the phenotype can be rescued by the introduction of wild-type PIKfyve [70].

The identification of PIKfyve and its importance in the endocytic pathway is quite recent, although its precise role(s) within the cell is far from clear. Studies that have taken place however have highlighted not only the importance of PIKfyve in membrane trafficking but in other membrane and signalling events, for example the regulation of specific trafficking pathways and the translocation of membrane transporters such as GLUT4 [141]. With regards to endo-lysosomal trafficking, kinase-dead mutants or cells that lack PIKfyve expression have been suggested to cause defects in the delivery and subsequent degradation of receptors to the lysosome [84, 88].

The study of this kinase is still relatively new and bearing in mind that the discovery of the phosphoinositide lipid PtdIns(3,5)P_2 is also relatively recent, it is understandable that much has to be discovered about PIKfyve and its specific cellular roles. However the current literature does provoke some confusion on PIKfyve's role within mammalian cells. There have been conflicting reports on its sub-cellular localisation, having been reported to be both early- [84-86] and late-endosomal [142]. The cellular events that PIKfyve may control have been reported to range from late endosomal maturation [131], to TGN retrograde trafficking [86], lysosomal maturation [84, 88], and even possibly nuclear transportation of receptors in tumour cells [87]. It is likely however that PIKfyve does not carry out a single task within the cell but has adapted to the complex system of mammalian trafficking to perform several cellular duties. The lipid PtdIns(3,5)P_2 itself may then consequently have promiscuity in its own cellular function.

Given the confusing state of research with PIKfyve as well as the importance of PtdIns(3,5)P_2 in proper MVB biogenesis and maturation, being able to better understand the role of PIKfyve in a cellular scenario is an important undertaking. It is possible there is some role of PIKfyve in endosomal trafficking and thus it is desirable to have tools to be able to investigate this protein more extensively in this context. Hence as PIKfyve has only recently begun to be characterised, useful tools such as commercial antibodies raised against PIKfyve have not been available for use. Thus the aim of the work described in this chapter was to generate a reliable and specific antibody that would recognise endogenous PIKfyve in mammalian cells. A small polypeptide that was taken from a hydrophilic portion of the PIKfyve protein was used to raise polyclonal antibodies to the human PIKfyve protein. As this antigen was a hydrophilic sequence, it was likely to be readily accessible on the exterior of the native folded protein for recognition by polyclonal antibodies.

4.2 Results

4.2.1 A polypeptide epitope for raising polyclonal anti-PIKfyve antibodies against

The human PIKfyve protein is a very large protein of approximately 235 kDa and 2098 amino acids long. Thus for raising polyclonal antibodies for recognition of this protein in its native form a region that should be exposed in the folded protein state is desired. Hydrophobic residues tend to be sequestered away from contact with aqueous surroundings such as the cytoplasm. Thus when a protein undergoes folding after synthesis, many of the hydrophobic residues are found buried in the protein's interior. Hydrophilic residues on the other hand are often left exposed at the exterior of the folded protein. By choosing a region of amino acids from the protein's sequence that consists of hydrophilic residues as an antigen, the epitope will be found at the surface of the protein. The surface of the protein is exposed and therefore is recognisable by antibodies raised against this epitope when the protein is folded.

One such hydrophilic polypeptide sequence can be found on the PIKfyve protein between the residues 1183 and 1200 (see hydrophobicity plot, Fig. 4.1). The DNA sequence coding for this region (118 amino acids in length) was cloned into a pET15b vector with a His_6 tag at the N-terminus (see Fig. 4.2), to give a polypeptide of 152 amino acids in length termed His_6-PIK. This recombinant polypeptide was expressed and purified as previously described in 2.2.7, and sent to Diagnostics Scotland for immunization of a sheep. An injection protocol into sheep was used which involved an initial subcutaneous injection of 1 mg of the polypeptide followed by booster injections every 28 days. Test bleeds were taken 7 days after injections for a total of three separate bleeds. The sheep were not exsanguinated at the end of the procedure. A total

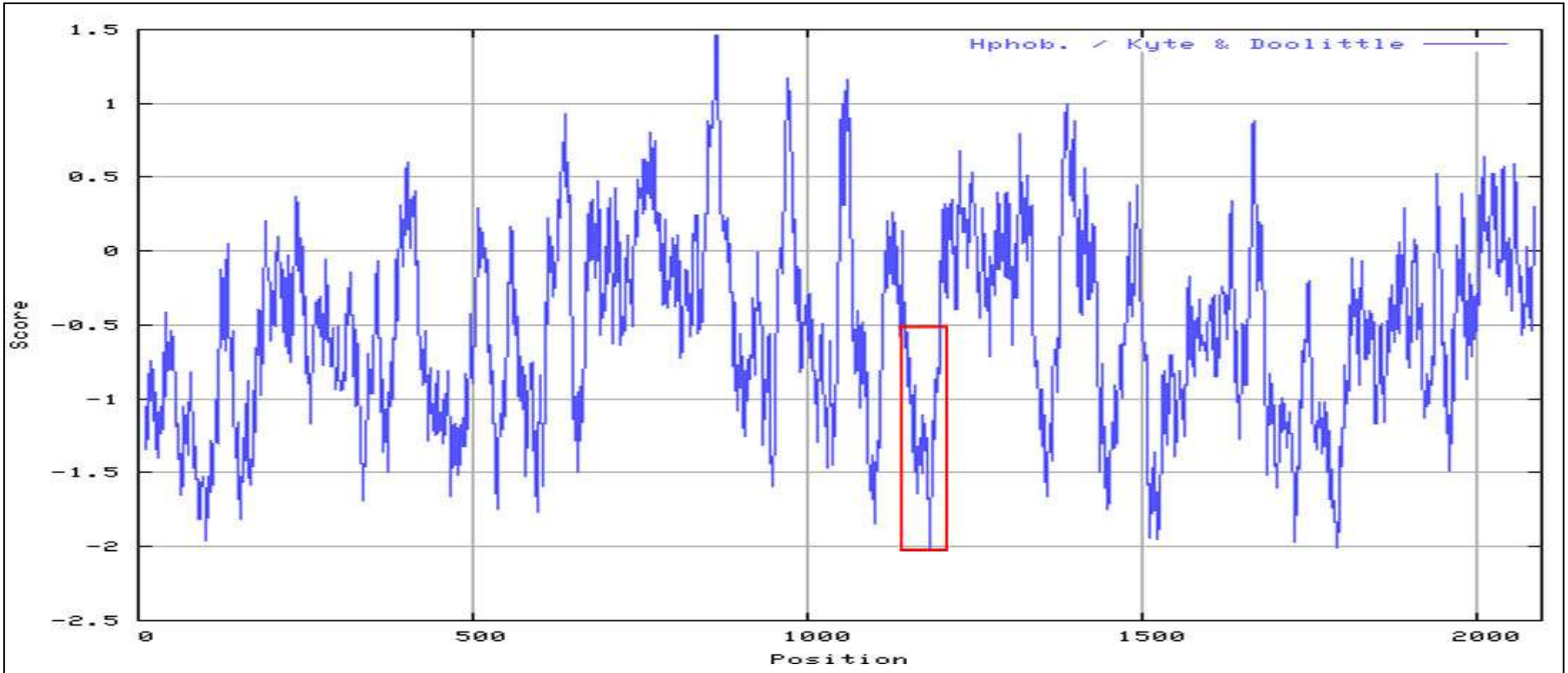

Figure 4.1 – Hydrophobicity plot of human PIKfyve. A hydrophobicity plot was performed using ExPASy Proteomics Server according to the Kyte and Doolittle method [143]. A positive score (y-axis) relates to a part of the sequence that is hydrophobic where a negative score indicates hydrophilic residues. The x-axis relates to the amino acid position of the PIKfyve sequence, with a frame set to 21. The area contained with then the red box indicates the sequence used for His_6-PIK.

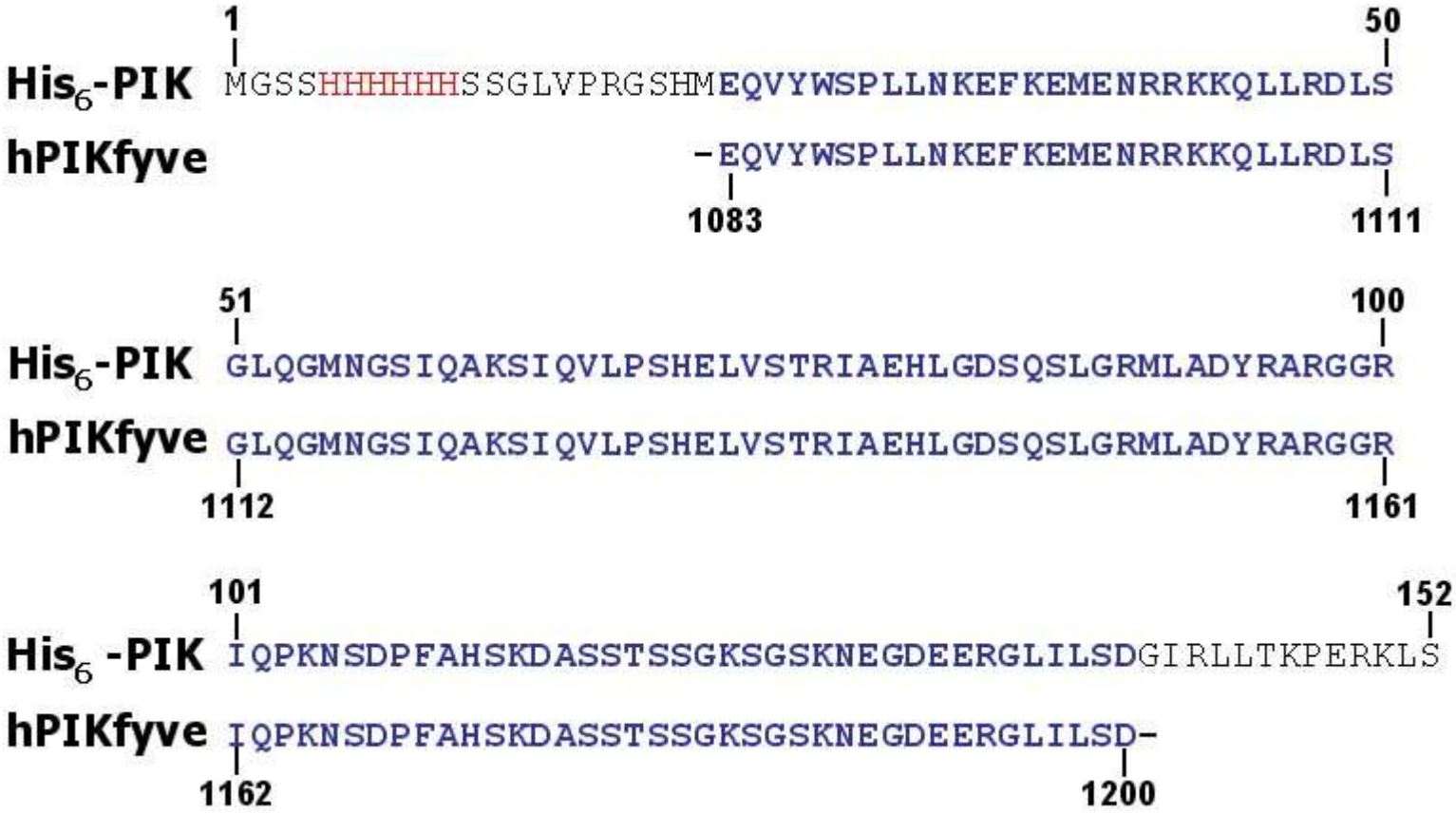

Figure 4.2 – Polypeptide used as an epitope for raising polyclonal anti-PIKfyve antibodies. The His_6-PIK peptide is 152 amino acids long in total to include restriction sites for original cloning into the pET15b vector as well as a His_6 tag (red). The relevant human PIKfyve (hPIKfyve) sequence that aligns to the His_6-PIK polypeptide spans from E1083 to D1200 and has been aligned in the figure (blue).

of three bleeds totalling roughly 200 ml each along with a pre-immune bleed from the sheep were obtained.

4.2.1.1 The purified His_6-PIK polypeptide is approximately 16.5 kDa when run on SDS-PAGE

Although the alignment of His_6-PIK to the corresponding region of PIKfyve is only 118 amino acids in length, the total purified polypeptide is of 152 amino acids long and thus can be estimated to be roughly 16.5 kDa in size. To confirm this, a small amount of the purified His_6-PIK was run on a high percentage SDS-PAGE gel and Coomassie stained (not shown).

4.2.2 The first bleed from a His_6-PIK immunized sheep shows greater specificity for the antigen than pre-immune serum

To determine the effectiveness of the post-immunization serum bleeds the first bleed serum was compared to the pre-immune serum, taken prior to the sheep being injected with His_6-PIK. To do this, both Western blotting and ELISA protocols were followed. Firstly, the purified His_6-PIK was run on a high percentage SDS-PAGE gel and transferred onto nitrocellulose membrane where it was incubated with a 1:1000 dilution of either the first bleed serum or the pre-immune serum. Western blotting techniques were used and the developed membrane shows recognition of His_6-PIK with the first bleed compared to the pre-immune serum (Fig 4.3). The strongest band is found to align with the 16.5 kDa marker, which would correlate to His_6-PIK having an estimated molecular weight of 16.5 kDa. Other bands are observed including one slightly above the 32.5 kDa marker and quite a few bands below. It is likely that the higher band is a dimerised form of His_6-PIK and bands smaller than 16.5 kDa may be degraded protein. It should be noted that the pre-immune and

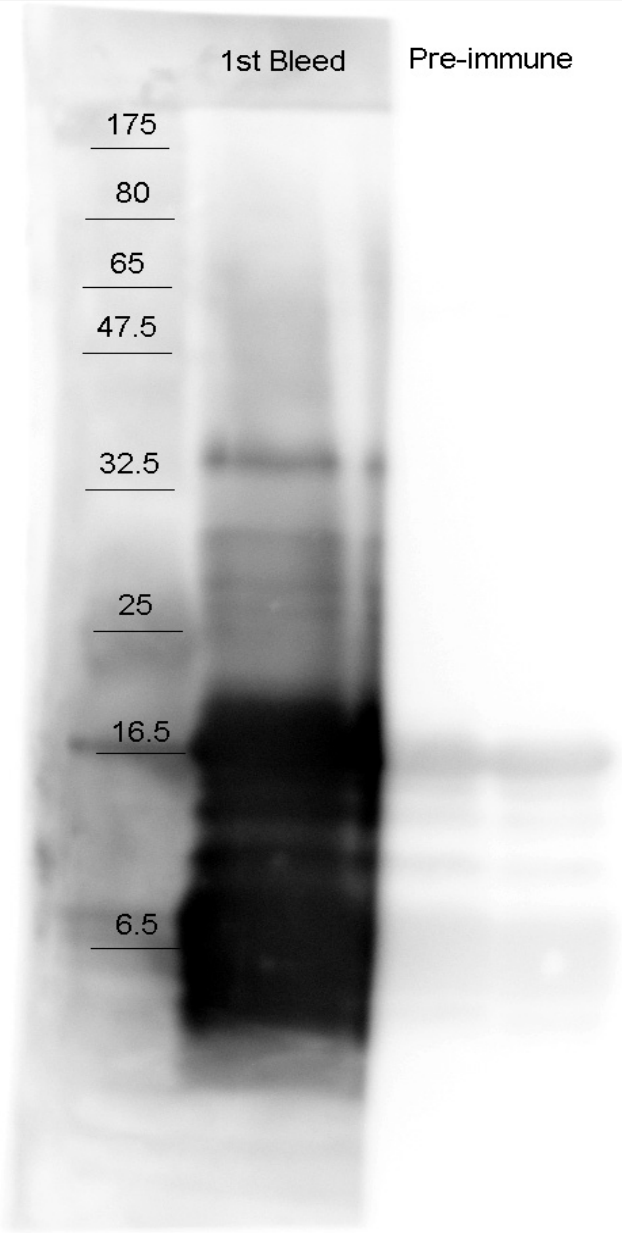

Figure 4.3 – The first bleed sera from a His_6-PIK immunized sheep shows high specificity for the His_6-PIK polypeptide in comparison with pre-immune serum. Two lanes of a 12% Tris-glycine SDS-PAGE gel were loaded with approximately 1 µg purified His_6-PIK along with pre-stained markers. Marker weights are drawn on and indicated where numbers represent kDa size of protein. Lane marked "1st Bleed" was blotted with a 1:1000 dilution of the first bleed of sheep serum obtained after injection of His_6-PIK. Lane marked "Pre-immune" was separated from the nitrocellulose the other lane was on, and similarly blotted at a 1:1000 dilution of the pre-immune serum from the sheep. Both lanes were incubated with goat α-sheep HRP-conjugated antibodies and developed at the same time for comparison of band intensities. Note estimated molecular weight of His_6-PIK is 16.5 kDa.

the first bleed were incubated with different halves of the membrane, but treated identically and exposed following secondary antibody anti-sheep-HRP-conjugate developing for the exact same amount of time for comparable results.

Following confirmation by Western that the first bleed serum recognised the antigen and the pre-immune largely did not, an ELISA was performed to further compare the specificity of the two bleeds at a range of serial dilutions from 1:100 to 1:250,000 (Fig. 4.4). As clearly seen in Figure 4.4, the binding of pre-immune sera to the antigen (His_6-PIK) starts to diminish just before the 1:1000 dilution range, and continues falling to virtually background level at the highest dilutions. In contrast, the first bleed appears to maintain practically the same level of antigen binding from the lowest dilution (1:100) to the highest dilution (1:248,000) suggesting that the recognition of the antigen by this sera is very good and that the sera has a very high affinity for the antigen. This is demonstrated by the fact that the OD_{450} for the first bleed at a 1:100 dilution is 1.242 compared with the OD_{450} at 1:124,000 and 1:248,000 being 1.2525 and 1.222 (averaged from duplicate readings).

4.2.3 Antibodies purified from the third bleed sera show greater specificity for His_6-PIK than antibodies purified from the first bleed

To obtain a purer form of the polyclonal antibodies that were raised against the His_6-PIK polypeptide, the serum was purified using a NHS-activated Hi-trap column prepared as described in 2.2.7.3. The His_6-PIK antigen was bound to this column and the serum run through the column allowing antibodies present in the serum to bind to the immobilised His_6-PIK polypeptides on the column. The bound antibodies were then eluted and collected into fractions. The fractions where the UV absorbance at 280 nm (tyrosine and tryptophan absorption; A_{280}) peaked were pooled

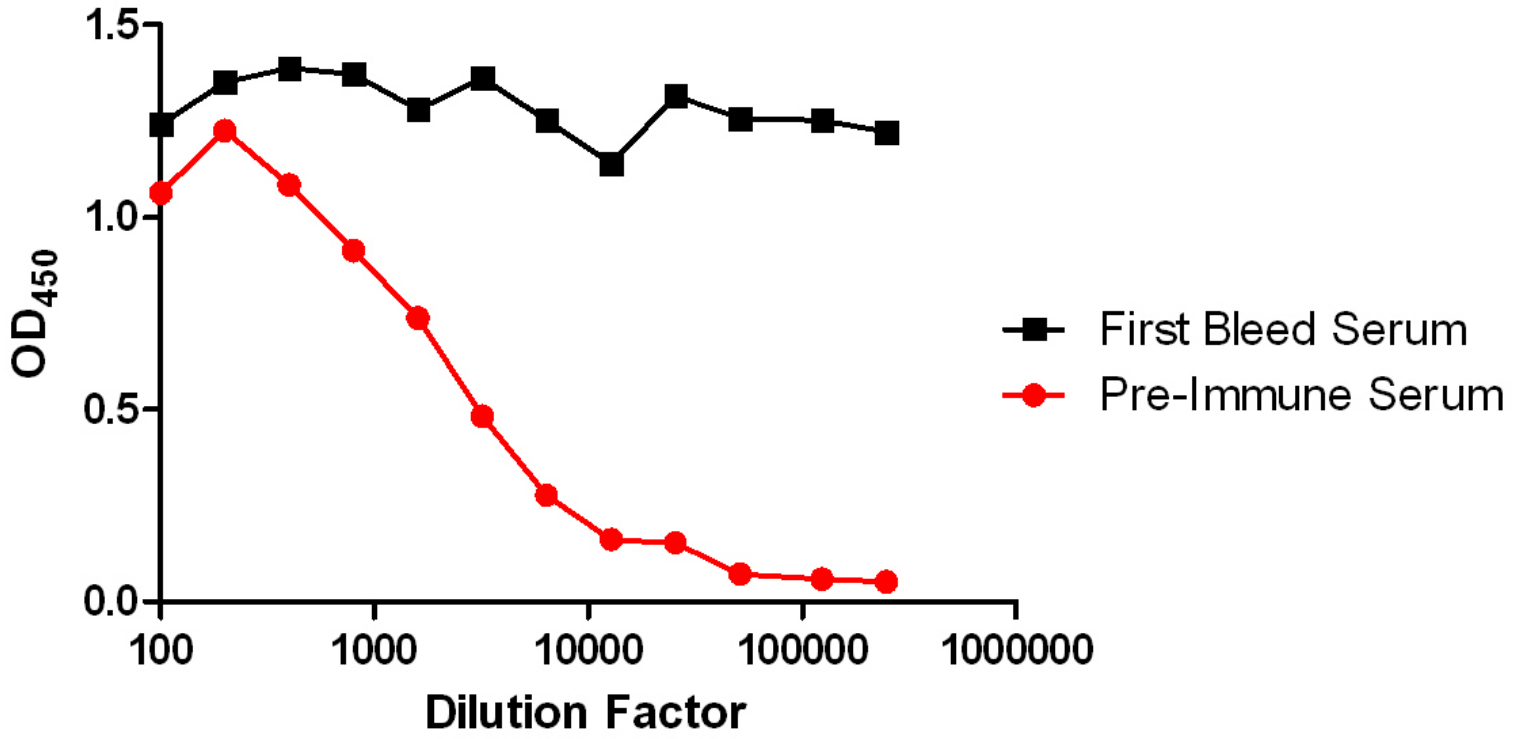

Figure 4.4 – ELISA of the pre-immune serum from sheep compared with the first bleed from the His_6-PIK immunized sheep. An ELISA was performed as described in 2.2.7.2 and the optical density at 450 nm was measured over a range of dilutions from 1:100 to 1:248,000. Values were determined in duplicate and the averaged value plotted on the graph. Red circles indicate values for pre-immune serum dilutions; black squares represent dilutions of the first bleed of immunized sheep serum.

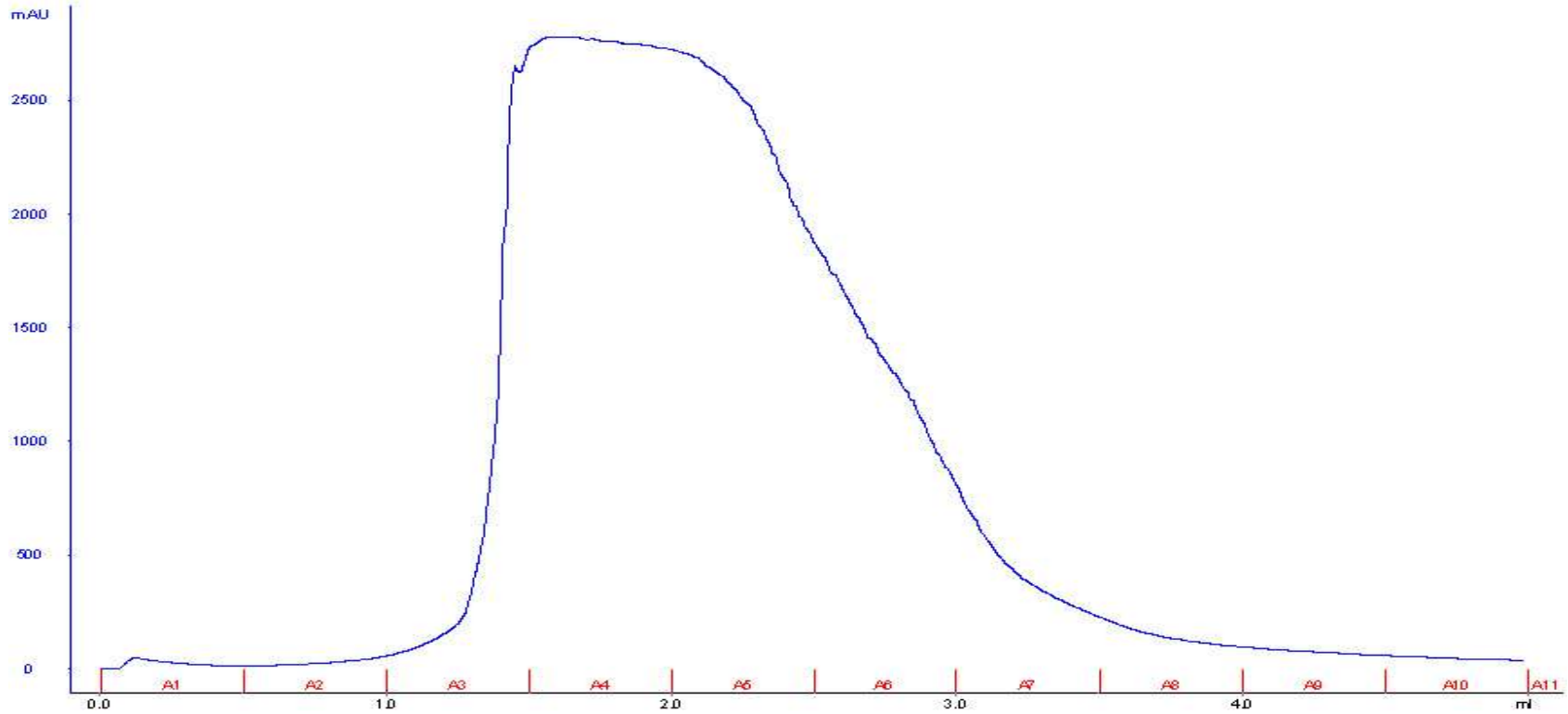

Figure 4.5 – Elution profile of α-PIKfyve[3] from a His_6-PIK-bound Hi-trap column. The column containing the bound antigen was prepared as described in 2.2.7.3 and serum from the third bleed of the host sheep was bound to this column and processed on an FPLC machine. To elute the affinity-purified antibodies, 100 mM glycine, pH 2.5 was run through the column and 0.5 ml fractions were collected as indicated by A1-A11 on the x-axis. Presence of eluted antibody was determined by the rise in the A_{280}, which is indicated, on the y-axis (arbitrary units). Fractions A3-A7 were pooled and used as the purified antibody.

together and used as the purified polyclonal α-PIKfyve (see Fig. 4.5 for elution profile). For the case of the first bleed, the purified antibodies are referred to as α-PIKfyve^{1} with the third bleed purification being α-PIKfyve^{3}. No purification of the second bleed was carried out or characterised.

To characterise the specificity and the ability of the affinity purified antibodies to recognise PIKfyve, CHO cells were transfected with a GFP-PIKfyve construct, and these cell lysates along with untransfected 3T3 cell adipocyte lysates (kindly provided by the Prof Geoff Holman lab) were run on an SDS-PAGE gel and blotted for using the sheep α-PIKfyve^{1} purified antibody at a range of dilutions (note that the stock concentration of α-PIKfyve^{1} was 2.2 mg/ml). Differentiated 3T3 adipocyte cells were what the human PIKfyve protein was first identified in [140], thus it was reasoned that they might provide a good source of endogenous PIKfyve for testing the antibody on. Although there appeared to be a fair amount of background bands appearing on the blots at lower molecular weights, there was an apparent intense band seen in the transfected CHO cell lysates that appeared to correlate to the expected size of GFP-PIKfyve (Fig. 4.6*A*). A much less intense band can be seen slightly below the proposed GFP-PIKfyve band in the 3T3 lysate lanes (at the 1:5000 and 1:10000 dilutions) that may relate to endogenous PIKfyve. Even at a high dilution of 1:50,000 giving a concentration of 44 ng/ml α-PIKfyve^{1}, there was clearly a band present in the GFP-PIKfyve transfected CHO lysate lane suggesting that the antibody has a very high affinity for the PIKfyve protein. This band appears to run to roughly 250 kDa when compared to a broad range protein marker used, despite estimations of GFP-PIKfyve's molecular weight being closer to 263 kDa. It should be noted however that when this broad range protein marker is run alongside the pre-stained protein marker also used in our lab, the 148 kDa marker from the broad range marker runs very close to the 175 kDa band from the pre-stained marker. As the pre-stained marker from past experience has been shown to run

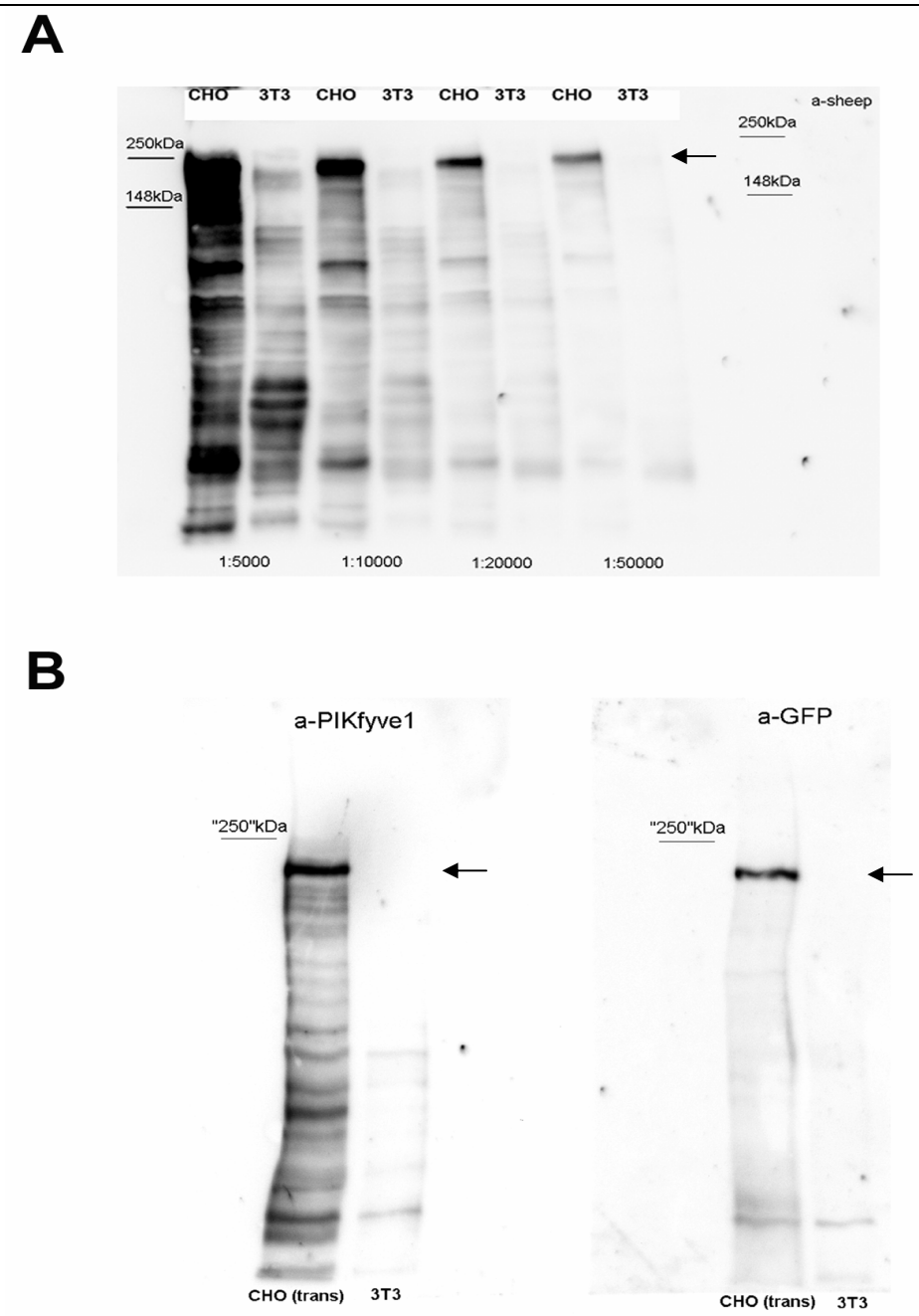

Figure 4.6 – α-PIKfyve[1] recognises transiently transfected GFP-PIKfyve in CHO cell lysates. CHO cells were transfected with GFP-PIKfyve as previously described. 16 hours post-transfection cells were lysed and a protein assay determined the amount of total protein. 50 µg of total protein for CHO and 3T3 (from stocks of known concentration) cell lysates were ran on gels. ***A***. A broad range marker was ran in Lane 1 and the two highest molecular weights indicated. Lanes 2, 4, 6 and 8 contained GFP-PIKfyve transfected CHO cell lysates and incubated with α-PIKfyve[1] at dilutions indicated on the bottom. Similarly, lanes 3, 5, 7 and 9 contained untransfected 3T3 cell lysates. The lane furthest to the right was blotted with the secondary antibody only for CHO lysate. ***B***. GFP-PIKfyve transfected CHO cells and 3T3 cells were run for an extended period of time on a low percentage Tris-glycine gel and blotted for either α-PIKfyve[1] (left) or α-GFP (right) along with broad range protein markers (250 kDa band indicated although this is suspected to run higher than it should). Arrows indicate the proposed band that represents GFP-PIKfyve.

fairly accurately with expected protein molecular weights, it is a possibility the broad range marker does not migrate as far as expected during SDS-PAGE.

To further confirm that the intense band seen in the transfected CHO lysate was indeed GFP-PIKfyve, the lysate was run again in separate lanes where one lane was incubated with the α-PIKfyve[1] antibody and another with an α-GFP antibody. The two lanes were realigned with each other and exposed together to see if the band recognised by α-PIKfyve[1] in the transfected CHO cell lysate was also detected by α-GFP. As shown in Figure 4.6*B* it appears quite clear that the band recognised by α-PIKfyve[1] is indeed GFP-PIKfyve as α-GFP also detects this band. This additionally suggests that either GFP-PIKfyve runs lower than its estimated molecular weight of 263 kDa or that the broad range protein markers used run higher than expected. Thus when using the broad range protein markers it may be assumed that endogenous PIKfyve of estimated molecular weight 235 kDa would run slightly further below the 250 kDa band.

Having confirmed that the intense band seen on the Western blots performed appeared to be GFP-PIKfyve, it was hypothesised that an antibody that produced a cleaner blot with less background may also give a better indication of endogenous PIKfyve. It is usually the case that later bleeds from an immunized animal can be more specific for the antigen the animal is immunized against. This is due to the fact that over repeated exposure to the antigen, the B-cell population matures to produce and replicate those clones that bind the most tightly to the antigen. In later bleeds then, many antibodies produced from B-cells that were not as specific in earlier bleeds are no longer produced as the B-cells were destroyed in the antibody selection process. A more specific antibody, or rather population of antibodies being a polyclonal antibody population, should result in less background and ultimately better protein detection (for example, Western blotting). As the original

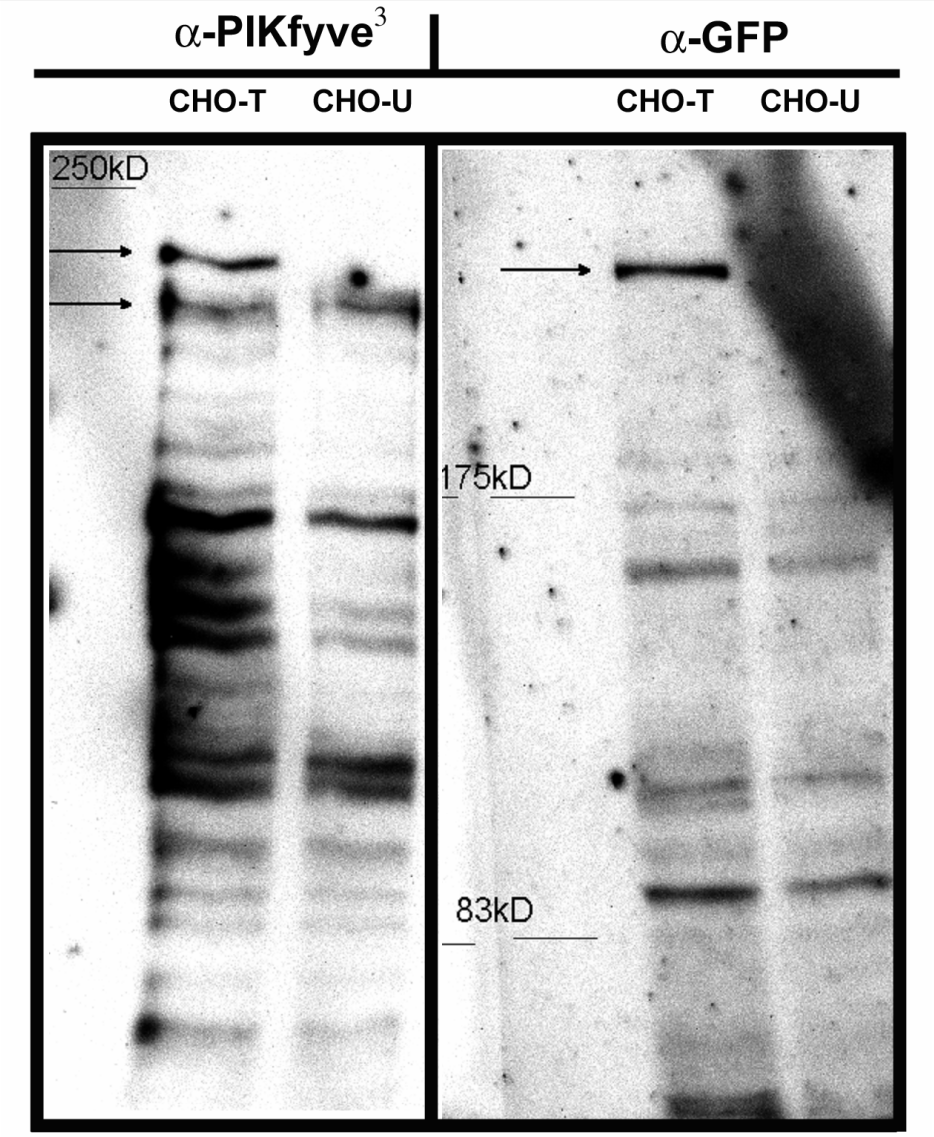

Figure 4.7 - α-PIKfyve^3 recognises GFP-PIKfyve on Western blots as well as apparent endogenous PIKfyve. Purified α-PIKfyve^3 (left) was used for Western blots to detect GFP-PIKfyve and endogenous PIKfyve in transfected and untransfected CHO cell lysates ("CHO-T" and "CHO-U" respectively). The same cell lysates were also used for detection of GFP with α-GFP antibodies (right) having been run on the same gel and transferred to nitrocellulose membrane where membranes were realigned when exposed for comparison of bands between the two antibody incubations. Both broad range markers (left) and pre-stained protein markers (right) were used and the molecular weights where the bands ran are indicated. The upper arrow in the left panel and the arrow in the right panel indicate GFP-PIKfyve as seen in CHO-T lanes. The lower arrow in the left panel indicates the proposed recognition of endogenous PIKfyve. Note that equal total protein was loaded for each lane on the basis of BCA protein assay (50 µg per lane).

first bleed was purified already, the decreased background expected from a later bleed may be marginal; however as the antigen-coupled column can be reused it was of minimal effort to also purify antibodies from later bleeds. The third bleed was hence purified similarly to the first bleed and this antibody was tested on western blots of GFP-PIKfyve transfected and untransfected CHO cell lysates.

As seen in Figure 4.7, the α-PIKfyve^3 purified antibody appears to give an overall cleaner blot with recognition of transfected GFP-PIKfyve in CHO cell lysates. Additionally, it is possible that the antibody is detecting endogenous PIKfyve at a dilution of 1:4000 (0.5 µg/ml from the stock α-PIKfyve^3 being 2 mg/ml). It should further be noted however that the transfection of GFP-PIKfyve typically resulted in < 0.1% of cells being successfully transfected. Various methods and optimisations were performed however the transfection efficiency was always very low. It is interesting to note then the comparable intensities of the bands for GFP-PIKfyve and suspected endogenous PIKfyve on the Western blot in Fig. 4.7. These bands appear to be of similar intensities, suggesting that if 1 in every 1000 cells were successfully expressing GFP-PIKfyve, that this expression was in the region of 1000-fold over endogenous PIKfyve expression in CHO cells. If then α-PIKfyve^3 was recognising endogenous PIKfyve, it may be assumed that this recognition is quite sensitive and can detect low levels of PIKfyve.

4.2.4 Characterisation of α-PIKfyve^3 for use in immunofluorescence studies

As the α-PIKfyve^3 antibody had been already shown to recognise the SDS-solubilised form of PIKfyve, to further characterise α-PIKfyve^3, immunofluorescence studies were performed. HeLa cells were transfected with the GFP-fusion PIKfyve protein to help determine the ability of α-PIKfyve^3 to recognise the native folded protein expressed in

the context of mammalian cells. Successful transient transfections of GFP-PIKfyve into mammalian cell lines had proved to be very difficult as already discussed. Despite varying the cell types used, transfection reagents and methods, ratios of transfection reagent to DNA and increasing the amount of DNA itself, the transfection efficiency of GFP-PIKfyve was always much less than 1%. On a typical 13 mm coverslip of ~80% confluency, there may have only ever been between one and ten successfully transfected cells, and this number was on the low side and often even zero when using a kinase dead mutant form of GFP-PIKfyve (GFP-PIKfyve^{mut}).

Despite these transfection issues, the ability of α-PIKfyve^{3} to recognise PIKfyve in a cellular context was still investigated based on the few transfected cells observed at different antibody dilutions (Fig. 4.8). A high dilution of the α-PIKfyve^{3} antibody at 1:2000 (stock antibody concentration of 2 mg/ml) resulted in some apparent low-level recognition of diffuse cytosolic protein in untransfected cells (Fig. 4.8*a*), confirmed by lack of staining with secondary only antibodies (not shown). Furthermore in some cells, there appeared to be concentrated areas of protein recognition by the antibody, as indicated by arrows in Fig. 4.8*a*. This was observed in a significant proportion of different untransfected cells and thus was not a rare phenomenon. There certainly did seem to be some small punctae with increased antibody binding, suggesting that if indeed the antibody was recognising endogenous PIKfyve, that it may be present in higher concentrations on specific membrane compartments. Previous work that was carried out during the work for this thesis looked at PIKfyve's localisation using GFP-PIKfyve and found it to localise to early endosomal compartments, which is in agreement with the findings in 3.2.3 which found colocalisation with SopB, shown to be early endosomally localised.

At the same dilution of 1:2000 of α-PIKfyve^{3}, there appeared to be potential recognition of the exogenously expressed GFP-PIKfyve as demonstrated in Fig. 4.8*b*. The sensitivity of the recognition was

apparently improved and a 1:1000 and 1:500 dilution (Fig. 4.8*c*-*e*), although the staining was starting to appear rather strong with the 1:500 dilution. Overexpression of GFP-PIKfyve can often result in slightly enlarged cellular structures and possible membranous compartments enriched with GFP signal, as seen in Fig. 4.8*d*. The α-PIKfyve^{3} antibody did however appear to partially recognise these protein enrichments at the 1:500 dilution (Fig. 4.8*d*) however whether this was a specific recognition was not determined. Furthermore, at such high levels of protein expression, it cannot be ruled out that these structures may simply be protein aggregates. At the lowest dilution of 1:100 however, the staining of PIKfyve appeared to be very strong, perhaps too strong for both the GFP-PIKfyve and endogenous PIKfyve (Fig. 4.8*f*).

As a result of these studies it appeared that the optimal dilution for use of α-PIKfyve^{3} in immunofluorescence studies was between 1:500 and 1:1000, with the latter being probably most suited for both exogenous and endogenous staining. Similar experiments were carried out with transfection of GFP-PIKfyve^{mut}, however in this case there were no positively transfected cells observed.

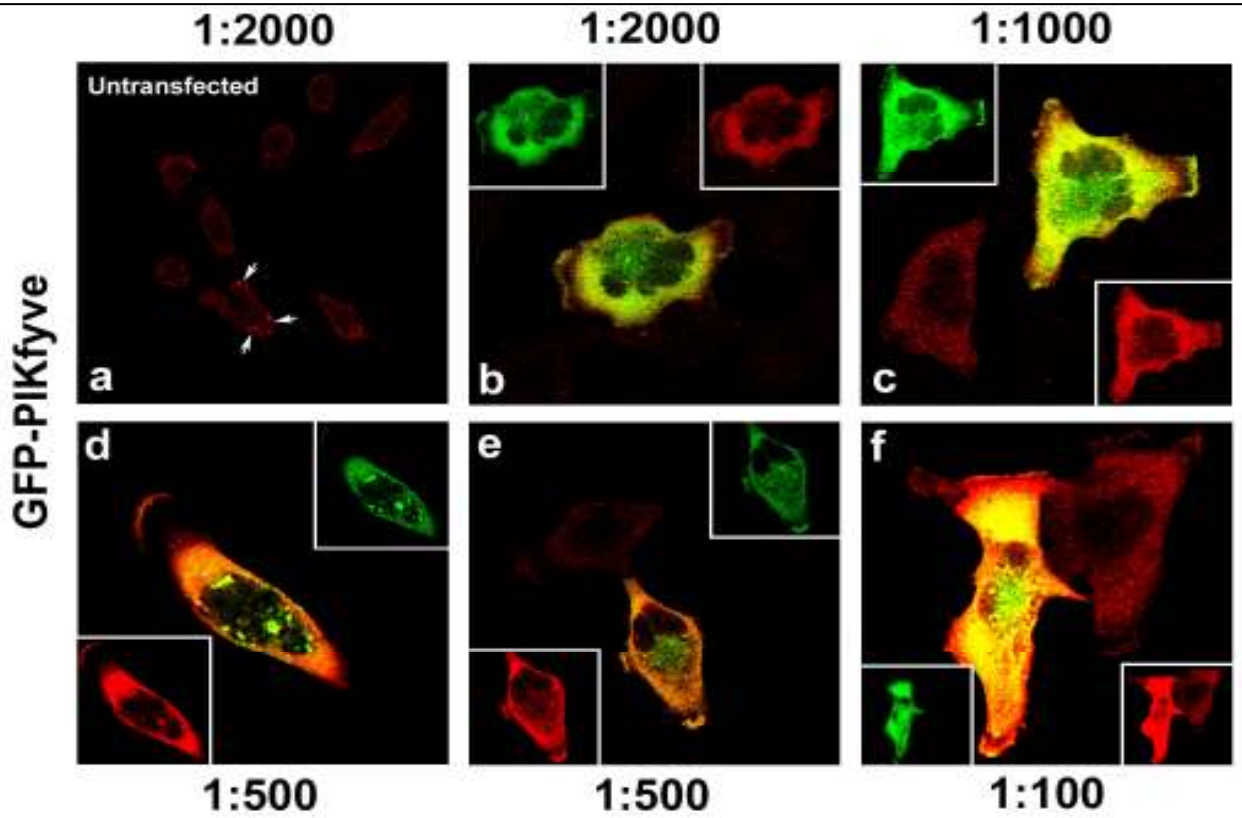

Figure 4.8 – The recognition of GFP-PIKfyve and endogenous PIKfyve at various antibody dilutions of α-PIKfyve[3]. HeLa cells were transfected with GFP-PIKfyve (green) and then fixed and stained with α-PIKfyve[3] followed by α-sheep Alexa® Fluor 594-conjugated IgG antibodies (red) and viewed under a confocal microscope. α-PIKfyve[3] dilutions are indicated above or below relevant panels. Insets in corners of panels represent the red and green channels of the corresponding transfected cells.

4.3 Discussion

The use of antibodies in research is clearly an important tool. Over-expression studies that involved tagged proteins are very useful approaches but offer limitations in interpretation of results due to the large amounts of dominant negative proteins or even wild-type proteins that result from an over-expressing cell. Additionally in studies such as gene silencing and knockdowns, it is often essential to show the lack of expression of the target gene via absence of the corresponding protein, for which an effective antibody is hence needed. Being able to detect endogenous proteins is a much more useful ability for a wide range of applications and coupled with studies such as over-expression and RNA silencing techniques, a better understanding of the protein at hand can be obtained by such methods. Additionally, the use of affinity isolations and pull-down experiments provide useful clues to potential protein interaction partners and cellular localisation of proteins. Having an antibody that one can be confident in detecting the protein of interest is vital for such studies.

As the field of research with regards to the lipid kinase PIKfyve is still relatively new and limited, the availability of good antibodies to this protein is somewhat scarce. Most publications that have made use of PIKfyve antibodies to date have relied on in-house production of such antibodies, with no apparent reliable commercial antibodies for PIKfyve seemingly available. A common animal to raise polyclonal antibodies in is rabbit, however much of the work done in our lab involves the use of other antibodies of which many have been raised in rabbit. Producing another antibody then that is from the rabbit species brings in limitations to the use of such an antibody in conjunction with detection of other proteins using common biochemical techniques such as immunofluorescence, immunoprecipitation and even Western blotting. Due to this reasoning, the animal used for α-PIKfyve production was a sheep.

The production of an antibody that recognises and specifically binds PIKfyve appears to have been successful, as demonstrated by these characterisation studies. This antibody has also been given to other labs that carry out research on PIKfyve. This antibody has been shown to recognise the same band that another antibody raised against PIKfyve recognises, and is currently being extensively used in the research of this lab (Prof Jeremy Tavare, personal communication).

As already discussed, the exact role of PIKfyve within the cell is not well established and under much scrutiny within the literature. There potentially are roles for PIKfyve in the endo-lysosomal trafficking pathway of some description. However given the conflicting findings of various studies on PIKfyve it is hard to draw firm and meaningful conclusions that take into account most of these findings. Some results may be cell-type specific, for example studies that suggest PIKfyve's involvement in EGFR trafficking to the nucleus may be rather specific to a certain cell type as it is hard to envisage a transmembrane protein being trafficked to the nuclei of many different cell types [87]. On the other hand the methods used as well as potential various roles for PIKfyve from some studies may explain the conflicting results, such as subcellular localisation of PIKfyve having been reported previously to be late endosomal with more recent studies suggesting an early endosomal association [84-86]. The personal data that has been found from not only this particular study described in this chapter but also in other chapters (for example Chapter 3) would be in agreement with an early endosomal localisation of PIKfyve. This would make sense given the FYVE domain that PIKfyve possesses; a domain that is known to bind the early endosomally localised lipid PtdIns(3)P. It may be the case that over-expression of mutant forms of PIKfyve results in a membranous bound PIKfyve that is associated with a compartment that ultimately matures into a late endosomal structure. This could explain the finding in over-expression studies of the kinase-dead mutant PIKfyve that it localises with late endosomal markers. In this scenario, the advantages of silencing endogenous genes become obvious.

A recent study has shown that PIKfyve appears to be necessary for the degradation but not silencing of endocytosed receptors, suggesting that PIKfyve is not needed for delivery of cargo into the MVB lumen [84]. Rusten *et al* showed that in mutant drosophila cells that did not contain the *fab1*/PIKfyve gene, enlarged MVBs were seen however there was a distinct lack of ubiquitylated cargo and endocytosed receptors were delivered into the lumens of MVBs [84]. Additionally, the lysosome was not correctly acidified and despite these endocytosed receptors being efficiently silenced, degradation was impaired in the mutant cells. This study displays parallels to Bache *et al*, who demonstrated similarly that the ESCRT-III component hVps24 (CHMP3) is not necessary for the silencing of EGFR but is needed for its degradation. By using gene silencing of CHMP3, Bache *et al* also showed that in CHMP3-depleted cells, EGFR was efficiently silenced despite the lack of CHMP3, in comparison to the ESCRT-I component TSG101 where silencing of this gene resulted in sustained activation of EGFR [56]. They then suggest that earlier ESCRT components (ESCRT-I for example) are necessary for delivery of cargo into the lumen of MVBs, however the ESCRT-III component CHMP3 plays a role in the fusion of the MVB with the lysosome. These two studies of PIKfyve and CHMP3 seem to suggest when taken in conjunction with each other that PIKfyve and ESCRT-III may be closely linked. Certainly this would explain then some of the findings that suggest that PtdIns(3,5)P_2 may play a role in this pathway and additionally add support to CHMP3 being an effector of PtdIns(3,5)P_2 despite the only current evidence for this comes from *in vitro* lipid binding studies [71].

4.4 Conclusion

Despite the confusing state of the literature with regards to PIKfyve, it is clear that this protein plays an important role in the proper function of endo-lysosomal pathways. This suggests that the phosphorylated products of PIKfyve, such as PtdIns(3,5)P_2 are hence important and perhaps more promiscuous than previously thought. The production and characterisation of a polyclonal antibody population that specifically and clearly recognises this protein even at endogenous levels is a very useful tool to have for further investigation of PIKfyve. This antibody is already being used by several other labs and has proven to be very effective for its given purpose, and certainly should be continued in its use to further our understanding of PIKfyve and help elucidate its precise role or roles within mammalian cells.

CHAPTER 5

5 Development of a pull-down assay of the Vps4^{E235Q} compartment as a potential proteomic approach for identification of novel ESCRT and MVB-related proteins

5.1 Introduction

The biogenesis and maturation of the mammalian MVB compartment is already known to be a highly complex process that is not completely understood. The formation of MVBs in mammalian cells bears many similarities to that in yeast, and certainly contains highly homologous proteins. However in comparison to yeast it is already evident that the mammalian MVB pathway is even more multifaceted and contains a wider spectrum of protein involvement and interactions. Many of these proteins and associated interaction partners are only recently beginning to be described and discovered. Additionally it has been strongly suggested and implicated that ESCRT proteins are involved in other non-endosomal functions as well as MVB formation. As a result, some interaction partners identified through yeast two-hybrid and other similar studies may not actually play a role in MVB biogenesis [reviewed in 4; 42].

Ideally, it would be advantageous for one to be able to observe the MVB compartment and the proteins found therein, allowing us to study the properties and functions of such proteins in terms of MVB formation and maturation, resulting in a better and more complete understanding of how this process occurs. Obviously the complexities of the MVB formation process itself limit such an approach of isolating an *in vivo* compartment; a compartment that is dynamic. Furthermore, despite the identification of ESCRT protein complexes, it is not clear as to whether or not these complexes purely consist of the identified ESCRT proteins. In

fact it is possible that there are other unidentified proteins involved in these complexes. New ESCRT proteins previously not known to be involved in the ESCRT complexes have recently been identified as being necessary for proper MVB function [144-146]. Being able to identify proteins directly involved with the endogenous ESCRT complex is an important undertaking; however current technology and reagents such as good antibodies to endogenous ESCRT proteins have not currently allowed such an approach. These approaches are also limited to pre-existing knowledge, for example in the case of antibodies you can only probe a complex or cellular compartment with an antibody to a known protein.

One approach that may yield a method for identification of proteins involved in ESCRT complexes and hence MVB formation is to isolate a stable compartment that is known to contain ESCRT components. It is widely accepted that the expression of an AAA-ATPase dead mutant form of Vps4 ($Vps4^{E235Q}$) results in a swollen endosomal phenotype in mammalian cells [53, 135]. This observed swollen endosomal structure can be referred to as the $Vps4^{E235Q}$ compartment. It is accepted that exogenous expression of this dominant negative protein results in a defective Vps4 protein that binds to membranes but cannot be removed due to its lacking ATPase activity. As the role of Vps4 is the removal of ESCRT components from the MVB limiting membrane, it should be expected that ESCRT proteins would colocalise with the dominant negative protein on swollen endosomal membranes, which has already been shown [53, 71, 73]. As Vps4 interacts with the ESCRT-III components for its localisation through its MIT domain [89, 91], its localisation is dependent upon ESCRT-III localisation. The removal of ESCRT proteins from the MVB membrane is necessary to complete cargo delivery to the lumen and a defective Vps4 is unable to facilitate this reaction [53, 135]. Furthermore, it has been previously shown that the $Vps4^{E235Q}$ compartment stabilises a structure of >670 kDa involving other proteins additional to CHMPs [147].

Given these findings, it was hypothesised that an affinity pull-down assay could be constructed that allowed for the isolation of intact Vps4^{E235Q} compartments that not only contained existing ESCRT components such as CHMPs but possibly other proteins not yet identified that are involved in MVB formation and associate with ESCRT complexes. This could ultimately then lead to a large-scale screening of the proteomic complement found on such a compartment, with possible identification of novel proteins contained on this compartment not yet identified as ESCRT-related proteins.

This chapter describes the work carried out to develop such an affinity pull-down assay of the Vps4^{E235Q} compartment. By transient transfection methods, a GFP-fusion Vps4^{E235Q} protein was expressed in mammalian cells and the resulting swollen endosomal compartment was pulled down using immunoprecipitation methods. Utilising a new tag developed by Promega called HaloTag® to better isolate Vps4^{E235Q} compartments, it was shown using 2-d SDS-PAGE gel methods that a large number of proteins can be detected from the Vps4^{E235Q} compartment. Hence such an assay may provide useful information on the proteomic complement associated with ESCRT complexes.

5.2 Results

5.2.1 The Vps4^{E235Q} GFP-fusion protein can be efficiently immunoprecipitated from non-detergent lysed cells

It was hypothesised that the membrane bound compartment that contains the GFP-Vps4^{E235Q} protein would be best isolated as an intact compartment to ensure any stability of a complex reliant on the compartment's lipid membrane was maintained. As a result of this, a detergent-free lysis method was employed. This involved using a non-detergent lysis buffer for gentle cell lysis, known as TES. Furthermore, it has been implied from a previously isolated ESCRT-complex that such a complex may need the presence of ATP to maintain assembled stability [147], thus 2 mM ATP was also added to this lysis buffer, resulting in a buffer termed TESA. Cells were gently lysed on ice in this buffer and then homogenised using a syringe homogeniser, which sheared the cells through a ball-bearing with a clearance distance of 4 µm. Further details of this process and the immunoprecipitation with α-GFP antibodies can be found in 2.2.8.

Initially, the transfection of GFP-Vps4^{E235Q} was optimised and it was determined that the use of Lipofectamine 2000™ was the optimal reagent for the most efficient transfection of GFP-Vps4^{E235Q}. Additionally, the α-GFP antibody used for Western blotting was tested on the detergent-free lysed cells that had been transfected using the Lipofectamine reagent to determine how well this antibody would detect GFP-Vps4^{E235Q}. A range of protein amounts from the cell lysates (25-75 µg protein) was loaded, and as seen in Figure 5.1, this antibody gives a very distinct band just below the 83 kDa marker with little background. The estimated MW of GFP-Vps4^{E235Q} is 76 kDa.

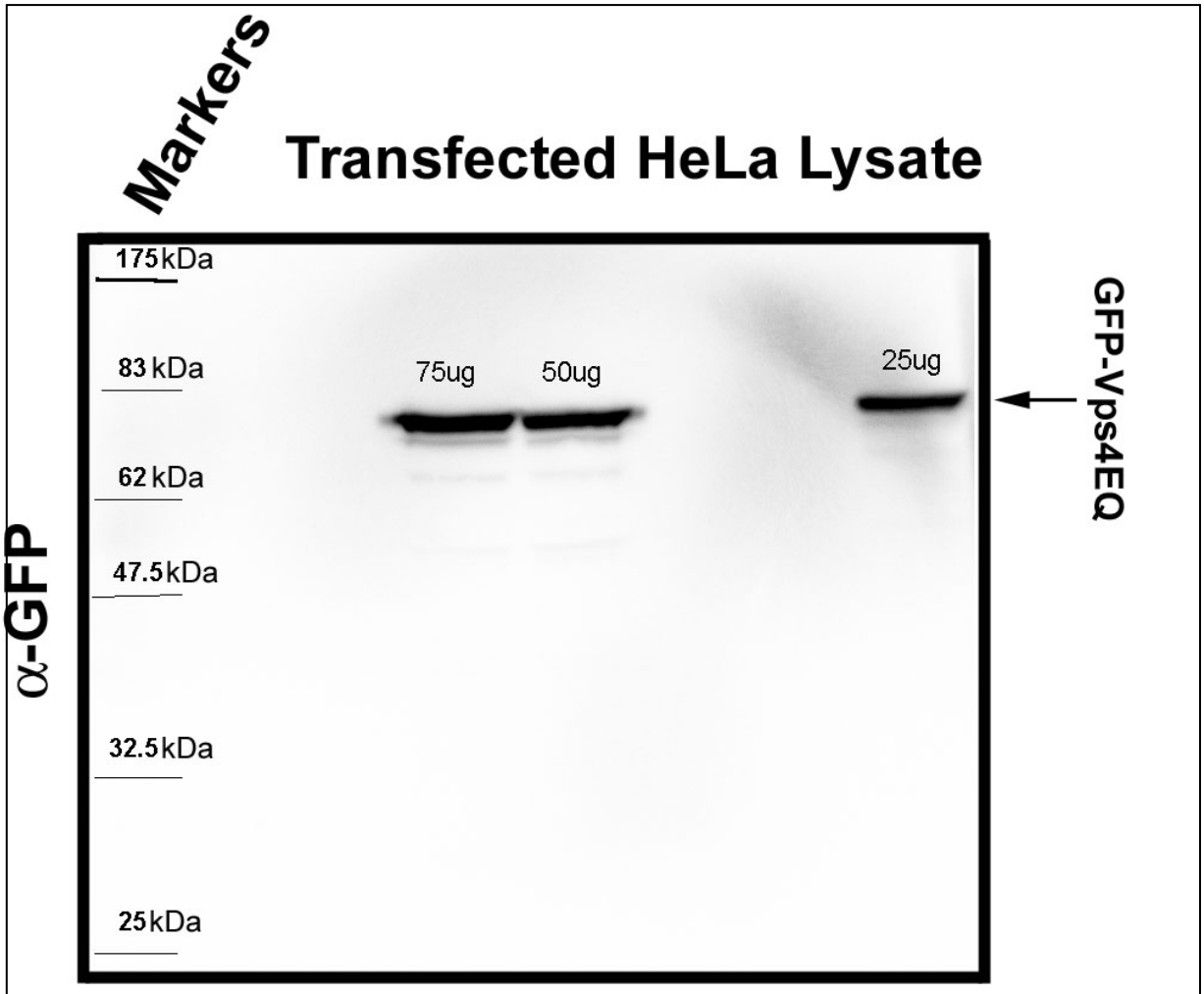

Figure 5.1 – Transfection with GFP-Vps4E235Q using Lipfectamine 2000™ in detergent-free lysed HeLa cells is detectable by Western blotting. HeLa cells were grown in a 25 cm^2 flask to 60-80% confluency and then transfected using Lipofectamine 2000™ reagent by standard protocol, allowing to express for 18 hours. The following day cells were trypsinised, pelleted and resuspended in a small volume of TESA buffer, with protein concentration determined by BCA methods. 75 µg, 50 µg and 25 µg of total protein was run on an SDS-PAGE gel, transferred, and blotted with rabbit α-GFP and α-rabbit-HRP, as indicated on the above blot (75ug, 50ug, and 25ug respectively). The bands appear between the 62 and 83 kDa markers suggesting a correlation to GFP-$Vps4^{E235Q}$, which has an estimated MW of 76 kDa. The same process was previously carried out using FuGene® 6 as the transfection reagent however no obvious GFP-$Vps4^{E235Q}$ was detected using this method (not shown).

Following successful transfection and Western blot detection of GFP-Vps4^{E235Q}, immunoprecipitations of GFP-Vps4^{E235Q} were performed to determine if GFP-Vps4^{E235Q} could be successfully immunoprecipitated using the α-GFP$_{IgG2a}$ antibody. Briefly, Protein G beads were bound with the mouse α-GFP$_{IgG2a}$ antibody and immunoprecipitations were performed on this affinity complex. As the antibody used for the precipitations was a mouse monoclonal antibody, rabbit polyclonal antibodies could be used for Western blots, as antibodies from non-mouse species should not detect the IgG bands that may have been detected with mouse antibodies, which could potentially provide confusing results. As seen in Figure 5.2, it is evident that there is a loss of GFP signal from the fraction not bound to the Protein G beads ('Unbound' lane). In contrast, the bound lanes show a signal of GFP detection, which appears to correlate to the correct size of GFP-Vps4^{E235Q} in the bound lanes ('Bound IP' lanes). Thus these results demonstrate that GFP-Vps4^{E235Q} can be successfully pulled out of a cell lysate using immunoprecipitation methods.

As CHMP proteins and other ESCRT components are generally small proteins, it is possible to blot for these proteins in the same lanes on Western blots where the GFP-Vps4^{E235Q} was being blotted for. By separation of the blot below the 47.5 kDa marker in addition to separation of the various bound immunoprecipitate lanes, various CHMPs could be probed for, using CHMP antibodies already developed and characterised in the lab. It was apparent that in the corresponding pull-down of GFP-Vps4^{E235Q} that there was possible enrichment of endogenous CHMP3, as demonstrated by the detection of a faint band at the approximate size of CHMP3 (Fig. 5.2). However, upon blotting the immunoprecipitate with the α-CHMP4A antibody, there appeared to be little to no band present, suggesting that CHMP4 was not pulled down. It should be noted that for detection of CHMP bands that the use of ECL Advance® solutions was necessary as regular ECL development resulted in no apparent bands.

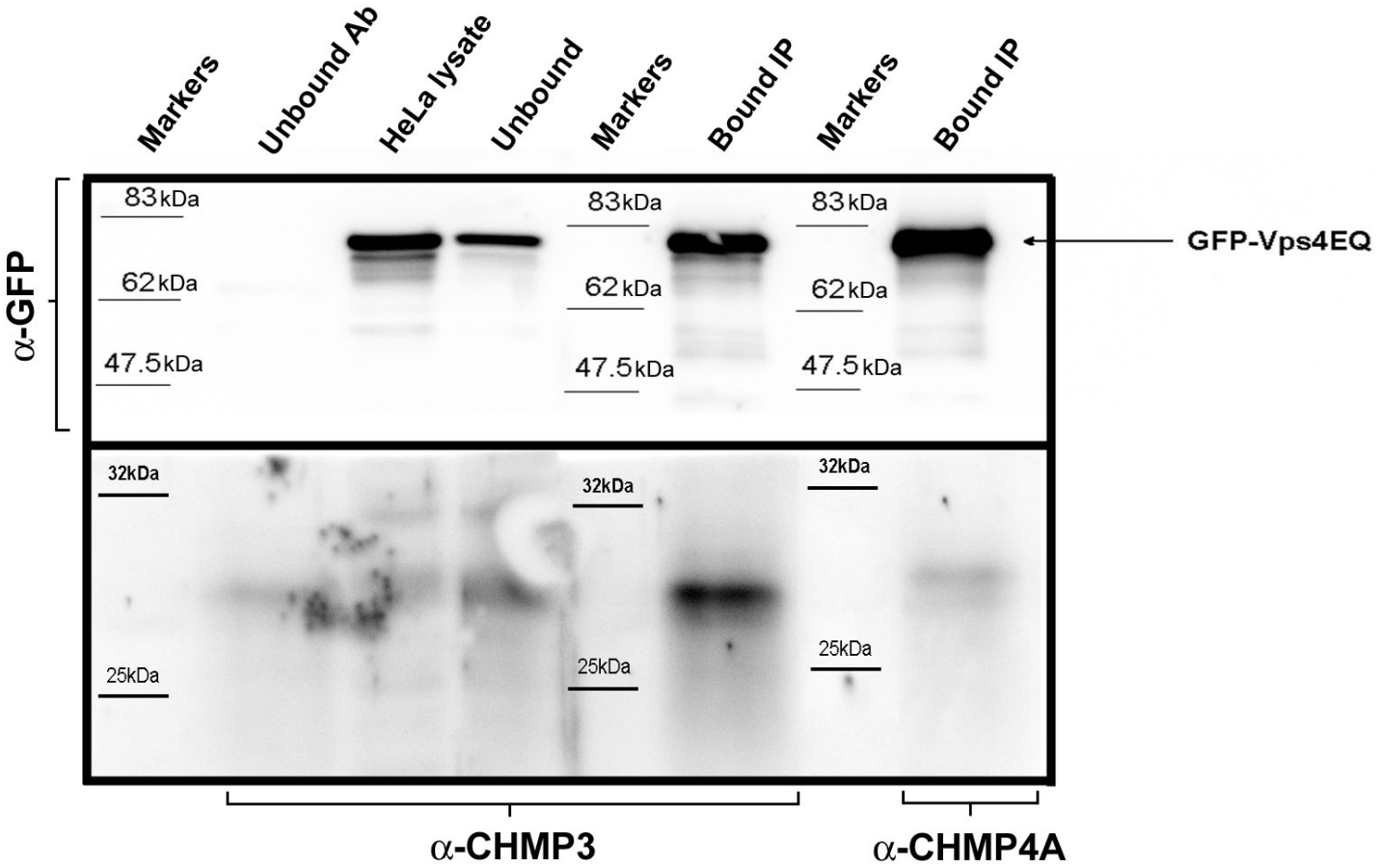

Figure 5.2 – GFP-Vps4^{E235Q} can be efficiently immunoprecipitated from a cell lysate and pull-down associated CHMP3. HeLa cells were transfected with GFP-Vps4^{E235Q} as already described, and immunoprecipitated with α-GFP$_{IgG2a}$ bound to Protein G beads. 'Unbound Ab' lane is a sample of the antibody not bound to Protein G beads after the 3 hr incubation. 'Unbound' lane refers to lysate content not bound to beads after overnight incubation with the antibody-bead complex. 'Bound IP' refers to the bound immunoprecipitate, that is, what was bound to beads post-washes. Upper panel was incubated with α-GFP and lower panel with α-CHMP3 or α-CHMP4A as indicated.

To address whether or not the pull-down was a specific immunoprecipitation, an IgG only control was needed. Thus the experiment was repeated using mouse IgG binding to Protein G beads in parallel to mouse α- GFP_{IgG2a} antibody. Initial experiments resulted in a GFP positive band of similar intensity in the IgG control bound lane compared with the α- GFP_{IgG2a} lane, suggesting that the pull-down of GFP-$Vps4^{E235Q}$ may be a non-specific interaction with IgG molecules (not shown). However upon increasing the number of washes and adding a small amount of BSA into some of the washes of the beads, the specificity of the α-GFP_{IgG2a} antibody appeared to improve greatly, although there did still appear to be some small amount of non-specific immunoprecipitation occurring (Fig. 5.3). Despite possible recognition of enriched CHMP3 in the bound immunoprecipitate of previous blots (see Fig. 5.2, *lower panel*), endogenous CHMPs were not detected again in HeLa cells using this method including the IgG control. Although pull-downs of GFP-$Vps4^{E235Q}$ seemed successful, we cannot be sure that we were pulling down an intact ESCRT-machinery complex.

5.2.2 Characterisation of the HaloTag® labelling system with $Vps4^{E235Q}$ for isolation of the $Vps4^{E235Q}$ compartment

A recent product that had been introduced by Promega is a novel tag that allows for expression of a fusion protein of a 33 kDa tag termed HaloTag®. There are several advantages of this tag over other large tags; one being the use of HaloLigands® which can be biotinylated or fluorescent ligands. Such fluorescent ligands are membrane permeable and bind specifically to the Halo-tagged protein, allowing for quick, easy and versatile detection of a tagged protein. A further advantage of the HaloTag® is the product referred to as HaloLink® which is a resin that covalently binds the HaloTag® thus allowing a tagged-protein to be covalently bound to a resin as opposed to other affinity and immuno-interactions which are less stable than covalent

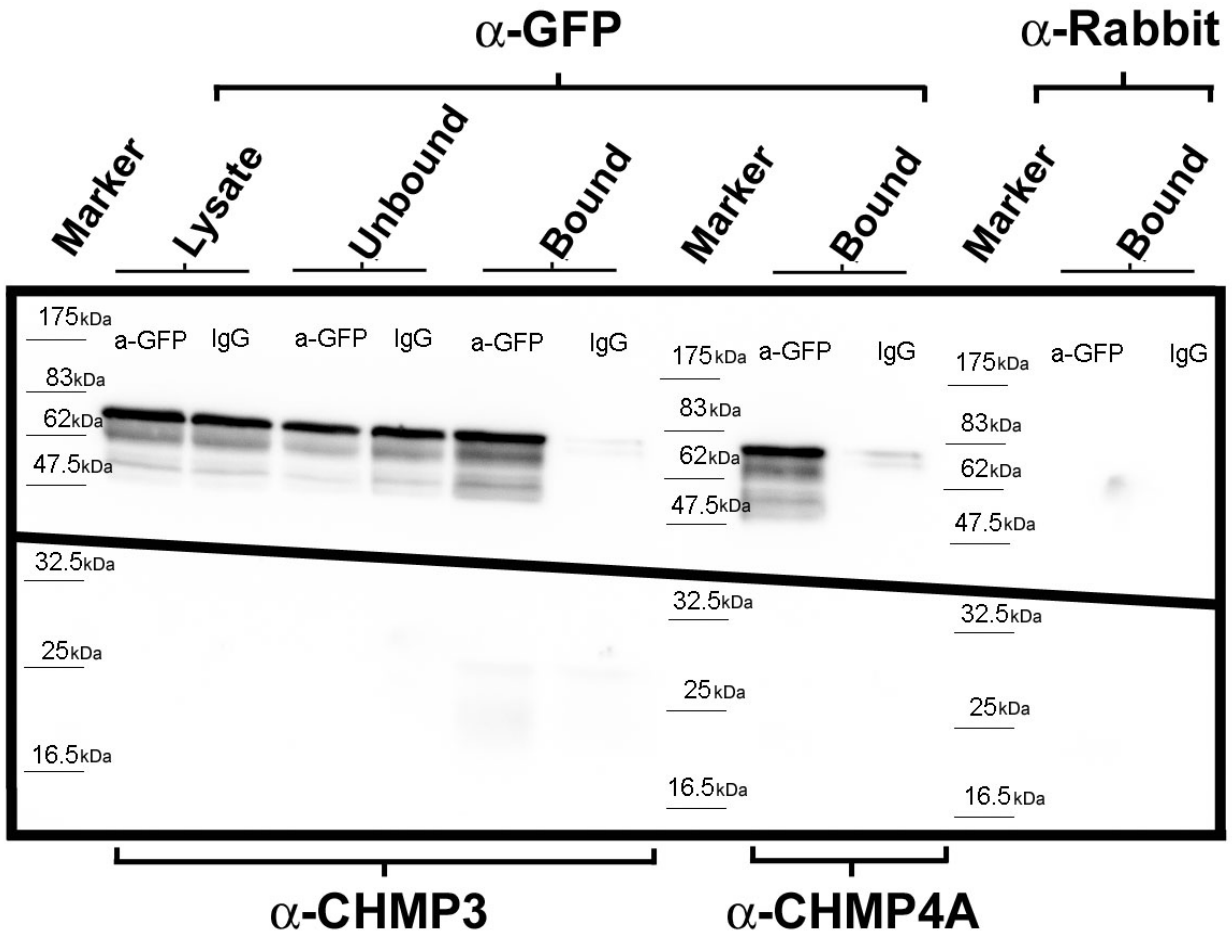

Figure 5.3 – Pull-downs of GFP-Vps4^{E235Q} are specific with the α-GFP antibody. HeLa cells were transfected and processed with detergent-free lysis buffer as already described. Lysates were incubated with IgG–Protein G or α-GFP–Protein G bead complexes and fractions run on SDS-PAGE gel, transferred, and blotted for using indicated antibodies. α-rabbit represents a secondary only control. 'a-GFP' refers to the α-GFP–Protein G beads; 'IgG' refers to IgG–Protein G bead control.

bonds. The HaloLink® resin then is a useful tool for pull-downs and can act as a replacement for using Protein G or Protein A beads in an immunoprecipitation pull-down assay. As the covalent link to the HaloTag® is specific, there should be a large decrease in non-specific proteins pulled down from a cell lysate. Using the pHT2 vector that contains the HaloTag® coding sequence, $Vps4^{WT}$ and $Vps4^{E235Q}$ were both cloned into this vector to give a fusion protein with the HaloTag® at the N-terminus of each protein when expressed. For details of this cloning, see Chapter 2.2.6. These Halo-tagged constructs were hence named Halo-$Vps4^{WT}$ and Halo-$Vps4^{E235Q}$.

To determine the phenotype of the Halo-$Vps4^{E235Q}$ protein when expressed in mammalian cells, constructs were transiently transfected into Cos-7 cells and examined by confocal microscopy after incubation with fluorescent Halo-ligands (Fig. 5.4*A*). As expected, the dominant negative expression of Halo-$Vps4^{E235Q}$ resulted in an enlarged endosomal phenotype, with a punctate staining obvious. There is however a difference in the phenotype visible by eye when observing positively transfected Halo-$Vps4^{E235Q}$ cells in comparison to GFP-$Vps4^{E235Q}$ expression, namely the size of swollen endosomes. In Cos-7 cells the expression of GFP-$Vps4^{E235Q}$ often results in giant aberrant endosomal structures with the overexpressed protein present on its membranes. However with expression of Halo-$Vps4^{E235Q}$ similarly in Cos-7 cells, the swollen vesicles did not appear to be as enlarged by comparison.

Additionally with transfection of Halo-$Vps4^{E235Q}$ it was typically noted that the general expression levels were lower than that often seen with GFP-$Vps4^{E235Q}$ transfection, with fewer more highly expressing cells present. Thus it was determined that the Halo-tagged constructs would be useful for trying to isolate the $Vps4^{E235Q}$ compartment using the HaloLink® resin, and subsequent studies were hence carried out with these constructs instead of the GFP-tagged constructs.

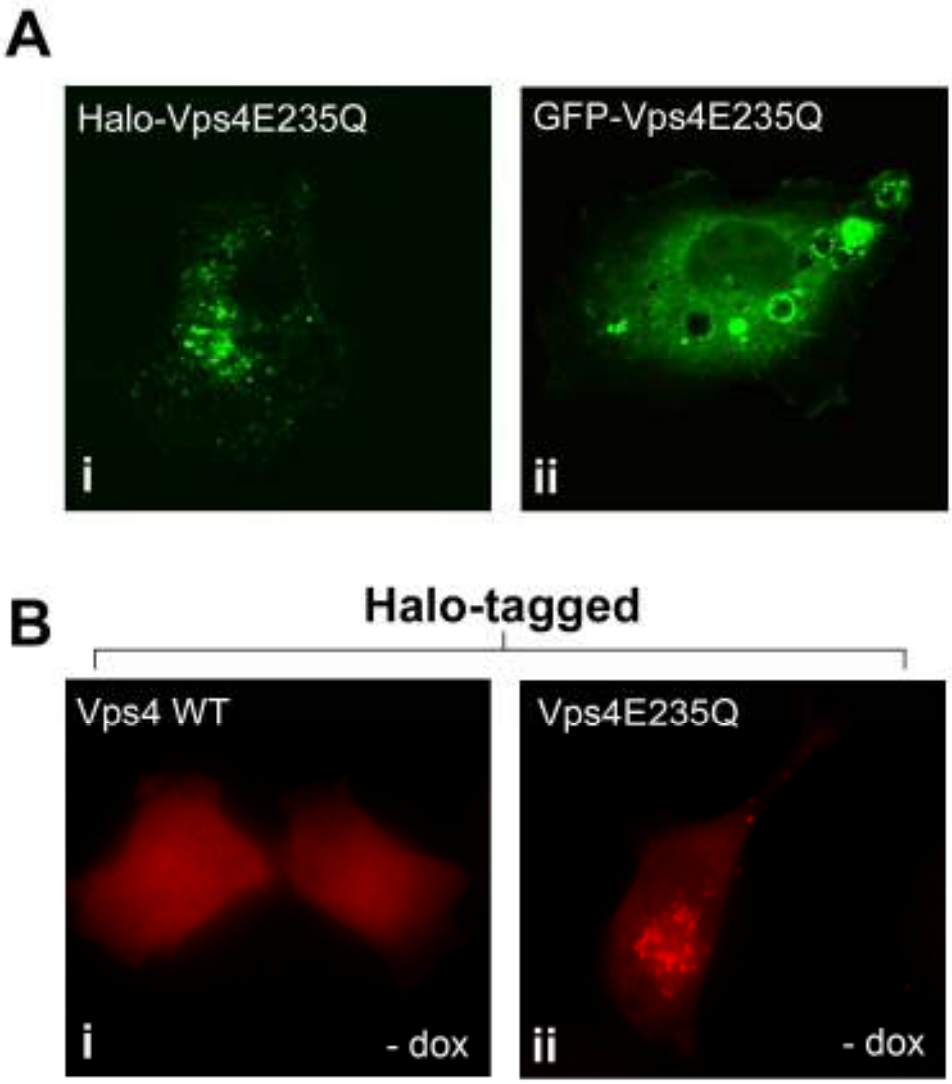

Figure 5.4 – Halo-Vps4E235Q expression gives enlarged endosomal structure and expression can be induced by removal of doxycycline when transfected into HeLa-Tet-Off® cells. *A*. Cos-7 cells were transfected with constructs as indicated and processed (described in 2.2.2). Expression of Halo-Vps4^{E235Q} and incubation with the green TMR® Halo-ligand (*i*; see 2.2.2.1) results in a punctate cellular localisation, with enlarged vesicles. GFP-Vps4^{E235Q} expression (green; *ii*) also results in enlarged vesicular structures however typically these structures are much more enlarged by comparison. *B*. HeLa-Tet-Off® cells were transiently transfected with Vps4^{WT} or Vps4^{E235Q} sequences cloned into the pTRE2pur vectors. Removal of doxycycline post-transfection allowed expression of appropriate proteins as indicated. Cells were incubated with the DiACFam red Halo-ligand and the Halo-Vps4^{WT} gives a diffuse cytoplasmic staining (*i*) whereas Halo-Vps4^{E235Q} localises to enlarged vesicular structures (*ii*).

5.2.3 Generation of stable cell lines that express Halo-Vps4^{WT} or Halo-Vps4^{E235Q} in an inducible manner

One problem with a transient transfection method for producing cell lysates with the Vps4^{E235Q} compartment is the inconsistency in and often low-level of successfully transfected cells. This will hence vary the endogenous proteins that will be detected by antibodies. This is because the degree of enrichment of these endogenous proteins associated with the complex will be dependant on the number of complexes in the cell lysate, which in turn is dependant upon the transfection efficiency. Having a stable cell line that expresses Vps4^{E235Q} would result in 100% of the cells expressing the Vps4^{E235Q} compartment thus allowing for a large quantity of these compartments to be isolated, enabling better detection of proteins that may be associated with the complex.

One potential dilemma with the use of a stable cell line is that the Vps4 protein is essential for proper cell function in terms of proper endo-lysosomal trafficking and receptor silencing. Continual expression of such a dominant negative protein is likely to be somewhat detrimental to a cell line, and it would be reasonable to expect that the cell would not grow and proliferate under such expression of a dominant negative Vps4 protein. The Tet-Off/On™ system provides a technique by which stable cell lines can be produced that possesses inducible protein expression. For these experiments the Tet-Off™ system was used which relies on the presence of tetracycline or doxycycline to keep the incorporated construct's expression constitutively turned off. By removal of tetracycline or doxycycline from the cell media, expression of the protein is no longer repressed and allowed to occur. For more details with regards to the Tet-Off™ system and methods used for cloning of the Halo-Vps4^{WT} and Halo-Vps4^{E235Q} constructs into appropriate vectors for production of stable cells, see Chapter 2.2.9.

For the generation of inducible stable cell lines, cells were transiently transfected and selected with appropriate antibiotic markers as outlined in 2.2.9. To test whether the constructs transiently transfected were indeed inducible, cells were transfected and fixed in both the presence (repression) and absence (expression) of doxycycline. This resulted in clear inducibility as the cells that had doxycycline removed for both Halo-Vps4^{WT} and Halo-Vps4^{E235Q} transfection both showed clear expression (Fig. 5.4*B*) compared with transfected cells in the presence of doxycycline which did not show any notable expression (not shown).

Despite screening of over 200 colonies that showed selectable antibiotic marker properties for both Halo-Vps4^{WT} and Halo-Vps4^{E235Q} stable cell lines, no colonies were found to obviously express either protein when doxycycline was removed from the cell media. Protein expression was assayed for by both immunofluorescence and Western blotting techniques using fluorescent Halo-ligands and α-Vps4 antibodies respectively. No fluorescence was seen in any of the colonies tested, and in the case of Western blotting, the endogenous Vps4 protein was detected, however the Halo-Vps4^{WT} or Halo-Vps4^{E235Q} protein (33 kDa heavier than endogenous Vps4) was not detected in the + or – doxycycline conditions (Fig. 5.5). Thus due to the time-scale and volume of unsuccessful screening for positive stable colonies being already greater than 6 months, it was decided to not further pursue this approach.

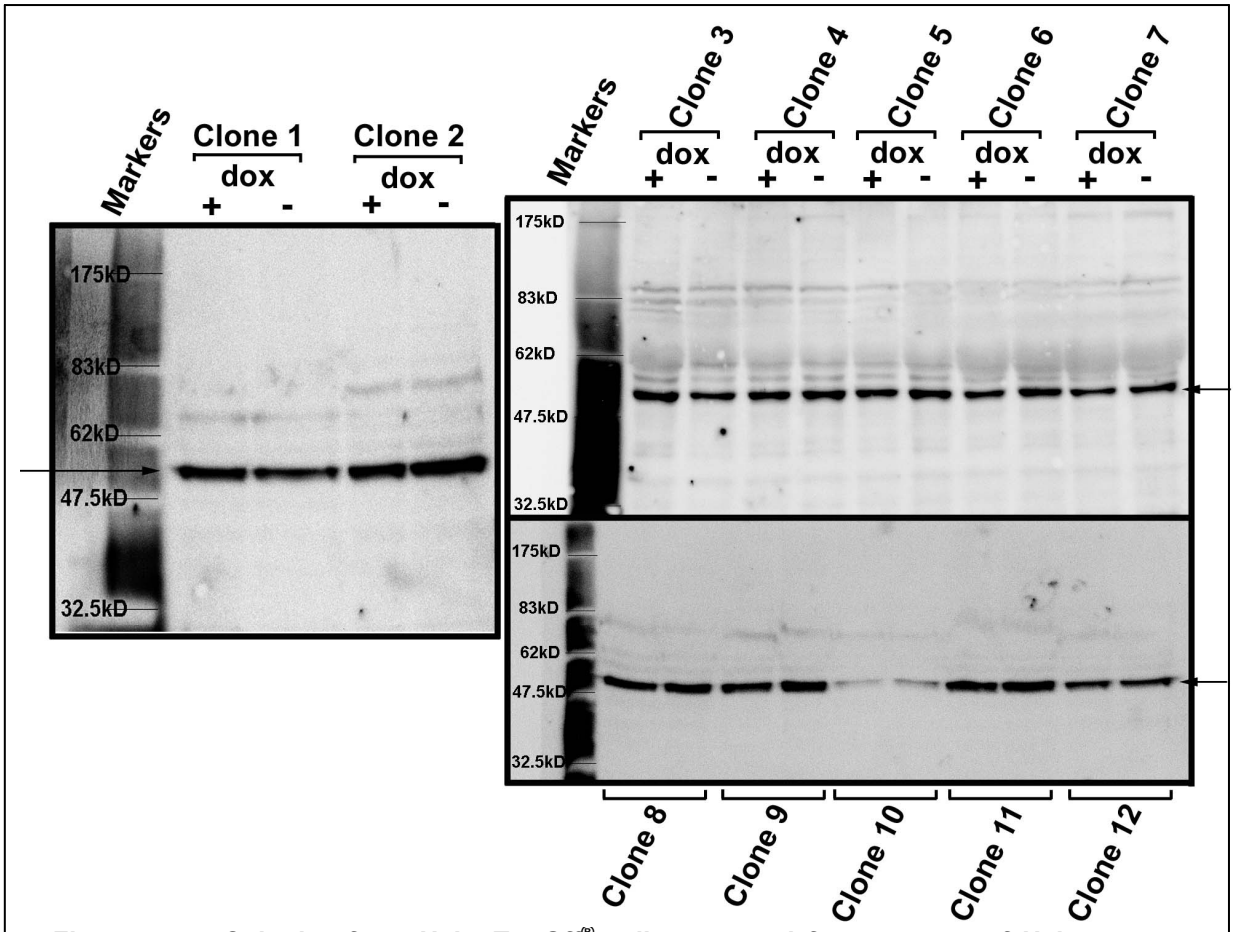

Figure 5.5 – Colonies from HeLa-Tet-Off® cells screened for presence of Halo-Vps4^{E235Q} in the presence and absence of doxycycline show no apparent expression. Colonies of HeLa-Tet-Off® cells showing resistance to selective antibiotic containing media were screened using Western blotting techniques by incubating 35 mm dishes with or without doxycycline for 24-48 hours prior to cell lysis. Protein content was determined by BCA methods and 30 µg of protein was loaded for each clone except clone 10 (which had too low a protein to load 30 µg). Lysates were run on SDS-PAGE gels, transferred and blotted using α-Vps4. The three blots represent twelve separate colonies, a fraction of the total number screened (>200). The estimated MW of Halo-Vps4^{E235Q} is 81 kDa; arrows indicate bands that represent endogenous Vps4. Doxycycline presence is indicated by 'dox +' (doxycycline present) or 'dox –' (doxycycline absent). No obvious bands are seen at the estimated MW of Halo-Vps4^{E235Q} that show doxycycline expression inducibility; any bands visible near the 83 kDa marker are fainter than endogenous Vps4 bands.

5.2.4 Pull-downs of Halo-Vps4^{E235Q} from detergent-free lysed cells shows the presence of ESCRT components TSG101 and CHMP3

From other studies carried out in the lab, it was found that NRK cells appeared to express higher amounts of some endogenous CHMP proteins when compared with other cell lines such as HeLa cells (Dr Judith Richardson, personal communication). Thus it was decided to use these cells for the pull-down experiments using the HaloLink® resin as an enrichment of CHMP proteins may be more easily detected. For full details of the methods used for pull-down with the resin see 2.2.8.

As the Halo-Vps4^{E235Q} protein binds covalently to the HaloLink® resin, one is unable to detect the transfection efficiency or successful pull-down by Western blotting as the Halo-Vps4^{E235Q} protein remains bound to the resin. However any proteins hence associated with the Halo-Vps4^{E235Q} compartment would be detected using SDS-PAGE and Western blotting methods as the gel sample preparation process disrupts the protein-protein and protein-lipid interactions. Using the HaloLink® resin to pull-down Halo-Vps4^{E235Q} compartments, the ESCRT-I component TSG101 and the ESCRT-III component CHMP3 were both detected to be enriched in bound fractions (Fig. 5.6). The ESCRT-III component CHMP4A however was not detected in the bound fraction of these experiments (Fig. 5.6*A*). These experiments were repeated with Halo-Vps4WT, however there was no detection by Western blotting of TSG101, CHMP3 or CHMP4A from these pull-downs (not shown). This suggests that the proteins detected in the Halo-Vps4^{E235Q} pull-downs are likely to be specifically pulled down due to Halo-Vps4^{E235Q} protein expression.

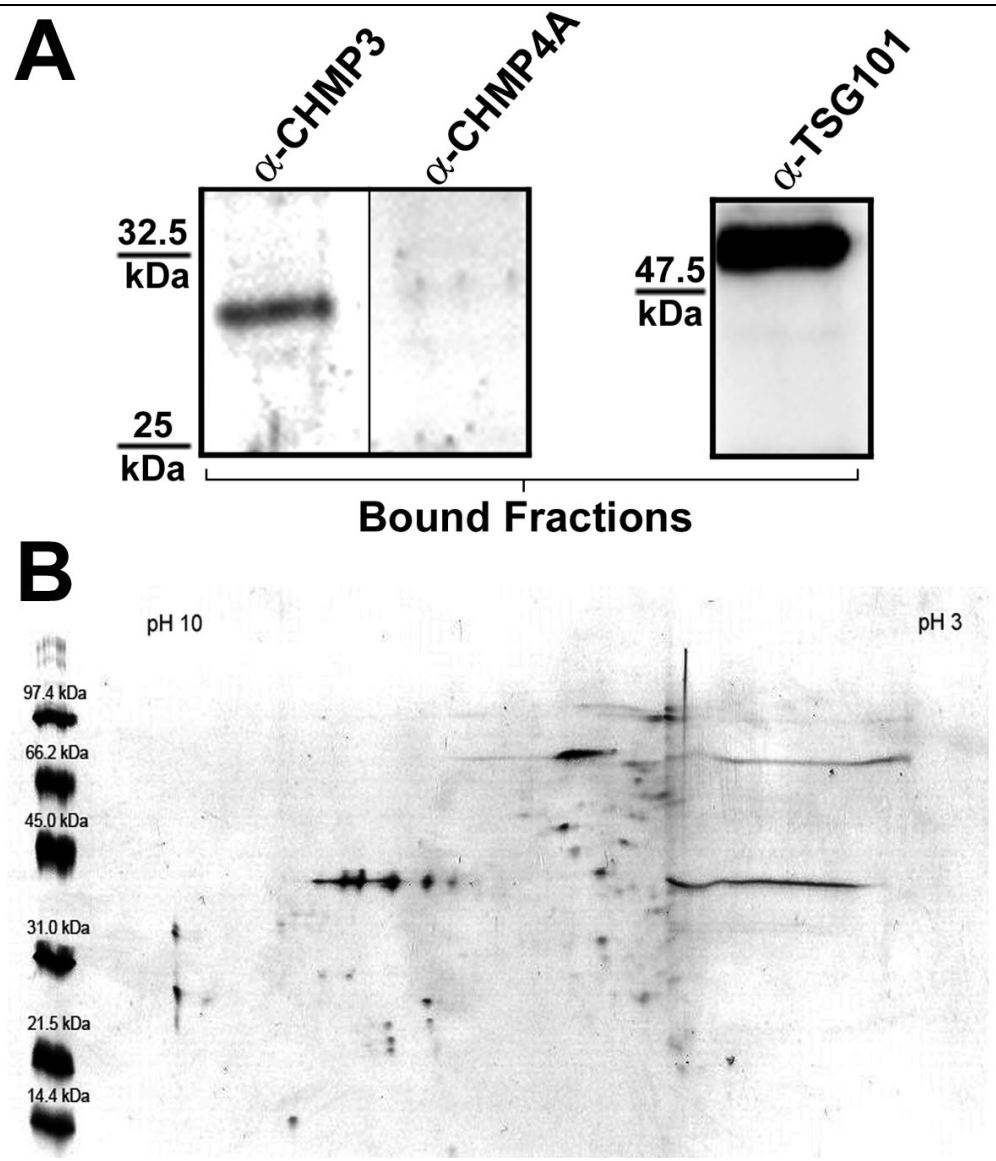

Figure 5.6 – Affinity pull-downs of Halo-Vps4^{E235Q} contain ESCRT proteins as well as a large number of other unknown proteins. NRK cells transfected with Halo-Vps4^{E235Q} were subjected to detergent free lysis and affinity purified for Halo-Vps4^{E235Q} via HaloLink® resin by methods described. *A*. The bound fractions were solublised from the resin using SDS sample buffer and boiling. Samples were run on an SDS-PAGE gel, transferred, and Western blotted for CHMP3, CHMP4 and TSG101 as indicated above the lanes. Known marker weights are indicated to the left of blots. *B*. Affinity pull-downs from NRK transfected lysates were solublised in SDS sample buffer, boiled, and run on a 2-d gel. Markers of known size are indicated on the far left; the pH range is from pH 3 (far right) to pH 10 (left) as indicated. Individual spots were counted as being in the range of 90-100 unique spots.

5.2.5 HaloLink® resin pulls down a significant number of different endogenous proteins from the Vps4^{E235Q} compartment that may be ESCRT-associated

To determine whether or not various different endogenous proteins could be pulled down using the recently developed HaloLink® pull-down assay, the resin from a pull-down experiment of NRK cell lysates transfected with Halo-Vps4^{E235Q} (lysed in detergent-free buffer) was loaded and run on a 2-d gel. This gel was run with appropriate markers, from a pH range of 3.0 to 10.0 by Dr Ursula Gereike (University of Bath). The 2-d gel shows a range of individual spots, approximately 90-100 in total, which suggests that there are many possible proteins that have yet to be identified as being present on the Vps4^{E235Q} compartment and thus potentially important in proper ESCRT function and MVB biogenesis (Fig. 5.6B).

5.2.6 Intact vesicles can be successfully pulled down using HaloLink® resin

The ability of the developed method to be able to pull down intact vesicles cannot be assumed simply by detection of other proteins. Indeed these proteins may simply have been pulled down as a result of protein-protein interactions between the Halo-Vps4^{E235Q} and other endogenous proteins that form a complex. Thus the detection of other proteins pulled down with Halo-Vps4^{E235Q} such as TSG101 and CHMP3 does not provide evidence that an integral vesicular compartment has been successfully affinity isolated. Being able to isolate such a compartment is a useful process as this could allow the possibility of many other *in vitro* experiments on such a compartment. To address this question, a simple dextran-red uptake assay was performed (for full details of the method see 2.2.8). Dextran-red will be taken up by endocytosis and traffic through the endocytic pathway. In cells with

perturbed MVB formation resulting in enlarged vesicles such as the Vps4^{E235Q} compartment, accumulation of dextran-red will be seen in these enlarged endosomal structures (Fig. 5.7*A*). Cells treated with dextran-red versus cells transfected with Halo-Vps4^{WT} or Halo-Vps4^{E235Q} and treated with dextran-red were compared for dextran-red accumulation by measuring the fluorescence in the wavelength range of dextran-red following detergent-free cell lysis and pull-downs with the HaloLink® resin. The Halo-Vps4^{E235Q} transfected cell pull-downs accumulated a large proportion of dextran red as indicated by the relative fluorescent units (Fig. 5.7*B*). In contrast, cells expressing the Halo-Vps4^{WT} protein showed little dextran-red detection, giving only a slight increase in fluorescence over untransfected cells treated with dextran-red (Fig. 5.7*B*). These findings provide evidence for the ability of this developed method to isolate intact Vps4^{E235Q} vesicular compartments.

5.2.7 Overexpression of Vps4^{WT} can negate the typical enlarged endosomal structures produced due to overexpression of Vps4^{E235Q}

As from previous work it was suggested that intact vesicular structures containing the Vps4^{E235Q} protein could be isolated, it may be hypothesised that a large-scale isolation of these compartments could result in assays being developed to study the uptake and inward vesiculation *in vitro* using these intact vesicles with endogenous ESCRT machinery already present. An initial predicament with such an approach is that the Vps4^{E235Q} remains bound to the membrane and inhibits the proper inward vesiculation process that occurs to deliver cargo to the MVB lumen. As a result, it was investigated as to what the consequence of overexpressing both wild-type and ATP-ase dead mutant proteins in the same cells would be. It was

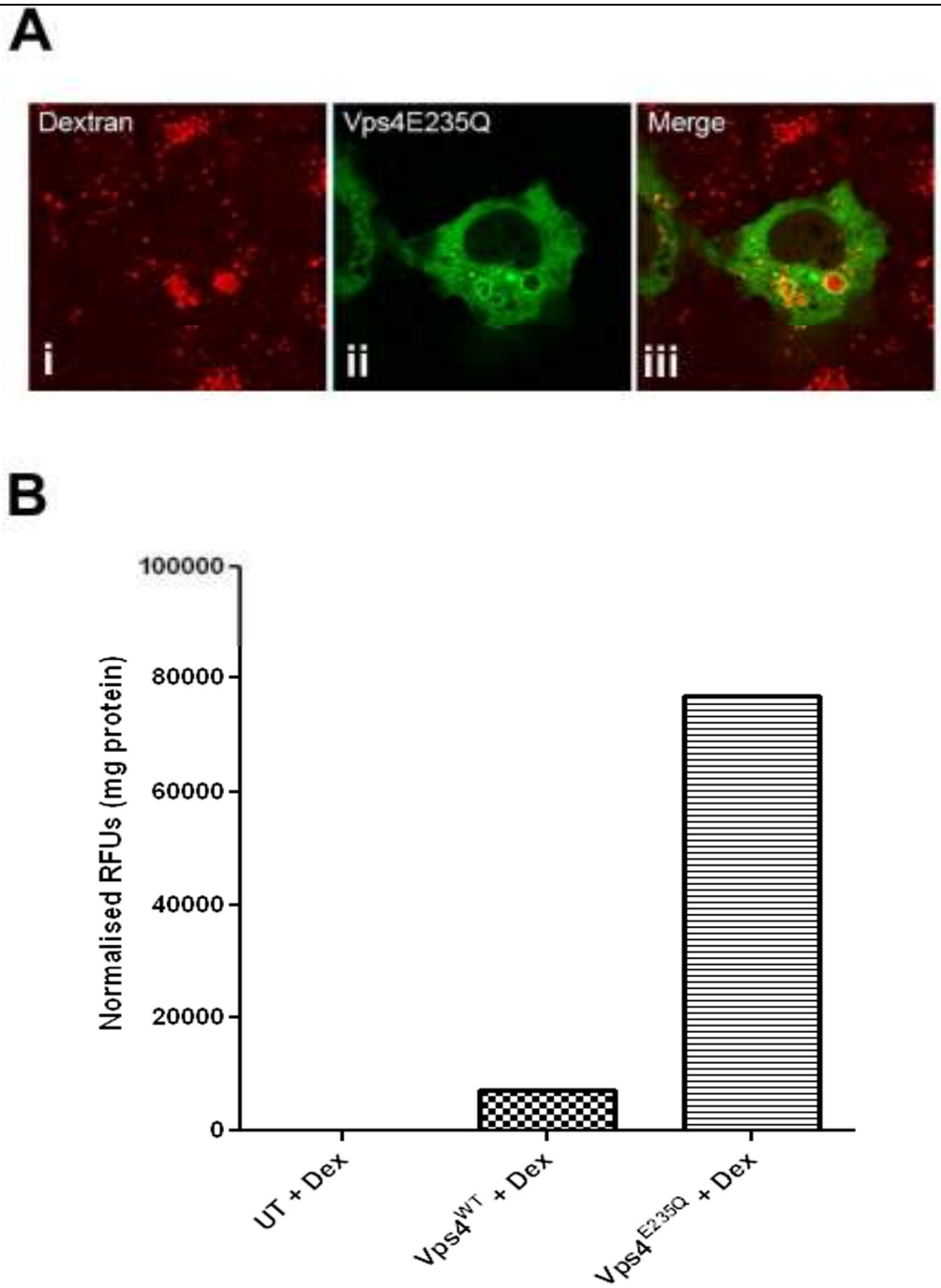

Figure 5.7 – Halo-Vps4^{E235Q} compartments loaded with dextran-red can be affinity purified as intact membranous compartments. *A*. Cos-7 cells were transfected with GFP-Vps4^{E235Q} (green) and loaded with dextran-red (red), fixed and processed for immunofluorescence. Note the Vps4^{E235Q} swollen compartments where dextran is contained within. *B*. NRK cells were untransfected (UT) or transfected with Halo-Vps4^{WT} or Halo-Vps4^{E235Q} and dextran-red (Dex) added post-transfection. Cells were lysed in detergent free TESA buffer, and affinity purified using HaloLink® resin. Bound fractions were read on a Fluoro-scan plate reader (see 2.2.8), with values normalised per mg of protein, and untransfected cells plus dextran-red taken as zero RFUs (averaged over two experiments).

discovered that upon expression of GFP-Vps4^{WT} with Halo-Vps4^{E235Q} in HeLa cells that the induced vacuolation by Vps4^{E235Q} was abrogated by co-expression of the wild-type Vps4 protein (Fig. 5.8). The resultant phenotype of this co-expression resembled a typified Vps4^{WT} alone overexpression phenotype, that is, diffuse cytoplasmic non-membranous staining. These results suggest that the Vps4^{E235Q}-induced vacuolation phenotype may possibly be rescued with wild-type Vps4 protein, which could be a useful finding if *in vitro* assays were to be performed on Vps4^{E235Q} vesicle compartment isolations. However, it should be noted that the GFP-Vps4 construct tends to express at higher levels than the Halo-Vps4 construct, thus this might account for the overcoming of the Vps4^{E235Q} vacuolation phenotype in this case.

Figure 5.8 – Co-expression of GFP-Vps4^{WT} with Halo-Vps4^{E235Q} negates the dominant negative phenotype of Halo-Vps4^{E235Q}. GFP-Vps4^{WT} (*a*; green) was co-transfected with Halo-Vps4^{E235Q} (*b*; red) using standard methods. 16 hours post-transfection cells were incubated with the diAcFAM Halo-ligand and then fixed, as described in 2.2.8. Cells were viewed under a confocal microscope, and the merged image is shown in *c*. Halo-Vps4^{E235Q} single transfections gave a swollen endosomal phenotype (not shown), which is not seen when co-transfected with the wild-type Vps4 protein as shown here.

5.3 Discussion

The MVB compartment has not yet fully been characterised. The development of an assay that allows for the isolation of the Vps4^{E235Q} induced compartment by affinity isolation methods may provide a unique approach to offer useful information with regards to the proteomic complement of the Vps4^{E235Q} compartment.

As the assay depends on the amount of GFP-Vps4^{E235Q} present for isolation, low and inconsistent transfection efficiencies provide difficulties in interpreting meaningful results, and is one problem that needs to be addressed. Thus it was decided to pursue the production of stable cell lines in order to avoid transfection issues and allow for larger scale isolation of Vps4^{E235Q} compartments. Furthermore, the recent introduction of the HaloTag® system by Promega allowed a seemingly more efficient and possibly more specific approach to affinity isolation. Transient transfections demonstrated that it was possible to produce cells that inducibly express Halo-Vps4^{E235Q} (and Halo-Vps4^{WT}). However despite isolation of a large number of cell colonies that grew under the harsh selective antibiotic-present conditions (for selection of stably transfected cells), none of the colonies screened showed any apparent Halo-Vps4^{E235Q} or Halo-Vps4^{WT} expression, with or without the presence of doxycycline. Given the timescale of the work already carried out in attempting to produce stable inducible cell lines, this was not further pursued.

Despite the failings of stable cell line production, transient transfections using HaloTag® technology for affinity isolation of Vps4^{E235Q} compartments yielded promising results, showing affinity isolation of the ESCRT-I component TSG101 as well as ESCRT-III component CHMP3. Notably however CHMP4A was not detected. The antibody used for detection of CHMP4 was raised against the CHMP4A sequence, and given the fact that there are two other isoforms of CHMP4 (B and C), it is

possible that the antibody used does not recognise these isoforms efficiently, if at all. These isoforms of CHMP4 may also be cell-type specific. It may be then that CHMP4A is not expressed in the cell lines used for these experiments. The possibility that CHMP4 is not present on this complex however cannot be fully excluded. Detection of two ESCRT proteins from affinity isolations provides evidence that an ESCRT-related complex can and has been successfully isolated. Whether the isolation was of a protein complex or rather of an actual membranous vesicular compartment containing protein complexes is not fully known. However, evidence from dextran-red studies performed show that in cells expressing Halo-Vps4^{E235Q} that pull-downs are likely to be of intact compartments when lysed under non-detergent conditions, given the increase in dextran-red fluorescence.

Running a 2-d gel from affinity purified Halo-Vps4^{E235Q} transfected NRK lysates has shown that various proteins may be isolated from the Vps4^{E235Q} compartment. A large number of individual spots were seen from this gel, and this suggests that there is a good possibility that there are a number of various MVB and ESCRT-related proteins not yet identified. It is possible and indeed likely that a significant proportion of these spots are in fact simply cargo and other proteins pulled down given the affinity isolation method. This is why a fuller approach utilising this method would involve a parallel running of Halo-Vps4^{WT} affinity purified cell lysates which would serve as an efficient control for identification of non-specific pull-downs and non-MVB related proteins (see Fig. 5.9). The other predicament with the approach used is the inconsistency and low percentage of successful transfection methods. With the pursuit of inducible stable cell lines resulting in little success, other approaches would need to be considered. Retroviral delivery of DNA constructs is an alternative to transient transfections however as dominant negative ESCRT components including Vps4^{E235Q} have been shown to inhibit retrovirus budding and thus perturb virus production, this approach is not viable when looking to express dominant negative ESCRT proteins. One further method however would be to use adenoviral delivery of DNA

encoding for dominant negative Vps4^{E235Q}. This approach has already been used for expression of Vps4^{E235Q} in mammalian cells [135]. This method should not be impaired by the expression of dominant negative ESCRT components (as adenoviruses are not dependant upon ESCRT machinery for their exiting infected cells) and gives near to 100% infectivity and thus expression of protein in practically 100% of the cell population, allowing for much better affinity isolation of Vps4^{E235Q} compartments and subsequent studies. Although the production of inducible stable cell lines was unsuccessful in this case, this approach could be further pursued. However, it may result in a very time-consuming process that is not guaranteed to result in positive stable cells.

The successful isolation of Halo-Vps4^{E235Q} vesicular compartments as demonstrated by dextran-red studies is an important finding. This method relies on the uptake of the dextran-red into swollen compartments induced by Halo-Vps4^{E235Q} expression. By lysing the cells in the absence of detergents, we hoped to keep the membrane compartment that Halo-Vps4^{E235Q} protein is contained to intact. Thus in the case of Halo-Vps4^{WT} expression, which is largely cytosolic, fluorescence corresponding to dextran-red should be limited as no compartments containing accumulated dextran-red would be expected to be isolated. In contrast, we might expect the HaloResin® to affinity isolate Halo-Vps4^{E235Q} compartments, and if these compartments have intact membranes then in the case of dextran-red loading, dextran-red would also be isolated. If our lysis method did not result in purification of intact membrane compartments but rather just protein complexes, the dextran-red should be released into the cell lysate and not affinity purified, giving a similar fluorescent result to Halo-Vps4^{WT} (see Fig. 5.9). Thus we interpret a rise in fluorescence with the Halo-Vps4^{E235Q} transfected cell pull-downs to be indicative of an intact membrane compartment having been isolated. The apparent findings that this method can isolate intact compartments opens up the possibility of various other experiments on such compartments, including the possible

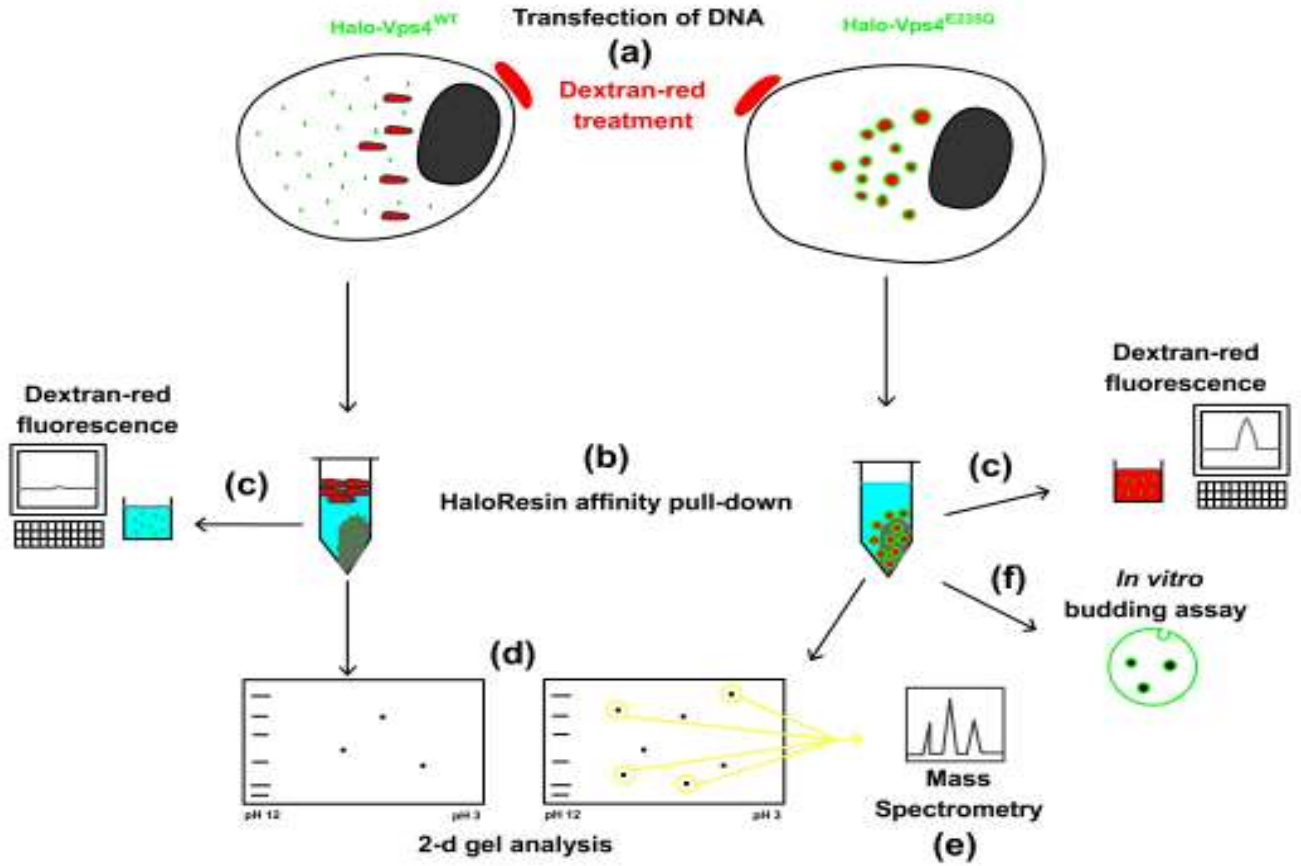

Figure 5.9 – Applications of isolating the Halo-Vps4^{E235Q} compartment. (a) Halo-tag fusion constructs containing either the wild-type (WT) or dominant negative forms of Vps4 are transfected into mammalian cells. Cells can be treated with dextran-red and this will be delivered to endosomal compartments. (b) Following non-detergent lysis, in-tact enlarged vesicles containing Halo-Vps4^{E235Q} may be isolated, whereas Halo-Vps4^{WT} isolation should largely not produce such compartments. (c) Dextran-red fluorescence can be measured of isolated Halo-tagged proteins. In the case of Halo-Vps4^{E235Q} a membranous compartment containing dextran-red may be isolated thus giving a fluorescent signal. (d) The WT and E235Q isolations using HaloResin are analysed by 2-d gel and spots present in the E235Q blots picked for mass spectrometry analysis (e). (f) Intact Halo-Vps4^{E235Q} compartments may potentially be isolated and used for setting up an *in vitro* budding assay using a quenchable marker.

development of an *in vitro* invagination assay, which to date there is no such assay known to have been developed. In theory, by affinity purification of Halo-Vps4^{E235Q} compartments from cells expressing this protein, a large-scale isolation could result in a large number of purified compartments that contain the endogenous proteinacious ESCRT machinery. By removal of the dominant negative Halo-Vps4^{E235Q} from the membranes of such compartments, a cell-free invagination assay could be set-up to investigate more fully the process of inward invagination and delivery of cargo into the lumen of the 'MVB' compartment. Results from co-transfections of Vps4^{WT} and Vps4^{E235Q} suggest that the dominant negative phenotype and membrane binding of the Vps4^{E235Q} protein can be overcome by expression of the wild-type protein. A scenario then can be envisaged where purification of Vps4^{WT} protein would allow one to incubate the Halo-Vps4^{E235Q} compartments with an excess of Vps4^{WT} and thus compete off the dominant negative protein, yielding the intact ESCRT-containing compartment and allowing invagination to occur.

Such an assay would rely on the fluid phase uptake of an assayable marker resulting in lumenal vesicles containing this marker. A fluorescent marker that is quenchable would be ideal, such as ANTS which is quenchable by the non-membrane permeable DPX. ANTS/DPX dye quenchable assays have already been used to measure the fusion between two populations of vesicles [148, 149]. Once a successful and consistent assay had been established, other effects on inward invagination could be investigated. For example, purified cell cytosols containing dominant negative proteins and possible inhibitors of ESCRT and related proteins could be added to this cell-free invagination assay and their effects on invagination investigated. Development of such an assay may be able to answer questions such as: What is the core machinery needed for invagination and lumenal delivery of cargo? Is PIKfyve necessary for proper invagination? How important are specific lipids? Is ESCRT-III alone sufficient for cargo delivery? In short, an assay like this could help us determine what proteins are needed

specifically for invagination of the MVB membrane, what proteins are needed for other processes on the MVB, such as cargo concentration and protein recognition, and if there is any overlap between such roles. Being able to answer these questions would vastly improve our understanding of trafficking events in the endo-lysosomal pathway. For example, although CHMP3 and the ESCRT-III complex has been proposed to be involved in the final stages of vesicle formation in the lumen of the MVB, recent evidence suggests that this may not be the case as gene silencing of CHMP3 does not inhibit the delivery of EGFR into the MVB lumen, but does inhibit its degradation [56]. Combining this with evidence that CHMP3 may bind PtdIns(3,5)P_2 and that PIKfyve is necessary for degradation but not silencing of signalling receptors [71, 84], it may be hypothesised that ESCRT-III may not be involved as first thought in the formation of vesicles at the MVB, but rather in proper trafficking and fusion of the MVB to the lysosome.

The HaloTag® is still a relatively recent technology. Much of the work contained in this chapter has relied on the viability of this tag for isolation using a resin that covalently binds this tag. Certainly the Halo-ligand use in this work suggests that this part of the technology is reliable given the distinct phenotypes seen in immunofluorescent studies. Despite the HaloTag® technology being so new, there are some studies in the literature that have successfully used this tag [150-153]. In particular, one study used the HaloLink® resin to develop a rapid single-tube method for small-scale isolation of polyclonal antibodies [150]. These studies suggest then that the HaloTag® technology is a viable and useful technology, and that the approach that has been utilised in this chapter for the isolation of the Vps4^{E235Q} compartment is feasible.

5.4 Conclusion

The full proteomic complement of the functional MVB compartment is not known. An affinity pull-down method has been developed that may enable us to be able to determine such an endogenous proteomic make-up of a cellular MVB compartment, which has yielded promising results with ESCRT components already having been affinity purified and detected. Further work using this approach may help us better understand the endogenous proteins involved in MVB biogenesis, and may result in the discovery of novel ESCRT-related proteins. Furthermore, by perfecting this method it may be possible to set up a further novel assay which would assay the invagination of MVB membranes, helping us more fully understand the process of mammalian MVB formation which is still not properly understood.

CHAPTER 6

6 Cellular effects of truncations and mutant forms of the ESCRT-III component CHMP3 and roles for ESCRT proteins in cytokinesis*

6.1 Introduction

One useful tool for investigating a protein's cellular function is the use of dominant negative forms of the given protein and over-expression of such mutants to investigate cellular effects of the mutation. Studies like these can help better understand a normal function of the protein, by seeing ways in which impaired function results in abnormal cellular processes. As already discussed in chapter 1, one of the effects that mutant forms of ESCRT and related proteins can have is perturbing proper retroviral budding in HIV-infected cells. These studies have often involved the use of dominant negative proteins which suggest the normally functioning protein counterparts play a key role in this process. Another useful approach is the use of siRNA which has also helped elucidate protein cellular function. This method relies on the silencing of endogenously expressed protein and thus offers a different approach to over-expression studies.

One truncation of CHMP3, which removed the whole C-terminus, resulted in a dominant negative N-terminal CHMP3 protein that displayed endosomal defects such as impaired MVB biogenesis and the swollen endosomal phenotype paralleled to the class E phenotype first described in yeast [71]. This dominant negative construct, termed $CHMP3^{1-112}$, has been previously used in our lab and in various studies, including those described in chapter 3 of this thesis. It has been suggested that the C-terminus acts as an autoinhibitory domain, which in the cytosolic form of CHMP proteins inhibits the N-terminal end of the protein from membrane localisation and proper protein function [78]. The C-terminal

autoinhibitory domain is proposed to be released from N-terminal inhibition prior to allowing full N-terminal binding to the endosomal membrane. One recent study has highlighted the importance of normal CHMP proteins, in particular, truncations of the C-terminus of CHMP3 [78]. This study showed that indeed the $CHMP3^{1-113}$ truncation had significant inhibitory effects on HIV-1 viral budding; however other truncations including $CHMP3^{1-150}$, $CHMP3^{1-179}$ and $CHMP3^{1-200}$ had much more pronounced effects on viral budding and particle formation [78]. From this study it was hypothesised that these truncations that produced a longer CHMP3 dominant negative protein (the native protein is 222 amino acids in length) than the $CHMP3^{1-112}$ truncation would also give stronger endosomal dominant negative phenotypes. This would then make such constructs quite helpful for studies relating to ESCRT proteins, given the usefulness of dominant negative proteins for understanding better the native protein's function.

It has also recently emerged that one function of the native ESCRT proteins seems to be that of playing an important role in the cellular process of cytokinesis [104, 105, 154]. The process of cytokinesis is a highly precise yet complex process necessary for the formation of two daughter cells from a single parent cell. During the final stages of cytokinesis, a mid-body is formed which is a thin membrane tether-like structure connecting the two daughter cells together. The end of cytokinesis is typified by the abscission of this structure at the mid-body, which seems to be an event heavily reliant on membrane dynamics [155-158]. There are several theories as to how this abscission occurs to separate the two daughter cells. Perhaps the most favourable theory is that of the trafficking of membrane vesicles to the mid-body where perhaps some apparent fusion event occurs allowing the separation of the two cells and abscission of the plasma membrane at this region [156]. It has recently been shown that some ESCRT and ESCRT-related proteins are present at the mid-body and mutations or silencing of such proteins results in impaired cytokinesis, which has been paralleled to impaired retroviral budding [104, 105].

Following on from this recent work, several of the already described constructs for expression of dominant negative truncated forms of CHMP3 that lack the C-terminal autoinhibitory domain were produced. Specifically, both GFP- and FLAG-tagged forms of $CHMP3^{1-150}$ and $CHMP3^{1-179}$ were made. The aim of this chapter was to better characterise these truncated proteins in terms of sub-cellular localisation and effects within the cell, namely receptor trafficking through the endo-lysosomal pathway, and the effects of such truncations on cellular events such as cytokinesis. Furthermore, to try and better understand the role of the N-terminus of CHMPs in endosomal membrane lipid binding, several further mutations were made which substituted positive residues from the N-terminus with uncharged residues, as these positive amino acids were thought to be essential for membrane binding of CHMP3. These mutations had recently been described and have been suggested to cause the loss of membrane association and swollen endosomal phenotypes when mutated from dominant negative CHMP3 constructs that typically bind membranes when overexpressed in mammalian cells [159]. Much of this work then was largely focussing on CHMP3, to provide better understanding of this protein and membrane events it is involved with. This focus was influenced by previous results that had been obtained that showed the importance of CHMP3 with regards to binding of endosomal lipids, in particular $PtdIns(3,5)P_2$, with the aim of being able to more clearly grasp the specificity of such events that occur at the endosomal membrane.

*****The work described in this chapter was submitted to the Biochemistry Journal and accepted for publication on 12 December, 2007:

Dukes JD, Richardson JD, Simmons R, Whitley P. *A dominant negative ESCRT-III protein perturbs cytokinesis and trafficking to lysosomes.* Biochem J, 2008. Apr 15; **411**(2): 233-239

6.2 Results

6.2.1 Expression of CHMP3 truncations result in swollen endosomal phenotypes and localisation to a hybrid early-late endosomal compartment

Previously, dominant negative truncation constructs of CHMP3 used in our lab included a GFP- and FLAG-tagged CHMP3$^{1-112}$ construct, a truncation that removed amino acids 113-222 from the C-terminus of CHMP3. Overexpression of the GFP form of this construct in mammalian cells resulted in some localisation in the nucleus, with endosomal localisation that resulted in swollen vacuoles (Fig 6.1). This construct has been further shown to localise in part to structures containing both early and late endosomal markers, thus being thought to be a 'hybrid' endosomal compartment. Despite this construct giving a swollen endosomal phenotype, the phenotype was not always regular. Additionally, the often overpowering level of GFP localisation in the nucleus often gave difficulties in viewing lower level expressing cells.

In an attempt to obtain a dominant negative construct more suited to giving a consistently distinct phenotype with perhaps less nuclear staining, several truncations resulting in dominant negative proteins of varying lengths were cloned. By using the pEGFPN1 and pFLAG-CMV5c vectors, both GFP- and FLAG-tagged (respectively) versions of CHMP3$^{1-150}$ and CHMP3$^{1-179}$ (deleting amino acids 151-222 and 180-222 respectively) constructs were made. It has been reported that expression of the full length wild-type CHMP protein with a GFP tag present at the N-terminus results in a swollen endosomal phenotype [78, 160]. However the constructs used for these studies were made with the fusion of GFP on the C-terminus, thus eliminating the likelihood of any endosomal defects with the wild-type protein expression (see Fig. 6.1 for full length CHMP3 expression).

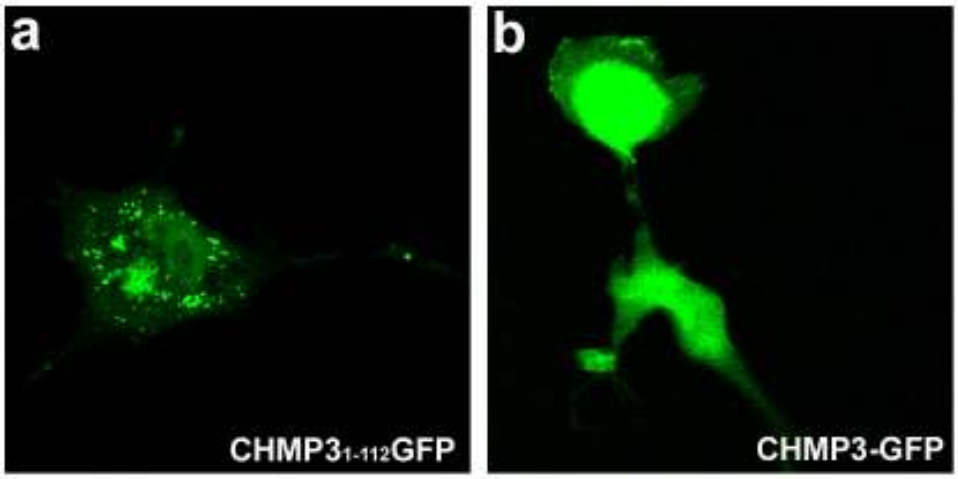

Figure 6.1 – Expression of an N-terminal CHMP3 construct and full length CHMP3 in Cos-7 cells. *(a)* Cos-7 cells were transiently transfected with CHMP3$^{1-112}$GFP (green) as previously described. This panel shows an example of a lower-level expressing cell with less nuclear expression than often seen. This cell has a distinct phenotype however expressing cells were not always consistently similar to this example, normally with large nuclear expression. *(b)* Cos-7 cells were also transfected with a full-length CHMP3 construct with a GFP tag (green) present at the C-terminus of the protein. Note in the upper cell the high nuclear expression and also the diffuse non-membranous cytosolic distribution of the protein in general.

To investigate the sub-cellular localisation of the truncated CHMP3$^{1-150}$ and CHMP3$^{1-179}$ constructs, transfected cells were co-stained with the early and late endosomal markers, EEA-1 and M6PR respectively. Previous reports had suggested that the overexpression of CHMP3$^{1-150}$ and CHMP3$^{1-179}$ proteins resulted in a largely plasma membrane localisation, in particular with CHMP3$^{1-150}$ [78]. In experiments carried out for this study however, it was found that overexpression by transient transfection of both CHMP3$^{1-150}$ and CHMP3$^{1-179}$ resulted in a largely peri-nuclear punctate membrane-bound distribution, with an apparent swollen endosomal phenotype (Fig 6.2*a, g, j*). At very high expression levels of CHMP3$^{1-150}$ some cells were seen to seemingly have a plasma membrane localisation of CHMP3$^{1-150}$ (Fig 6.2*d*),

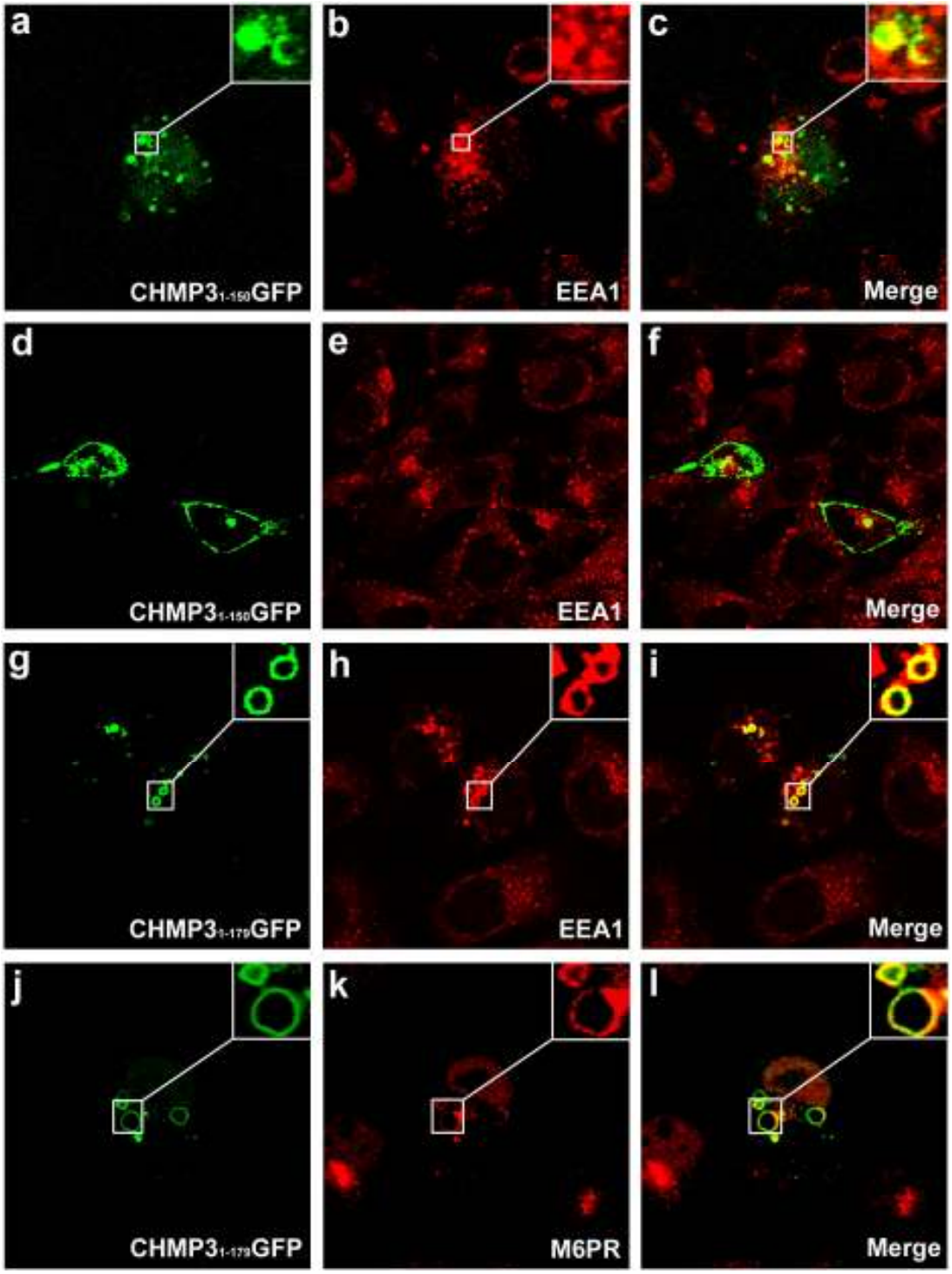

Figure 6.2 – Overexpression and sub-cellular localisation of truncated CHMP3 proteins in mammalian cells. Cos-7 cells were transfected with either CHMP3$^{1-150}$GFP (*a-f*; green) or CHMP3$^{1-179}$GFP (*g-l*; green) and either stained for EEA1 (*b*, *e, h*; red) or M6PR (*k*; red). Panels *c*, *f*, *i* and *l* show merged image, with yellow indicating co-localisation. Insets in upper right corner of panels represent magnified images of boxed area in panel. Note the difference in EEA1 and M6PR staining in transfected cells when compared with neighbouring untransfected cells (*b, e, h, k*). Also note panel *d*, which represents two cells highly over-expressing CHMP3$^{1-150}$GFP with a large localisation to the plasma membrane.

however this was not a typical observation nor was it seen in cells expressing at lower levels. Despite a few cells that were very highly expressing CHMP3$^{1-150}$GFP exhibiting some plasma membrane localisation, the overwhelming majority of transfected cells showed a typical endosomal staining as seen in Fig. 6.1*a*. Furthermore, expression of dominant negative truncations resulted in localisation to both early endosomal structures as indicated by colocalisation with EEA1 (Fig. 6.2*a-i*) and late endosomal structures, demonstrated by colocalisation with the late endosomal marker M6PR (Fig. 6.2*j-l*). This phenomenon was seen for expression of both CHMP3$^{1-150}$GFP and CHMP3$^{1-179}$GFP (CHMP3$^{1-150}$ localisation with M6PR not shown). This suggests that these truncations localise to what may be considered a hybrid compartment containing both early and late endosomal markers, and is a similar finding to previous studies carried out with the CHMP3$^{1-112}$ construct. It should be noted that these findings were also seen when expressing the FLAG-tagged constructs described instead of the GFP-fusion versions and were also expressed in HeLa cells where similar results were obtained (data not shown).

The studies carried out that focused on the expression of the two dominant negative CHMP3 truncations, CHMP3$^{1-150}$ and CHMP3$^{1-179}$, revealed interesting immunofluorescence results. From an endosomal-defect phenotypic point of view, the CHMP3$^{1-179}$ truncation appears from immunofluorescence studies to give the clearest, most consistent, and most drastic swollen endosomal phenotype. As a result of this general finding, which appeared to be true for both FLAG- and GFP-fusion proteins, the CHMP3$^{1-179}$ construct was the favoured truncation when used for overexpression studies. An additional advantage of the CHMP3$^{1-179}$ protein is that it appeared to give very low nuclear staining, which was a desired trait for overexpression immunofluorescence studies involving the GFP-fusion protein.

6.2.2 Expression of truncated CHMP3 results in the accumulation of ubiquitin on endosomal structures containing the truncated protein

One of the key events in the sorting of receptor membrane proteins into MVBs for ultimate degradation via the lysosome is the addition of a single or several ubiquitin molecules onto the target receptor protein. ESCRT-related proteins as well as actual ESCRT components contain ubiquitin recognition motifs that allow delivery of ubiquitylated cargo into the MVB lumen. Defects in proper MVB biogenesis then can result in the accumulation of ubiquitylated cargo on endosomal membranes, cargo that has failed to be sorted into the MVB lumen and deubiquitylated. To test the effects of truncated CHMP3 protein expression on proper trafficking to the lysosome via the MVB, $CHMP3^{1-179}$ constructs were expressed in mammalian cells and stained for ubiquitin. Overexpression of $CHMP3^{1-179}$ resulted in large accumulation of ubiquitin when compared with untransfected cells (Fig. 6.3). This ubiquitin colocalises to the GFP signal indicating that in such cases the ubiquitylated cargo is present on the $CHMP3^{1-179}$-containing endosomal membrane. Note in untransfected cells the distribution of ubiquitin within the cell is much more diffuse and very little appears to be membrane-bound unlike cells expressing $CHMP3^{1-179}$GFP where a large proportion of ubiquitin is membranous.

6.2.3 CHMP3 truncations perturb proper EGF degradation

Colocalisation of the truncated CHMP3 protein with ubiquitin does provide some evidence that this dominant negative protein causes trafficking defects by the accumulation on enlarged endosomal membranes of ubiquitylated cargo. However, it is possible that the GFP-fusion constructs themselves

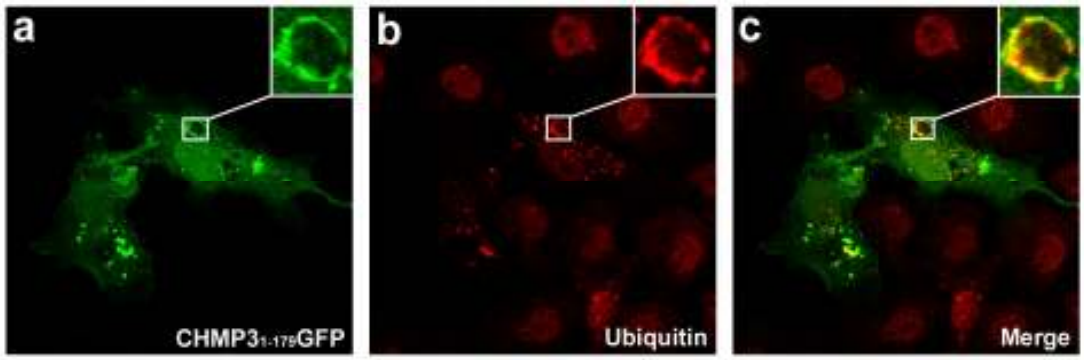

Figure 6.3 – Expression of CHMP3$^{1-179}$ results in the accumulation of ubiquitin on enlarged membranes in mammalian cells. Cos-7 cells were transfected with the CHMP3$^{1-179}$GFP construct (green; *a*) and 24 hours post-transfection were stained for ubiquitin (red; *b*). Merged images are shown in panel *c* where yellow indicates colocalisation. Boxed areas are magnified in the upper right corner of each panel. Note the distribution of ubiquitin staining in panels *b* and *c* in cells that are not expressing CHMP3$^{1-179}$GFP.

undergo ubiquitylation and thus this may account for some of the colocalisation observed. To better clarify whether or not CHMP3$^{1-179}$ actually perturbs proper receptor sorting into MVBs and delays subsequent lysosomal degradation, a more relevant assay is needed that actually monitors such an endocytosed receptor that would typically follow the MVB-lysosomal pathway. EGFR is such a receptor that is commonly used in such studies as it has been shown to almost exclusively follow the MVB-lysosomal pathway of degradation following stimulation with EGF and endocytosis into the cell. There are two simplistic approaches that one could use for such an assay; firstly EGF stimulation followed by staining of the EGFR protein for immunofluorescence studies, or alternatively one could use a fluorescent or similarly labelled EGF and follow this ligand (which would relate to the degradation state of the receptor) via immunofluorescence. One practical problem with the former of the two approaches is that despite numerous commercial antibodies to EGFR are available, it appears to be very difficult to detect any EGFR with antibodies in HeLa and other mammalian cell lines. A431 cells do express high amounts of EGFR [161], and thus this can be detected better with antibodies. However as A431 cells do not grow in monolayers and are relatively small cells, they

are not very amenable from an immunofluorescent imaging perspective. The advantage of using the approach of fluorescently labelled EGF is also that very little to no background would be picked up in immunofluorescence staining as no staining with antibodies would be required. Thus for these studies it was decided that a fluorescently labelled EGF would be used to follow the degradation of EGFR in cells expressing CHMP3$^{1-179}$GFP.

After 2 min of stimulation with EGF in HeLa cells there was a clear accumulation of EGF at the plasma membrane suggesting that EGF was rapidly binding to its receptor (Fig. 6.4*a-c*). On separate coverslips, cells were stimulated with fluorescent EGF for 60 min. Cells were then washed, fixed and viewed on a confocal microscope, where it was found that in cells which expressed the truncated CHMP3$^{1-179}$ protein there appeared to be impaired degradation kinetics of EGFR as indicated by the accumulation of fluorescent-EGF in transfected cells (Fig. 6.4*d-f*). This was not seen in untransfected cells treated similarly that were not expressing CHMP3$^{1-179}$ (Fig. 6.4*d-f*, indicated by cells marked with '*').

6.2.4 Mutants of N-terminal truncated CHMP3 display similar phenotypes and sub-cellular localisation to non-mutated truncations

To try and better understand the mechanisms by which CHMPs (in particular CHMP3) bind the endosomal membrane in a specific manner via their N-terminus, mutations in positive residues that were thought to be key to membrane binding have been recently performed. It was reported that particular mutations in the N-terminal region resulted in a loss of membrane association with the truncated CHMP3$^{1-150}$ construct.

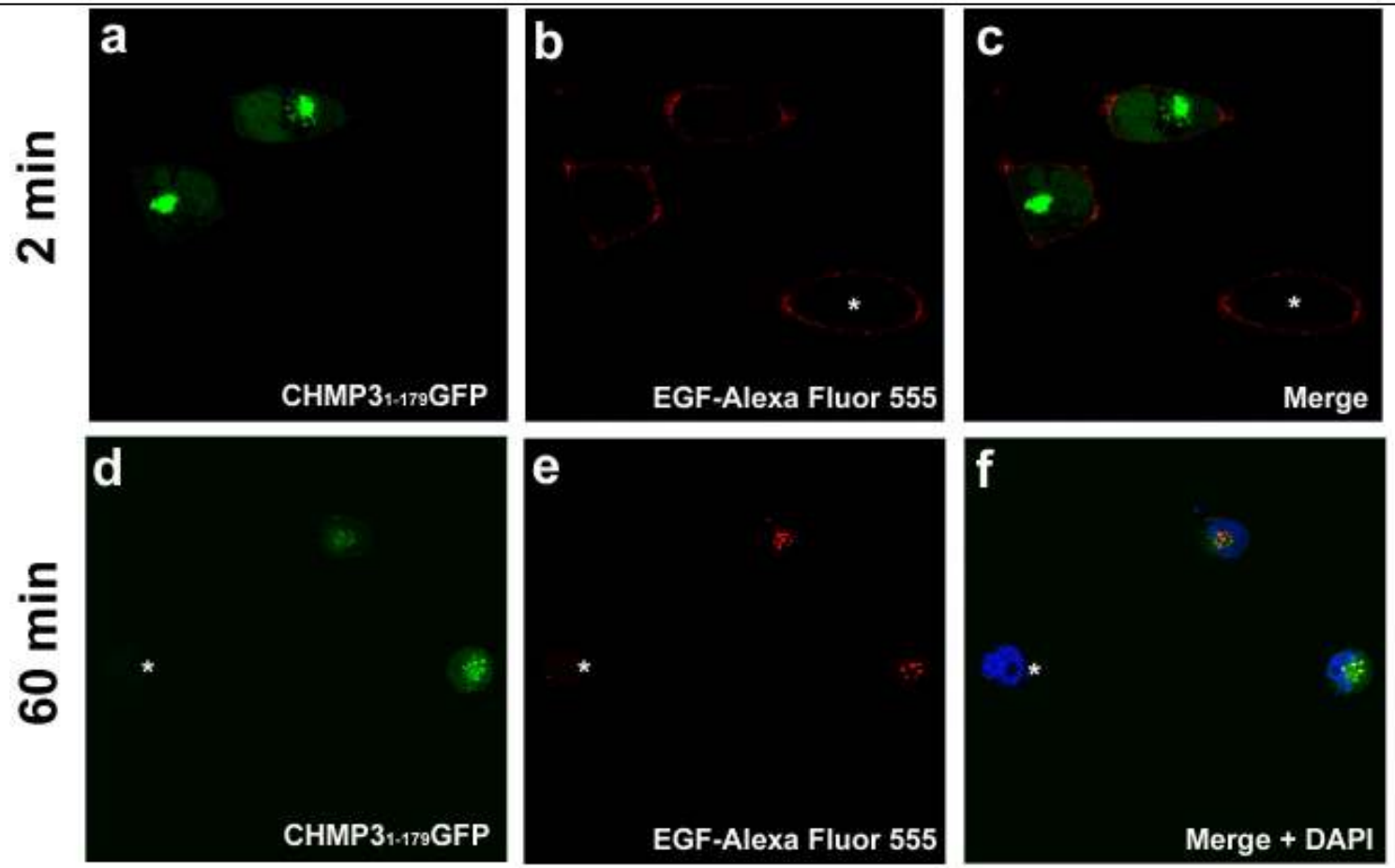

Figure 6.3 – Expression of CHMP3$^{1-179}$GFP delays degradation of EGF-simulated EGFR. HeLa cells were transfected with CHMP3$^{1-179}$GFP (green) and allowed to express for 24 hours. Cells were then serum-starved overnight and stimulated with Alex® Fluor 555-conjugated EGF (red) for times indicated and then fixed and mounted in Mowiol containing DAPI. (*a-c*) The result of a 2 min EGF stimulation. (*d-f*) 60 min EGF stimulation. '*' represents an untransfected cell.

Furthermore, these mutations reversed the dominant negative effect on HIV-1 viral budding, allowing budding to occur in contrast to the non-mutated CHMP3$^{1-150}$ which drastically inhibited viral budding [159]. It was decided to introduce two of these mutations into the CHMP3$^{1-179}$GFP constructs to more extensively characterise their effects on membrane binding and possibly look at other effects they may have in mammalian cells. The first mutant, which has been termed CHMP3$^{1-179}$GFP^{M1}, was a triple point-mutation which resulted in the amino acid changes R24S, K25A, and R28N (the original mutation previously described was R24S/K25A/R28S). The second mutation was a double point mutation of R32A and R35S and has been termed CHMP3$^{1-179}$GFP^{M2}.

Despite previous reports of these mutations leading to loss of membrane binding compared with their non-mutated dominant negative counterparts [159], it was found that expression of the mutants CHMP3$^{1-179}$GFP^{M1} and CHMP3$^{1-179}$GFP^{M2} still resulted in being largely membrane bound, giving a swollen endosomal phenotype (Fig. 6.5, M2 mutant not shown). The swollen endosomes appear by eye to not be as severe as the CHMP3$^{1-179}$GFP construct induces; however there was still a clear phenotype observed. As the CHMP3$^{1-150}$GFP^{M1} mutant was reported in a previous study to give the most dramatic effect in reversal of viral inhibition especially when compared with CHMP3$^{1-150}$GFP^{M2}, most of the ensuing studies were carried out using this mutant for characterisation. It was further found that much like CHMP3$^{1-179}$GFP, the CHMP3$^{1-179}$GFP^{M1} mutant also localised to compartments containing both EEA1 and M6PR, thus as described earlier seem to be found in a hybrid early-late endosomal sub-cellular localisation (Fig. 6.5*a-f*). Moreover, expression of the CHMP3$^{1-179}$GFP^{M1} mutant also resulted in the accumulation of ubiquitin on membranes (Fig 6.5*g-i*), and similarly to CHMP3$^{1-179}$GFP expression, inhibited the degradation of EGF *l*), suggesting that it too perturbs proper MVB-lysosomal trafficking (Fig 6.5*j-l*).

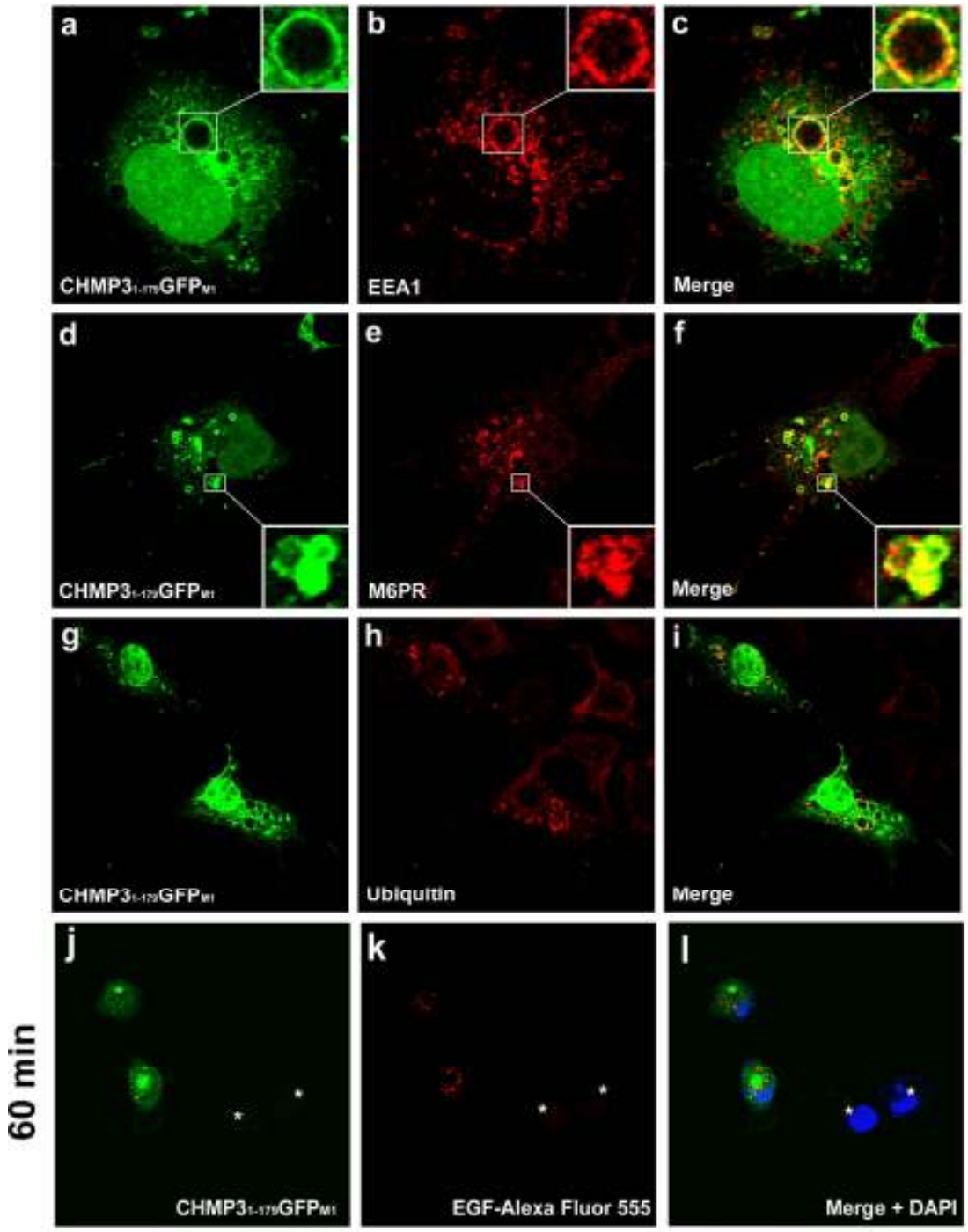

Figure 6.5 – Expression of N-terminal truncation mutant CHMP3$^{1-179}$GFP^{M1} results in similar sub-cellular localisation and cellular phenotypes compared to its non-mutated counterpart. Cos-7 cells (*a-i*) and HeLa cells (*j-l*) were transfected with CHMP3$^{1-179}$GFP^{M1} (green), fixed and stained for EEA1 (*a-c*), M6PR (*d-f*) or ubiquitin (*g-l*; red). Magnified panels represent the boxed insets, where yellow indicates colocalisation. (j-l) Transfected cells were serum-starved overnight and stimulated with Alexa® Fluor 555-conjugated EGF (red) for 60 min and the fixed and mounted in Mowiol containing DAPI. '*' represents an untransfected cell.

6.2.5 Truncated CHMP3 and its mutants as well as other ESCRT-related proteins localise to the mid-body of cytokinesis

As it has been recently reported that ESCRT components may play a key role in cytokinesis, the effects of various dominant negative ESCRT constructs on cytokinesis were investigated. When cells overexpressing the dominant negative truncation CHMP3$^{1-179}$ were fixed, those at the late stages of cytokinesis were observed to contain high concentrations of the CHMP3$^{1-179}$ protein apparently present on vesicles at the mid-body (Fig. 6.6*a-f*). In particular, CHMP3$^{1-179}$ appears to specifically localise to the central region of the mid-body, where □-tubulin staining is not observed, leaving an apparent "pseudo-gap" upon tubulin staining. This phenomenon was observed in both Cos-7 cells as well as HeLa cell lines, implying that this may not be cell type specific (Fig. 6.6*a-f*). There also appears to be equal contribution of CHMP3$^{1-179}$ vesicles at the mid-body from each daughter cell, and vesicles distributed along the tubulin network were often observed. It is possible that these vesicles were being trafficked towards the mid-body, however with the lack of live-cell imaging such conclusions as to their direction of travel cannot be made. The localisation of the N-terminal mutant of CHMP3$^{1-179}$ and CHMP3$^{1-179M1}$ was also investigated. Despite reports of the triple point mutation abrogating inhibition of HIV-1 budding, it was found that CHMP3$^{1-179M1}$ was also present in high concentrations at the mid-body, showing very similar results to expression of CHMP3$^{1-179}$ (Fig. 6.6*j-l*).

In addition to dominant negative CHMP3 being present at the mid-body of cytokinesis, the dominant negative ATP-ase defective Vps4^{E235Q} protein when overexpressed in transient transfections was also found to be concentrated at the mid-body (Fig. 6.7*a-c*). Vps4^{WT} and full length CHMP3-GFP expression were not found to form vesicular structures, but did appear to possibly be more concentrated at the mid-body of

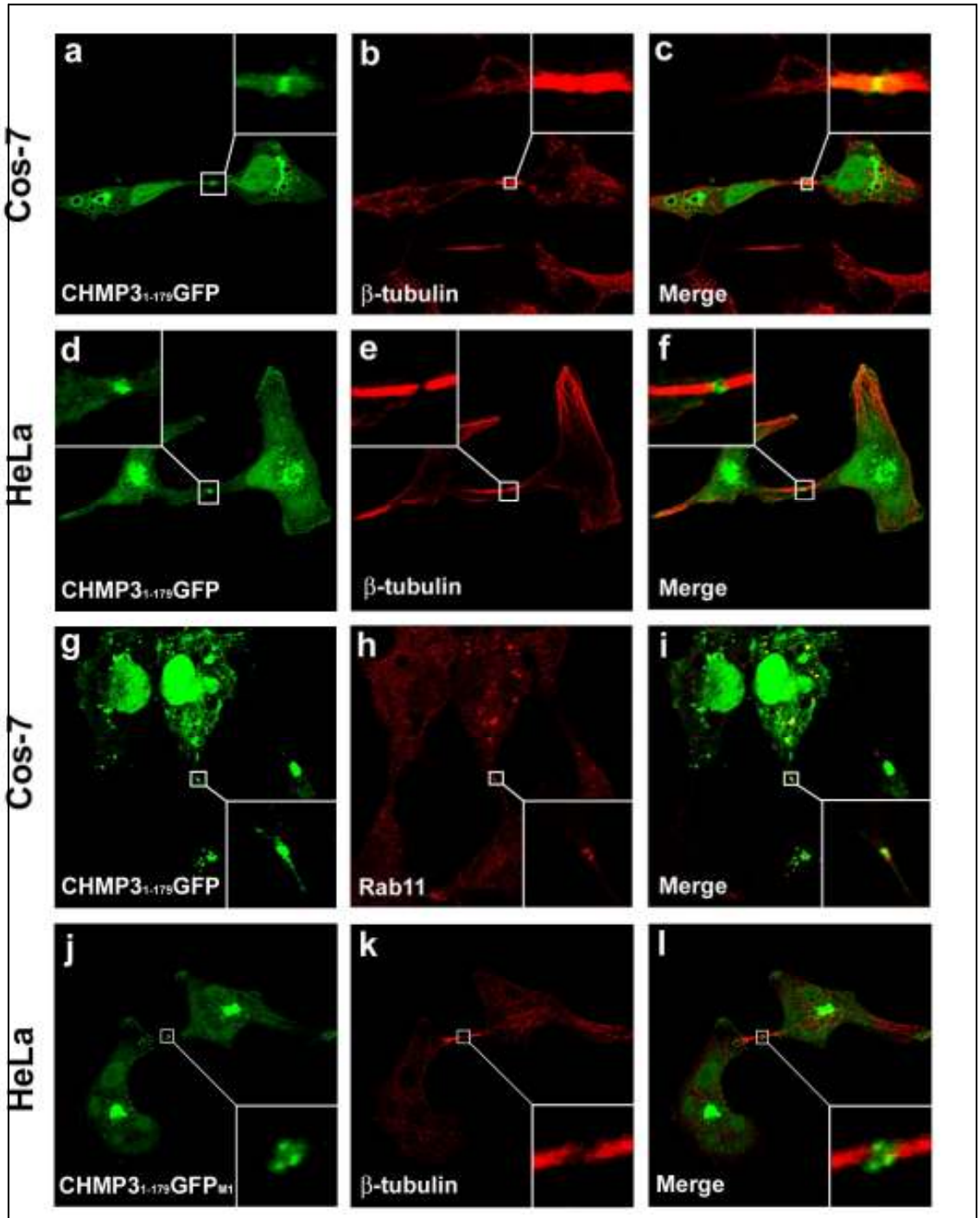

Figure 6.6 – Dominant negative CHMP3 truncations localise to the mid-body of cytokinesis. Cos-7 and HeLa cells (as indicated on left of panels) were transfected with CHMP3$^{1-179}$GFP (*a-i*) or CHMP3$^{1-179}$GFP^{M1} (*j-l*; green) and allowed to express for 24 hours before fixing. Cells were stained for β-tubulin (*a-f*, *j-l*) or Rab11 (*g-i*; red) and viewed on a confocal microscope. Boxed insets are magnified in corners of each panel. Note the mid-body shown usually lacks β-tubulin staining at the very centre. Transfected cells are considered as one cell as they have yet to complete cytokinesis.

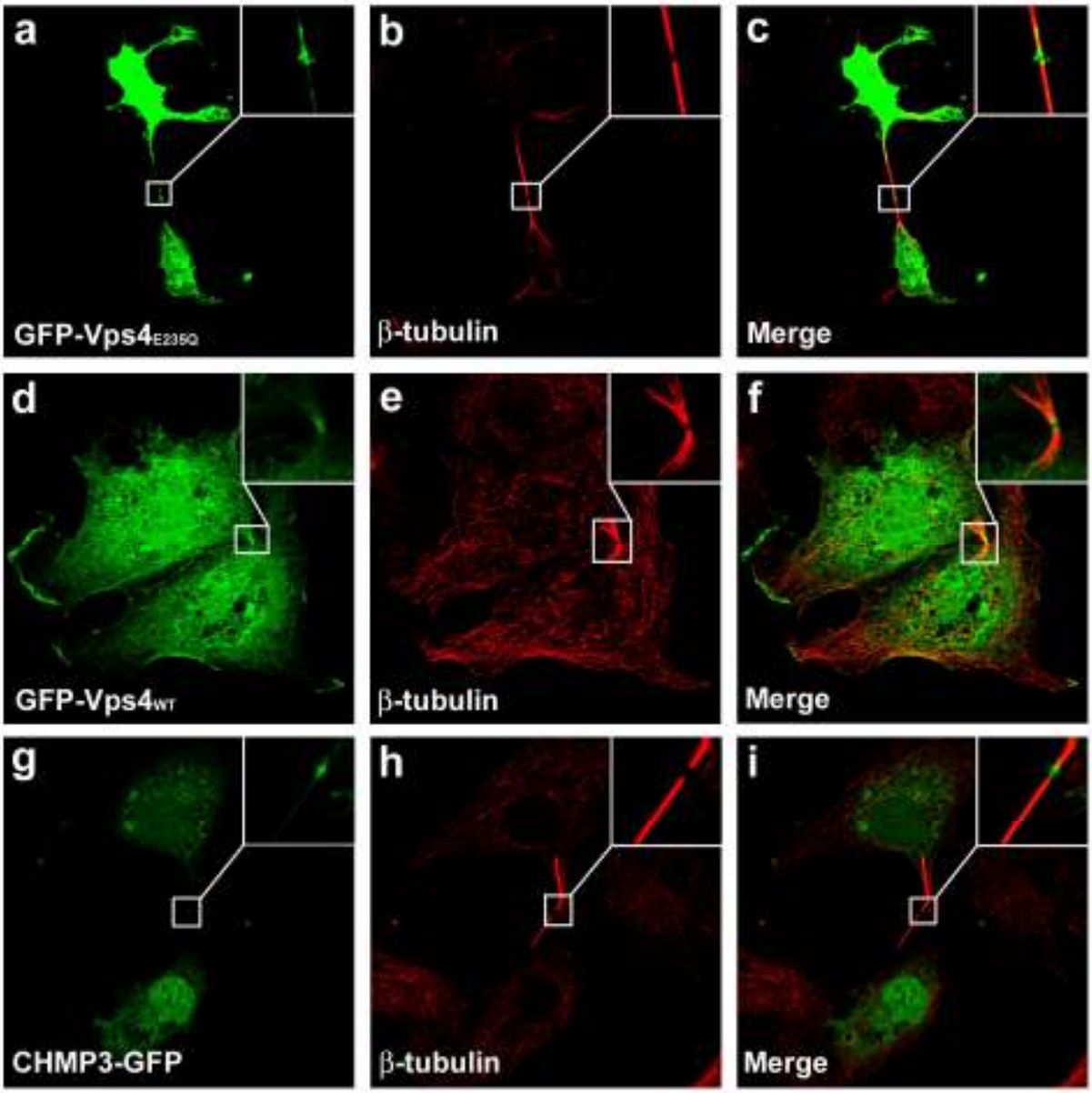

Figure 6.7 – Dominant negative GFP-Vps4^{E235Q}, but not GFP-Vps4^{WT} or CHMP3-GFP localises to membrane compartments at the mid-body of cytokinesis. Cos-7 cells were transfected with appropriate GFP-fusion constructs as indicated. 24 hours post-transfection cells were fixed and stained for β-tubulin (red). (*a-c*) GFP-Vps4^{E235Q} (green) localises to the mid-body of cytokinesis on vesicular structures. (*d-f*) GFP-Vps4^{WT} (green) shows a diffuse cytosolic expression with some non-membranous expression apparent at the mid-body. (*g-i*) CHMP3-GFP (green) expression is similar to GFP-Vps4^{WT} being cytosolically localised with apparent higher concentrations at the mid-body. Note CHMP3-GFP is fused to the GFP tag at the C-terminus thus is not typically membrane-bound when overexpressed in mammalian cells.

cytokinesis when compared with their distribution in the rest of the cytoplasm (Fig. 6.7*d-i*).

Rab11 has been shown to be a recycling endosomal Rab protein, which may play a role in vesicle trafficking within the cell [162]. It has also been previously shown to localise to the mid-body of cytokinesis, and cause defects in cytokinesis when dominant negative versions of it are expressed in mammalian cells [163]. This suggests that it is necessary for cell abscission during the late-stages of cytokinesis. Transfected cells expressing CHMP3$^{1-179}$GFP were found to have Rab11 at the mid-body as well (Fig 6.6*g-i*) although it should be noted that the Rab11 does not appear to fully colocalise with CHMP3$^{1-179}$GFP at the dense area of the mid-body in which it is found.

6.2.6 Expression of dominant negative ESCRT-III and related proteins results in cytokinesis defects

HeLa cells plated on 13mm coverslips were transfected with various constructs including Vps4^{E235Q}, CHMP3$^{1-179}$GFP and CHMP3$^{1-179}$GFP^{M1}. Cells were fixed after 24 hours then stained for β-tubulin and DAPI. Transfected cells were counted for the number of multinucleate cells, which was defined as any cell which was connected to another cell with a continuous plasma membrane, and included cells with two or more nuclei. As seen in Fig. 6.8*A*, the control cells expressing the parental plasmid only (GFP) gave a 12.0% multinucleate cell count, compared with only a very slightly increased 13.9% for the GFP-Vps4^{WT}. However for the cells expressing dominant negative components CHMP3$^{1-179}$GFP and Vps4^{E235Q} it was found that the percentage of multinucleate cells was significantly higher, at 48.1% and 44.4% respectively.

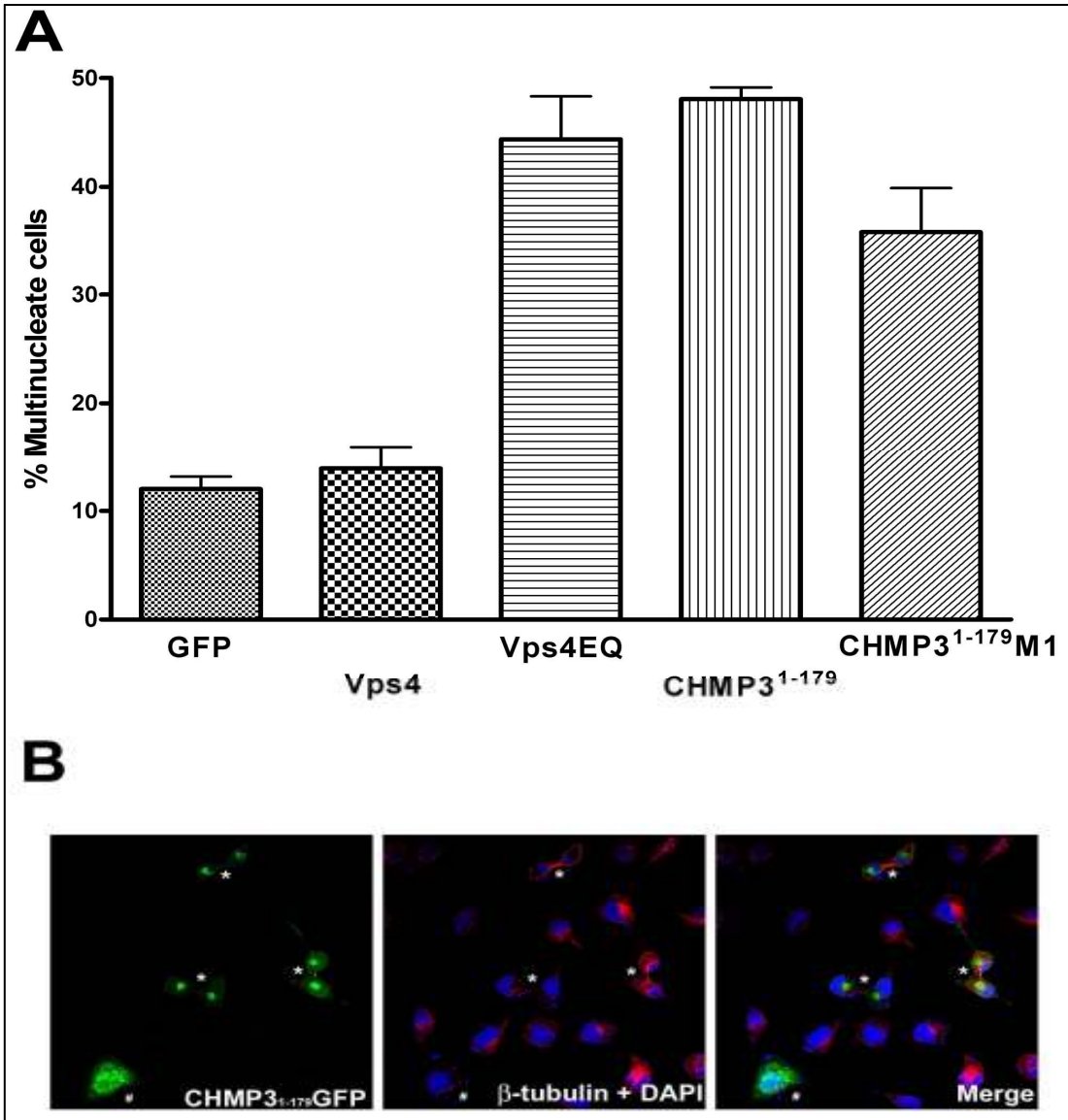

Figure 6.8 – CHMP3 and Vps4 dominant negative mutants impair proper cytokinesis. HeLa cells were seeded on 13 mm coverslips 24 hr prior to transfections. Cells were then transiently transfected with GFP-Vps4, GFP-Vps4^{E235Q}, CHMP3$^{1-179}$-GFP, CHMP3$^{1-179}$GFP^{M1} or GFP alone. Cells were fixed 24 hr post-transfection and immunostained with anti-β-tubulin followed by Alexa® Fluor 568-conjugated IgG secondary antibodies and DAPI. *A.* All transfected cells present on the coverslip were scored for multinucleation and the results were represented graphically as percentages of multinucleate cells (averaged over 3 experiments; error bars are $\pm SD$, $n=3$). Results were analysed by Chi-squared analysis and dominant negative mutants found to be significantly different to GFP control ($p<0.001$). Total numbers of cells over 3 separate experiments counted: GFP = 867, Vps4 = 1440, Vps4EQ = 871, CHMP3$^{1-179}$ = 1441, CHMP3$^{1-179}$M1 = 1800. *B.* A field of view at 400 x magnification to show cells transfected with CHMP3$^{1-179}$GFP and its effects on cytokinesis. Cells denoted by '*' represent a single multinucleated transfected cell. Cells marked as '#' represent a transfected cell that is mononucleate. In this case a multinucleation count would have resulted in 3 positive cells and 1 negative cell for multinucleation.

Furthermore, expression of the mutant CHMP3$^{1-179}$GFP^{M1} also resulted in impaired cytokinesis, giving a 35.7% multinucleate count. All percentages of multinucleate cells stated were taken as an average of three separate experiments. Chi-squared analysis was performed on the data to determine if the various constructs gave percentages that were significantly different to expression of GFP alone. It was found that for GFP-Vps4^{E235Q}, CHMP3$^{1-179}$GFP and CHMP3$^{1-179}$GFP^{M1} that all three were highly significantly different to GFP alone, with $p < 0.001$. Error bars on the graph represents the standard deviation for each condition.

6.3 Discussion

To provide insight into proper ESCRT function and mechanisms, dominant negative ESCRT constructs have previously been useful in identification of cellular activities and localisations. The expression of $Vps4^{E235Q}$ in mammalian cells is a good example of this approach. The N-terminal construct of CHMP3 previously used in our lab was the $CHMP3^{1-112}$GFP construct. It is important to note that this and other truncated constructs used bear the GFP-fusion tag at the C-terminus. This is an important point to make as it has been reported that a GFP-tag present at the N-terminus of CHMP proteins can result in a vacuolation phenotype and endosomal membrane binding of GFP-CHMP3, for example [41, 73, 100, 102, 160]. As shown in Fig. 6.1 however, expression of CHMP3-GFP results in a diffuse cytosolic distribution, much more consistent with the distribution expected of the wild-type CHMP protein. The reason for endosomal membrane-binding of wild-type CHMP3 with a bulky tag at its N-terminus may be the same reason truncated CHMP3 binds to membranes, that is, perturbing proper function of the C-terminal autoinhibitory domain. This auto-inhibition of the C-terminal domain has been proposed to regulate the assembly and oligomerisation of ESCRT-III components, such as CHMP3 [78]. Through specific intramolecular interactions between the acidic C-terminus and the basic N-terminus, the C-terminal domain is proposed to place the CHMP protein in an 'inactive' closed form. By some mechanism that may be either one of protein or lipid interactions, the C-terminus is released from its intramolecular binding of the N-terminus, allowing the CHMP protein to be in an open conformation that can result in the oligomerisation of CHMP proteins and proper ESCRT-III assembly at the endosomal membrane. The exact mechanism that allows for the conversion of the CHMP protein from a closed, inactive autoinhibited form to its open and active ESCRT-functioning state is rather speculative at this stage and not precisely known.

Truncations that remove the auto-inhibitory C-terminal domain have been shown to cause dominant negative phenotypes associated with impaired CHMP function, such as the inhibition of proper HIV-1 budding. It is additionally apparent that removal of even a very short portion of the C-terminus of some CHMPs results in impaired cellular functions. These defects are often more perceptible than the removal of the whole C-terminal half of the protein, suggesting that particular C-terminal residues are significant in proper CHMP function. The $CHMP3^{1-179}$ truncation, which is a deletion of the last 43 amino acids from CHMP3, appeared to give a more pronounced and penetrant phenotype with respect to endosomal swelling when compared with truncations that removed the whole C-terminus, namely the $CHMP3^{1-112}$ truncation. Furthermore this observed phenotype was more consistent in cells transfected with $CHMP3^{1-179}$ compared to $CHMP3^{1-112}$. It should be noted however that the Vps4 interacting domain is contained at the C-terminus of CHMP proteins [77, 89, 90]. As Vps4 is necessary for removal of ESCRT proteins from the endosomal membrane and in turn this removal is necessary for proper MVB formation, removal of this Vps4 interacting domain may be the mechanism for the phenotype observed.

It is interesting to note that previous studies have reported a plasma membrane localisation of truncated CHMP3 [78]. In this study however this was only seen rarely, and even then only in cells massively overexpressing $CHMP3^{1-150}$GFP. The general trend in transfected cells for both $CHMP3^{1-150}$ and $CHMP3^{1-179}$ was a clear, endosomal-membrane localised distribution, with a swollen vacuolar phenotype. Interestingly, the truncated CHMP3 localised to a compartment that contained both early and late endosomal markers. Such a compartment has been previously described with the $CHMP3^{1-112}$ protein [71]. It is possible that the dominant negative proteins inhibit the maturation of the MVB from an early endosome to a late endosomal compartment, thus resulting in a hybrid compartment seen with such studies. Another possibility is that the MVB that has typically been described as a subset of late endosomes, is in fact a hybrid compartment that can contain early and

late endosomal markers. It is likely that at some point in the maturation of an MVB that it will be a compartment that possesses early and late endosomal characteristics.

This work on the C-terminal truncations of CHMP3, in particular the $CHMP3^{1-179}$ mutant, have revealed clear trafficking defects as a result of their expression, with accumulation of ubiquitin on $CHMP3^{1-179}$ containing enlarged endosomal structures. It may be suggested that accumulation of ubiquitin that colocalises with $CHMP3^{1-179}$GFP may simply be a result of ubiquitylation of the GFP-fusion protein itself. However, there were certainly swollen vesicular structures present in transfected cells that stained positive for ubiquitin but did not have $CHMP3^{1-179}$GFP associated with them, in contrast to the more diffuse non-membranous ubiquitin staining in untransfected cells. Furthermore some enlarged endosomes that were $CHMP3^{1-179}$GFP positive did not exhibit any obvious ubiquitin staining. Thus these two points are important to note which favour the ubiquitin staining being largely due to ubiquitylated cargo other than the overexpressed dominant negative protein. Despite this, it was important to demonstrate that the truncated proteins did in fact disrupt normal receptor trafficking and degradation through the endo-lysosomal pathway. Indeed this was found to be the case with the EGF degradation study, and a clear accumulation of undegraded EGF was seen in cells expressing $CHMP3^{1-179}$GFP, which was not visible in untransfected cells. This further emphasises the need for a fully functional CHMP3 protein for proper MVB maturation, cargo sorting and degradation via fusion with the lysosome.

The mechanism of N-terminal interaction of CHMP proteins, in particular CHMP3, with the endosomal membrane is not well understood. There is some evidence to suggest PtdIns(3,5)P_2 may play a role in this process [62, 71]. It may be argued that localisation to the endosomal membrane is a result of protein-protein interactions, to provide the specificity for endosomal localisation. The problem with this proposal is quite simply that in overexpression studies the dominant negative proteins still bind to

endosomal membranes. If in fact it was an initial protein-protein interaction to provide the specificity for endosomal membrane binding, vastly increasing the numbers of dominant negative CHMP proteins but not the interacting partner for this mechanism would not result in such large accumulations of the CHMP protein at the endosomal membrane. Due to the fact that there appears to be a fair degree of specificity for endosomal membrane binding by CHMP3, it might be reasonable to assume that localised lipids allow this specificity to occur. This notion is further supported by work on CHMP3 that has shown PtdIns(3,5)P_2 binding occurs *in vitro*, and also that this lipid may be important in proper MVB maturation [62, 71]. Contrary to this line of thinking, it could be conceived that a cascade of events occurs in the activation and endosomal membrane recruitment of ESCRT complexes. If indeed an initial ESCRT-III activation was necessary for oligomerisation of the complex, one could envisage perhaps how a protein-protein interaction could provide this initial activation of CHMP proteins, and thus in turn these activated CHMPs subsequently activate further CHMP proteins in a cascade manner. In such a scenario as this, the number of "activating proteins" would not need to equal the number of CHMP proteins, rectifying why membrane recruitment still occurs in overexpression studies. There has however still been no definitive mechanism described that accounts for the apparent specificity of CHMP3's binding to endosomal membranes.

As the N-terminus of CHMP3 is enriched with positive residues, it may be that particular residues at the N-terminus provide the specific interactions with negatively charged lipids such as PtdIns(3,5)P_2. A recent study took one of the truncated CHMP3 constructs known to inhibit HIV-1 viral budding, $CHMP3^{1-150}$, and mutated several positive residues at the N-terminus [159]. Normal expression of $CHMP3^{1-150}$ has been reported to bind membranes, however the N-terminal mutants of $CHMP3^{1-150}$ were reported to lose membrane association, having a cytosolic distribution and losing the ability to inhibit HIV-1 viral budding [159]. Surprisingly when these mutants were made in this study to

further characterise them and their effects, there was no loss of membrane association found with CHMP3$^{1-179}$GFP^{M1} expression. This mutant being a triple mutation of R24S/K25A/R28N, showed very similar properties to its non-mutated counterpart, CHMP3$^{1-179}$GFP and it also localised to a similar compartment giving comparable trafficking defects with CHMP3$^{1-179}$GFP. Furthermore the double mutant CHMP3$^{1-179}$GFP^{M2} (R32A/R35S) gave identical results to that of the M1 mutant. It should be noted that these results were seen in Cos-7 and HeLa cells whereas the original mutations were expressed in 293T cell lines, so it cannot be completely excluded that there is some cell-type specificity, however this seems quite unlikely. One possible reason for this discrepancy of results may be that of the bulky GFP tag's position on the constructs. In the previously reported study that showed loss of membrane localisation of the triple M1 mutant, the GFP tag appears to have been fused to the N-terminus, compared with this study that cloned the GFP tag onto the end of the protein at the C-terminus. It is possible that this bulky tag by being at the N-terminus of the protein affects the membrane binding in some capacity. The bulky GFP tag present at the N-terminus may interfere in some way with the membrane association that occurs in the absence of C-terminal autoinhibition. When positive residues at the N-terminus that may be involved in electrostatic membrane binding are removed by point mutations, the remaining electrostatic charges present at the N-terminus are not strong enough to maintain membrane association, thus the protein resides largely in the cytosol. In the case of a bulky GFP tag being present at the C-terminus, this stoichiometric hindrance at the N-terminus is not present, hence membrane association without certain positive residues can still occur. This is just one suggested possibility for why these findings contradict those previously reported, and would obviously need further investigation to see if this was the case.

Cytokinesis is a crucial process that is necessary for the growth and proliferation of any mammalian cell. Much work has been done to help us understand the processes involved in cytokinesis better, however the

final stages that involve the separation of the two daughter cells is not well understood. In mammalian cells it seems apparent that some Rab GTPase proteins are essential for cytokinesis, in particular Rab11 [164, 165]. Rab11 has been shown to be an endosomal recycling Rab, involved with vesicular trafficking to and from endosomes [reviewed in 10, 166, 167]. These results suggest then that the events that occur at the mid-body prior to abscission involve a range of endosomal proteins and trafficking events for successful completion of cytokinesis.

Previous work involving ESCRTs and cytokinesis has mainly looked at the localisation of ESCRT-1 components with regards to the mid-body in cytokinesis late-stages [105]. Carlton and Martin-Seranno showed that TSG101 and possibly other ESCRT-I proteins were recruited to the mid-body just prior to abscission and are necessary for proper completion of cytokinesis [105]. It was speculated then that as ESCRT-III may be the last ESCRT complex before cargo delivery into the MVB lumen that this ESCRT complex along with other ESCRT components would also be found at the mid-body. As clearly seen in Fig. 6.6 it has been demonstrated that this is indeed the case, and not only are dominant negative ESCRT proteins found at the mid-body, but also in a similar fashion we see $Vps4^{E235Q}$, the dominant negative form of Vps4.

The expression of dominant negative ESCRT proteins clearly resulted in impaired cytokinesis, as demonstrated by Fig. 6.8. The large increase in percentage of multinucleated cells with dominant negative constructs indicates that the function of these proteins is necessary for proper cytokinesis. As immunofluorescence studies exhibit, this is particularly true of the late stages of cytokinesis when the mid-body has been formed. Interestingly, when overexpressing $Vps4^{WT}$, it was found that slightly higher concentrations were possibly present at the mid-body between the staining of the two tubulin stacks. This may simply be due to its cytosolic localisation. Alternatively, it may also demonstrate the importance of this protein in the completion of cytokinesis, hence why it is observed at the mid-body in slightly higher concentrations compared

with the cytosol. It must be noted that these concentrations did not appear to be obviously membranous bound, unlike the dominant negative CHMP3$^{1-179}$GFP or GFP-Vps4^{E235Q} where expression was clearly vesicular at the mid-body (see Fig. 6.6). Interestingly, GFP-CHMP3$^{1-179}$ expression resulted in a very high percentage of multinucleate cells, where almost every other transfected cell was multinucleate. This is the highest percentage of multinucleate cells that has been seen also upon examination of the literature.

It is much hypothesised that the AAA-ATPase Vps4 is involved in the final delivery of cargo into the MVB lumen, via a mechanism that involves ESCRT-III machinery removal. Through some mechanism not yet clear, the removal of this ESCRT complex by Vps4 allows the completed formation of inwardly budding vesicles to occur and delivery of such vesicles into the MVB lumen. This process requires an assembled ESCRT complex that includes ESCRT-III as well as ESCRT-I and -II, and a functional Vps4 protein [4]. It may be hypothesized then that in the late stages of cytokinesis, ESCRT-positive vesicles are trafficked to the mid-body with equal contribution from each daughter cell, where in the presence of Vps4, budding events occur with the plasma membrane which allows for final abscission of the two daughter cells, completing cytokinesis. There are obviously many other proteins involved in this process and present at the mid-body. However it is likely that the main events leading to abscission certainly involve participation from Vps4 and functional ESCRT complexes along with other proteins that help direct this event.

Overexpressing N-terminal mutants of truncated CHMP3 has been previously shown to resolve the inhibition of HIV-1 viral budding [159]. However in the case of cytokinesis, there seems to be very little difference in the impairment that CHMP3$^{1-179}$ and the M1 mutant have on this process. This is somewhat of a surprise, as there can be many parallels drawn between the events of viral budding and mid-body abscission in cytokinesis, thus one might expect similar effects of a

mutant on these processes. These findings may highlight the fact that there are important differences between these two events in terms of membrane dynamics, or alternatively it could as already suggested be the result of altered membrane association due to the size and position of the fusion tag used for the construct. One issue these results do seem to emphasize however is the importance of a fully functional CHMP3 protein for the proper completion of cytokinesis to occur.

6.4 Conclusion

Dominant negative proteins have in the past provided useful clues for a protein's cellular function and processes that rely on such a functional protein [71, 78]. This study has further demonstrated the necessity of a fully functional CHMP3 protein in the process of cytokinesis by expression of various truncated forms of CHMP3. This is an exciting time in the field of cytokinesis, membrane trafficking and viral budding as there appears to be many parallels between these events and the protein machinery required for such membrane events to occur. There is some very recent evidence to support the role of ESCRT proteins in cytokinesis, which comes by way of analysis of archaeal genomes, which has found homologues of ESCRT-III proteins present despite the fact that archaea do not have an endocytic pathway [90]. Thus given these recent advances in ESCRT proteins and cytokinesis it may be hypothesized that these bacterial homologues could play a role in cell division.

The dominant negative truncations of the ESCRT-III component CHMP3 also highlight the importance of this protein in receptor trafficking but also the importance of the separate domains contained within the protein. Our lab currently operate with a working model that the localisation of the ESCRT-III components is largely due to endosomally localised lipids, in particular PtdIns(3,5)P_2 which CHMP3 has been shown *in vitro* to

specifically bind to. Overexpression of mutant forms of CHMP3 results in the vast majority of the expressed protein being bound to endosomal membranes, lending weight to the theory that lipid specificity is necessary for ESCRT-III complex formation. However to define this specificity more work needs to be done as it appears that even with point mutations of apparent key positive residues at the N-terminus of CHMP3 still results in a membrane-bound truncated CHMP3 protein when expressed in mammalian cells.

CHAPTER 7

7 Overall Discussion

The recent advances in our understanding of MVB formation and the endo-lysosomal trafficking pathway have been intriguing and demonstrated that these processes are highly complex yet also tightly regulated [57, 75, 79, 89, 168]. Despite this, several of the fundamental processes involved are not understood at all. With regards to the work carried out in this thesis and the components that work has been focused on, there are four key questions that have yet to be fully answered.

(i) What is the basis or mechanism for CHMP binding to the endosomal membrane and removal of autoinhibition? The work in chapter 6 of this thesis demonstrates the importance of a functional autoinhibitory C-terminal domain in CHMPs for proper cellular function. It may be suggested that CHMP binding to the membrane occurs via interactions with other proteins such as earlier ESCRT complexes (ESCRT-I or –II) or other ESCRT-related proteins, such as ALIX. As already discussed however, one dilemma with this mechanism is that in overexpression studies, dominant negative CHMPs display endosomal binding phenotypes where the majority of the protein appears to be membrane associated [4, 35, 45, 65, 78, 159]. If the localisation of CHMPs to the MVB membrane was dependent upon protein-protein interactions we might expect there to be less binding to the membrane than that seen in these overexpression studies. This would be due to the limited relative (endogenous) expression of the protein interacting partner. One possible mechanism to explain membrane association of overexpressed protein would be a cascade mechanism. This would allow for significantly less of the interacting partner to recruit the CHMP to the membrane if in turn these CHMP proteins recruited further CHMPs to the membrane, once recruited themselves. Alternatively, direct association with membrane lipids could provide the basis for CHMP membrane recruitment. Certainly PtdIns(3)P is required for ESCRT-0 components (HRS) to be recruited to the endosomal membrane, and its

phosphorylated product PtdIns(3,5)P_2 also seems to be important in endo-lysosomal trafficking [62, 67, 71, 87]. CHMP3 has been shown to bind PtdIns(3,5)P_2 *in vitro* and so may be an effector of this lipid, however there is little current *in vivo* evidence to support the *in vitro* binding studies [71]. The studies carried out on SopB in chapter 3 of this thesis demonstrate the importance of PtdIns(3,5)P_2 in the normal degradation kinetics of endocytosed receptors that traffic through the MVB-lysosomal pathway. Furthermore, there are parallels in the literature between RNA gene silencing of CHMP3 and similar silencing of PIKfyve, which produces PtdIns(3,5)P_2. However, these studies suggest a role for both proteins not in MVB vesicle formation *per se* but rather in trafficking and fusion of the MVB to the lysosome [56, 84]. Very recently a study used a PIKfyve inhibitor to demonstrate the effects of PIKfyve inhibition within mammalian cells, resulting in enlarged endosomal structures, impaired endosomal trafficking and viral budding, similarly to truncations of CHMP3 [78, 138]. It would be very interesting then to see the effects of this inhibitor on CHMP membrane binding. If indeed CHMP3 is an effector of PtdIns(3,5)P_2 one might expect a dominant negative form of CHMP3, such as the CHMP3$^{1-179}$ construct, to not associate with endosomal membranes due to the lack of PtdIns(3,5)P_2 production. Additionally, it has been reported that the truncated dominant negative CHMP3 localises to the plasma membrane [78]. In studies carried out in this thesis, plasma membrane association of truncated CHMP3 was rarely seen and even then only in cells with abnormally high levels of protein expression. However this evidence may suggest a lipid interaction is the cause for membrane association. It may be that at very high protein levels the CHMP3 protein will interact promiscuously with negatively charged lipids found at the plasma membrane, hence why this localisation has been described. Despite this, the highly charged nature of the CHMP proteins itself may be enough to explain non-specific localisation to the plasma membrane at very high protein expression levels. This may occur when the positively charged N-terminus is exposed through release of the C-terminus, which would allow electrostatic interactions with negatively charged lipids.

It must also be questioned whether the release of the C-terminal autoinhibitory domain is a consequence of membrane binding or a necessity for membrane binding? How is the autoinhibitory domain removed from interacting with the N-terminus? It is likely that protein-protein interactions may serve to allow the C-terminus to be removed from binding the N-terminus which in turn exposes the membrane binding region of the CHMP protein, and allows specific binding to the endosomal membrane. What protein(s) and specific membrane components serve this purpose however are unknown, if indeed this is the mechanism that is occurring.

(ii) Does ESCRT-III play a role in MVB formation and vesicle formation or rather some other role such as trafficking to and fusion with the lysosome? The studies carried out in this thesis demonstrate the importance of normally functioning CHMP3 in receptor degradation. This evidence however does not specify where the CHMP3 functions in terms of receptor degradation. For example, in chapter 3 the phosphatase SopB delayed the degradation of EGFR, and in chapter 5, EGF degradation was inhibited by expression of truncated CHMP3 proteins. The lack of normal degradation kinetics of EGF and EGFR then could be attributed to either failed delivery into the MVB lumen or failed fusion/trafficking of the MVB to the lysosome, as these experiments did not allow for the two situations to be distinguished. Both scenarios would result in an elevated amount of the endocytosed receptor/growth factor being detected. Traditional models for ESCRT complexes have shown the three separate complexes in a 'conveyor-belt' style mechanism, where cargo is fed from one ESCRT complex to the next, with the ESCRT-III complex being the last ESCRT complex prior to delivery of cargo into the lumen of the MVB [4]. This mechanism did seem probable considering the fact that ATPase defective Vps4 protein expression resulted in cargo failing to be delivered into the lumen of the MVB [52, 53, 89, 90]. Furthermore, Vps4 has been shown to interact with CHMP proteins of the ESCRT-III complex via its MIT domain. Thus although Vps4 may be necessary for removal of all ESCRT proteins from the MVB

membrane, its membrane recruitment would appear to be dependent upon ESCRT-III [89, 90]. This evidence would seem to suggest that ESCRT-III may be involved in the formation and possible fission of vesicles that invaginate into the MVB lumen.

More recently however, it has been shown that gene knockdown of CHMP3 by siRNA does not impair the silencing of endocytosed receptors that traffic through the MVB, however the degradation of these receptors are impaired by CHMP3 silencing [56]. This evidence then suggests that the ESCRT-III complex, or components of it, may actually play a role in lysosomal fusion as opposed to MVB vesicle formation. This on the other hand poses problems with rectifying the exact role of Vps4 in MVB formation, as Vps4 has been shown to bind CHMPs for its localisation, and is necessary for CHMP removal as well as ESCRT-protein removal in general from the endosomal membrane. It has further been proposed that this action by Vps4 of removing ESCRT proteins may be the driving force behind vesicle fission, although strong evidence for this mechanism is still lacking [57]. Additionally, CHMPs have been implicated in both HIV-1 budding and membrane events at the mid-body of cytokinesis (chapter 6). This would suggest that these proteins are involved in some manner with membrane events that lead to fission or abscission. Alternatively, one must remember that although ESCRT-III has been described as a complex consisting of at least four separate CHMP proteins, there have been to date seven different CHMP families described in mammals [76]. Vps4 has been also shown to interact with CHMP5, which is not traditionally attributed to being part of the ESCRT-III complex [90]. It is possible that the various CHMP proteins in mammalian cells may play slightly different roles than their counterparts play in yeast. For example, some CHMPs may be involved in vesicle formation at the MVB, whereas others may play a role in lysosomal fusion. However this is purely speculative at this point in time. It is apparent though that as the literature becomes more in depth with studies on ESCRT-III proteins, that the roles of these proteins are more complex than initially thought. This also further highlights the relevance

of the assay development carried out in chapter 5, as purification and characterisation of an endogenous Vps4E235Q compartment may allow for identification of novel ESCRT proteins that help explain the apparent gaps in our understanding of the process of MVB biogenesis and the role of ESCRT-III in this process.

(iii) What drives the inward invagination at the MVB? This question has been the basis for much of the work carried out in the literature with ESCRT proteins. Our understanding of the invagination process that takes place away from the cytoplasm is very limited, and likely to be very different to the mechanisms that take place when vesicles bud towards the cytoplasm. For example, much of the budding that occurs in endocytosis is coat-driven, for example with proteins such as clathrin. There is little evidence however to suggest the budding at the MVB is driven by the coating with such proteins. Although ESCRT proteins seem to be key players in this process, other proteins such as SNARE proteins may mediate the reactions that allow inward budding at the MVB. However no SNARE-like proteins have yet been identified as being necessary or present with the ESCRT machinery [168]. This again demonstrates that proteomic analysis of the $Vps4^{E235Q}$ compartment as described in chapter 5 could be of great benefit. A recent attractive model that has been proposed for vesicle formation is the concentric circle model, which diverges away from the traditional conveyor-belt model and suggests an alternative circular model [57]. This model starts with ESCRT-0 components at the centre of where invagination occurs, with circular formations of ESCRT-I, -II and –III complexes occurring where the size of the vesicle is determined by ESCRT-III, being the outer circle. In this model, cargo is delivered to the centre of the circle, and along with the physical concentration of cargo and possible local asymmetrical lipids such as LBPA, a vesicular pit is formed. The removal of the ESCRT machinery by Vps4 then in some way allows the invagination and fission of the membrane of the inwardly budded vesicle. The authors remark that in cells infected with HIV-1 that are also expressing the ATPase dead $Vps4^{E235Q}$ protein, the diameter of the stalk

from the budding virus that has not undergone fission is approximately 100 Å [39]. This is then comparable to the estimated width of the dodecameric Vps4 molecule which has been estimated at 110 Å [169]. ESCRT protein removal by Vps4 has been suggested to occur via the pore of the functional Vps4 homomeric complex. One could envisage that the binding of CHMP proteins to the Vps4 may occur at the periphery of the Vps4 complex, where CHMP proteins are then 'pulled' towards the central pore for removal. This may then result in the membrane drawn together in a circular fashion also towards the centre due to the CHMP proteins being bound to the membrane, which may produce fission and successful vesicle formation in the MVB lumen (see Fig 7.1a-d). Much of this is again very speculative and needs more work to support the theory. However, it does provide an attractive hypothetical mechanism for vesicle formation and fission that may be closer to the exact mechanism than previous models have proposed. This would also provide potential explanations for how viruses use ESCRT proteins for budding from the plasma membrane as well as provide clues for the membrane events that take place for the abscission of cytokinesis (see Fig 7.1e-h).

(iv) What is the role of PIKfyve and its product PtdIns(3,5)P_2 in the endocytic pathway? The state of the literature with regards to the function of PIKfyve in the endocytic pathway suggests the cellular function of this protein is rather complex. Many different roles have been proposed for PIKfyve and consequently PtdIns(3,5)P_2. The work in this thesis suggests that this lipid plays a role in endo-lysosomal trafficking. As CHMP3 has been shown to bind PtdIns(3,5)P_2 *in vitro*, more work should be done to determine the relationship of CHMP3 with this lipid *in vivo* [71]. This was attempted in chapter 3 by use of SopB however due to the toxicity of SopB when expressed at high levels from a plasmid, this approach could not be taken. If indeed CHMP3 is shown to be an effector of PtdIns(3,5)P_2 *in vivo* then this would lend further weight for PIKfyve's involvement in the MVB-lysosomal pathway. Several studies

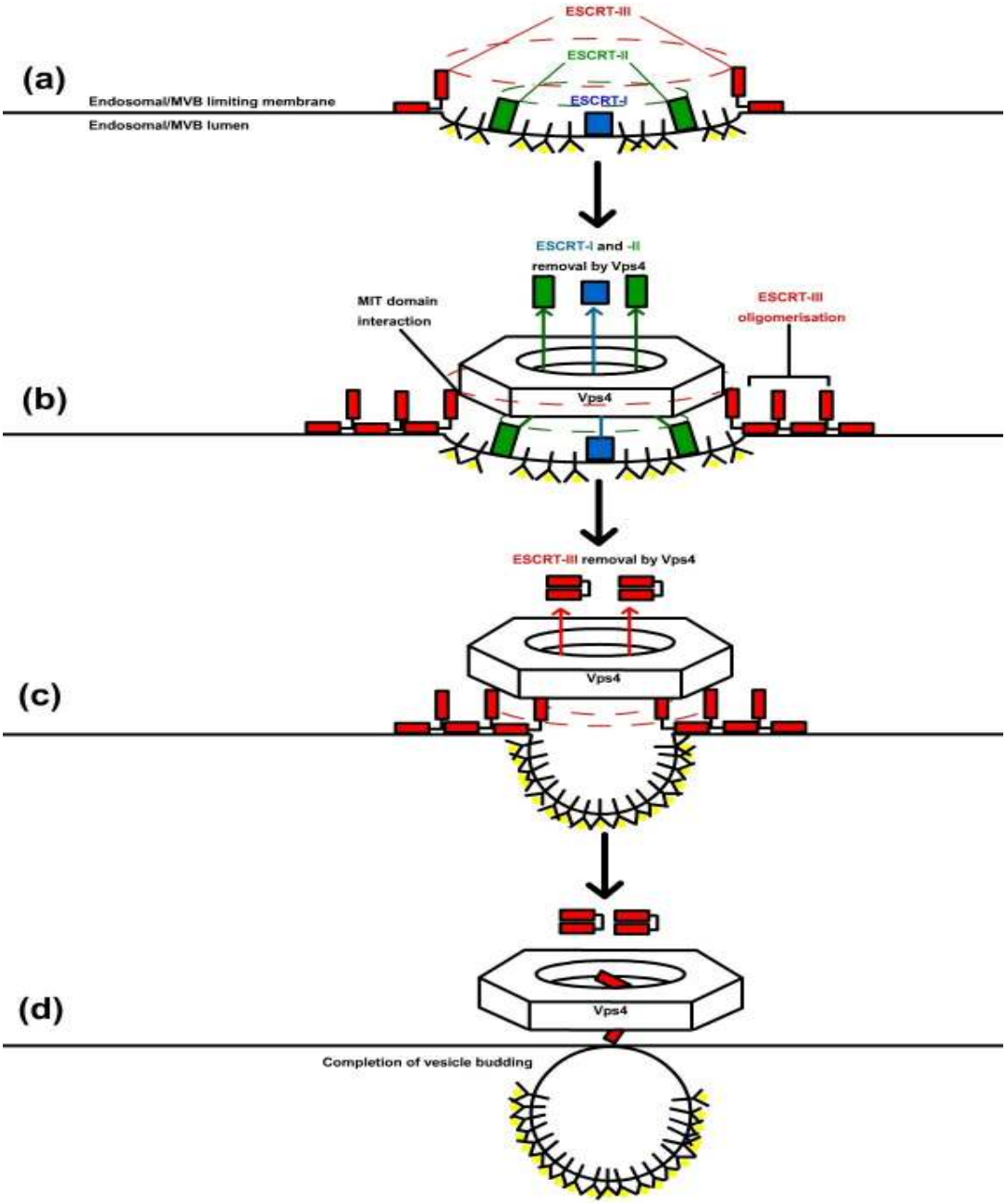

Figure 7.1a-d – A proposed mechanism for vesicle budding at the MVB lumen. *(a)* Vps27/HRS recruits the ESCRT-I complex (blue) components to the endosomal membrane. ESCRT-I may form a circle itself around Vps27 (not shown). Ubiquitylated cargo ('Y'-shaped structures with yellow ligands) is concentrated and the ESCRT-II complex (green) is recruited by ESCRT-I. ESCRT-III (red) is further recruited and is bound to the membrane by its N-terminal domain. The dashed green and red circles represent the 3-d circular nature of the oligomerised ESCRT-II and –III complexes. *(b)* The dodecameric Vps4 is recruited by interaction of its MIT domain with the C-terminus of ESCRT-III components. The ESCRT-III complex is highly oligomerised. Removal of ESCRT-I and –II complexes occurs by Vps4. *(c)* The removal of ESCRT-III components through the central pore of Vps4 brings the circumference of the budding vesicle closer together and hence closer to fission, possibly due to the strong electrostatic interactions of ESCRT-III's N-termini and negatively charged lipids. *(d)* The fission of the budding vesicle is complete when Vps4 removes the last ESCRT-III components. Figure based on concentric circle model [57].

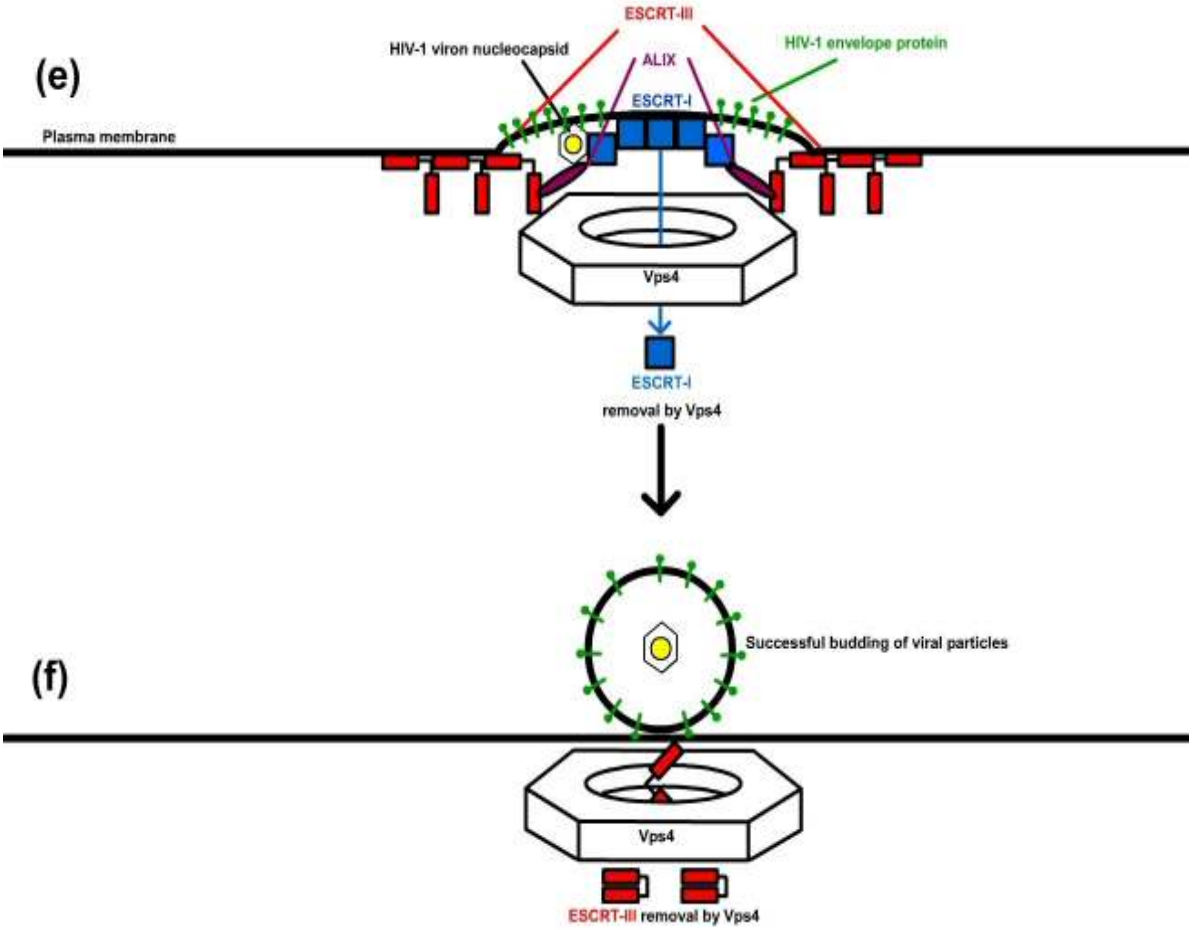

Figure 7.1e-f – A possible mechanism for viral budding from the plasma membrane of mammalian cells with the ESCRT machinery. *(e)* Viral particles are recruited to the plasma membrane, along with the ESCRT machinery. ESCRT-I (blue) is recruited and through interactions with ALIX (purple), which can act as a "bridge" that links ESCRT-I and ESCRT-III (red). ESCRT-III is in its uninhibited form allowing the N-terminus to bind to the plasma membrane, possibly through electrostatic interactions with negatively charged lipids. The C-terminus of ESCRT-III interacts with Vps4 which removes the ESCRT-I complex. *(f)* Removal of ESCRT-III oligomers allows fission of the membrane and successful budding of viral particles encapsulated in a membranous compartment.

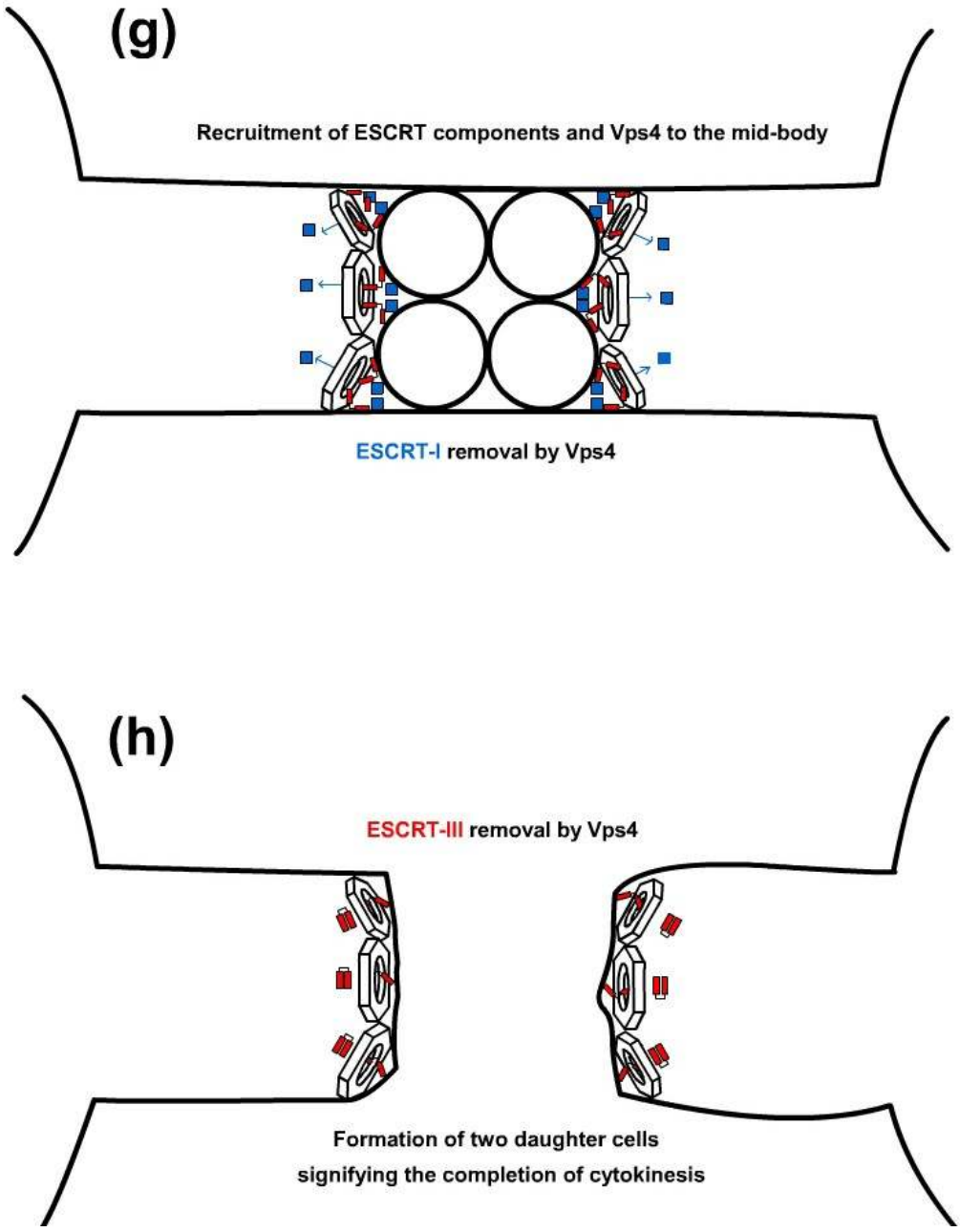

Figure 7.1g-h – A potential role for the ESCRT machinery in completion of cytokinesis. *(g)* Vesicles are trafficked to the mid-body of cytokinesis. ESCRT-1 (blue) and ESCRT-III (red) components as well as Vps4 are also trafficked to this compartment, where ESCRT-III binds to membranes of the trafficked vesicles and the tethered membrane, and recruits Vps4 via interactions with its MIT domain. Vps4 removes the ESCRT-I components after ESCRT-III is successfully recruited to membranes. *(h)* Removal of oligomerised ESCRT-III components at multiple locations at the mid-body allows for the abscission event to occur, and membrane fusion events that lead to two separate daughter cells being formed, signifying the completion of cytokinesis. It should be noted this is a very simplistic mechanism represented and that there are likely to be many other proteins involved in this complex process.

are in agreement however that PIKfyve's role is likely to be one that involves proper cargo delivery to the lysosome [84, 88]. This would be consistent with the findings of SopB's actions within the cell, and also would not rule out the possibility of CHMP3 being an effector of PtdIns(3,5)P_2. Currently however, the role of PIKfyve appears to be not well understood, and further studies to characterise this protein and the cellular function of its phosphorylated product PtdIns(3,5)P_2 are needed. The work in chapter 4 of this thesis then of producing a reliable polyclonal antibody that specifically recognises endogenous PIKfyve is important and this antibody should be used for further PIKfyve studies, such as in verifying gene silencing and PIKfyve inhibition studies.

In conclusion, there has been much recent advancement in the field of MVB biogenesis and ESCRT function. The recent findings of ESCRTs being involved in vital cellular processes such as cytokinesis (chapter 6) have made this field an even more exciting one to be working in, and demonstrate the importance as well as the multi-faceted nature of the ESCRT proteins. The work in this thesis has helped to further characterise components of the ESCRT-III complex, as well as provide new useful tools in the detection of important cellular proteins that are involved in these pathways. Additionally the development of a method that could result in affinity purification of endogenous MVB compartments is an exciting prospect. Such an approach may allow for the identification of novel ESCRT proteins, as well as the further development of an *in vitro* budding assay.

REFERENCES

8 References

1. Ungewickell, E.J. and L. Hinrichsen, *Endocytosis: clathrin-mediated membrane budding.* Curr Opin Cell Biol, 2007. **19**(4): p. 417-25.

2. van der Goot, F.G. and J. Gruenberg, *Intra-endosomal membrane traffic.* Trends Cell Biol, 2006. **16**(10): p. 514-21.

3. Bonifacino, J.S. and R. Rojas, *Retrograde transport from endosomes to the trans-Golgi network.* Nat Rev Mol Cell Biol, 2006. **7**(8): p. 568-79.

4. Babst, M., *A protein's final ESCRT.* Traffic, 2005. **6**(1): p. 2-9.

5. Gruenberg, J. and H. Stenmark, *The biogenesis of multivesicular endosomes.* Nat Rev Mol Cell Biol, 2004. **5**(4): p. 317-23.

6. Maxfield, F.R. and T.E. McGraw, *Endocytic recycling.* Nat Rev Mol Cell Biol, 2004. **5**(2): p. 121-32.

7. Mellman, I., *Endocytosis and molecular sorting.* Annu Rev Cell Dev Biol, 1996. **12**: p. 575-625.

8. Piper, R.C. and J.P. Luzio, *Late endosomes: sorting and partitioning in multivesicular bodies.* Traffic, 2001. **2**(9): p. 612-21.

9. Raiborg, C., T.E. Rusten, and H. Stenmark, *Protein sorting into multivesicular endosomes.* Curr Opin Cell Biol, 2003. **15**(4): p. 446-55.

10. Saraste, J. and B. Goud, *Functional symmetry of endomembranes.* Mol Biol Cell, 2007. **18**(4): p. 1430-6.

11. Stahl, P.D. and M.A. Barbieri, *Multivesicular bodies and multivesicular endosomes: the "ins and outs" of endosomal traffic.* Sci STKE, 2002. **2002**(141): p. PE32.

12. Schaub, B.E., P. Nair, and J. Rohrer, *Analysis of protein transport to lysosomes.* Curr Protoc Cell Biol, 2005. **Chapter 15**: p. Unit 15 8.

13. Gruenberg, J., *The endocytic pathway: a mosaic of domains.* Nat Rev Mol Cell Biol, 2001. **2**(10): p. 721-30.

14. Gorden, P., et al., *Epidermal growth factor: morphological demonstration of binding, internalization, and lysosomal association in human fibroblasts.* Proc Natl Acad Sci U S A, 1978. **75**(10): p. 5025-9.

15. Haigler, H.T., J.A. McKanna, and S. Cohen, *Direct visualization of the binding and internalization of a ferritin conjugate of epidermal growth factor in human carcinoma cells A-431.* J Cell Biol, 1979. **81**(2): p. 382-95.

16. Miller, K., et al., *Localization of the epidermal growth factor (EGF) receptor within the endosome of EGF-stimulated epidermoid carcinoma (A431) cells.* J Cell Biol, 1986. **102**(2): p. 500-9.

17. Felder, S., et al., *Kinase activity controls the sorting of the epidermal growth factor receptor within the multivesicular body.* Cell, 1990. **61**(4): p. 623-34.

18. Cereghino, J.L., E.G. Marcusson, and S.D. Emr, *The cytoplasmic tail domain of the vacuolar protein sorting receptor Vps10p and a subset of VPS gene products regulate receptor stability, function, and localization.* Mol Biol Cell, 1995. **6**(9): p. 1089-102.

19. Katzmann, D.J., G. Odorizzi, and S.D. Emr, *Receptor downregulation and multivesicular-body sorting.* Nat Rev Mol Cell Biol, 2002. **3**(12): p. 893-905.

20. Raymond, C.K., et al., *Morphological classification of the yeast vacuolar protein sorting mutants: evidence for a prevacuolar compartment in class E vps mutants.* Mol Biol Cell, 1992. **3**(12): p. 1389-402.

21. Haglund, K., P.P. Di Fiore, and I. Dikic, *Distinct monoubiquitin signals in receptor endocytosis.* Trends Biochem Sci, 2003. **28**(11): p. 598-603.

22. Hicke, L. and R. Dunn, *Regulation of membrane protein transport by ubiquitin and ubiquitin-binding proteins.* Annu Rev Cell Dev Biol, 2003. **19**: p. 141-72.

23. Shih, S.C., K.E. Sloper-Mould, and L. Hicke, *Monoubiquitin carries a novel internalization signal that is appended to activated receptors.* Embo J, 2000. **19**(2): p. 187-98.

24. Urbanowski, J.L. and R.C. Piper, *Ubiquitin sorts proteins into the intralumenal degradative compartment of the late-endosome/vacuole.* Traffic, 2001. **2**(9): p. 622-30.

25. Bache, K.G., et al., *Hrs regulates multivesicular body formation via ESCRT recruitment to endosomes.* J Cell Biol, 2003. **162**(3): p. 435-42.

26. Biederer, T., C. Volkwein, and T. Sommer, *Role of Cue1p in ubiquitination and degradation at the ER surface.* Science, 1997. **278**(5344): p. 1806-9.

27. Bilodeau, P.S., et al., *The Vps27p Hse1p complex binds ubiquitin and mediates endosomal protein sorting.* Nat Cell Biol, 2002. **4**(7): p. 534-9.

28. Hofmann, K. and P. Bucher, *The UBA domain: a sequence motif present in multiple enzyme classes of the ubiquitination pathway.* Trends Biochem Sci, 1996. **21**(5): p. 172-3.

29. Hofmann, K. and L. Falquet, *A ubiquitin-interacting motif conserved in components of the proteasomal and lysosomal protein degradation systems.* Trends Biochem Sci, 2001. **26**(6): p. 347-50.

30. Hofmann, R.M. and C.M. Pickart, *Noncanonical MMS2-encoded ubiquitin-conjugating enzyme functions in assembly of novel polyubiquitin chains for DNA repair.* Cell, 1999. **96**(5): p. 645-53.

31. Koonin, E.V. and R.A. Abagyan, *TSG101 may be the prototype of a class of dominant negative ubiquitin regulators.* Nat Genet, 1997. **16**(4): p. 330-1.

32. Ponting, C.P., Y.D. Cai, and P. Bork, *The breast cancer gene product TSG101: a regulator of ubiquitination?* J Mol Med, 1997. **75**(7): p. 467-9.

33. Raiborg, C., et al., *Hrs sorts ubiquitinated proteins into clathrin-coated microdomains of early endosomes.* Nat Cell Biol, 2002. **4**(5): p. 394-8.

34. Shih, S.C., et al., *Epsins and Vps27p/Hrs contain ubiquitin-binding domains that function in receptor endocytosis.* Nat Cell Biol, 2002. **4**(5): p. 389-93.

35. Babst, M., et al., *Escrt-III: an endosome-associated heterooligomeric protein complex required for mvb sorting.* Dev Cell, 2002. **3**(2): p. 271-82.

36. Babst, M., et al., *Endosome-associated complex, ESCRT-II, recruits transport machinery for protein sorting at the multivesicular body.* Dev Cell, 2002. **3**(2): p. 283-9.

37. Katzmann, D.J., M. Babst, and S.D. Emr, *Ubiquitin-dependent sorting into the multivesicular body pathway requires the function of a conserved endosomal protein sorting complex, ESCRT-I.* Cell, 2001. **106**(2): p. 145-55.

38. Martin-Serrano, J., et al., *Divergent retroviral late-budding domains recruit vacuolar protein sorting factors by using alternative adaptor proteins.* Proc Natl Acad Sci U S A, 2003. **100**(21): p. 12414-9.

39. von Schwedler, U.K., et al., *The protein network of HIV budding.* Cell, 2003. **114**(6): p. 701-13.

40. Katoh, K., et al., *The ALG-2-interacting protein Alix associates with CHMP4b, a human homologue of yeast Snf7 that is involved*

in multivesicular body sorting. J Biol Chem, 2003. **278**(40): p. 39104-13.

41. Strack, B., et al., *AIP1/ALIX is a binding partner for HIV-1 p6 and EIAV p9 functioning in virus budding.* Cell, 2003. **114**(6): p. 689-99.

42. Bowers, K., et al., *Degradation of endocytosed epidermal growth factor and virally ubiquitinated major histocompatibility complex class I is independent of mammalian ESCRTII.* J Biol Chem, 2006. **281**(8): p. 5094-105.

43. Bowers, K., et al., *Protein-protein interactions of ESCRT complexes in the yeast Saccharomyces cerevisiae.* Traffic, 2004. **5**(3): p. 194-210.

44. Malerod, L., et al., *Vps22/EAP30 in ESCRT-II mediates endosomal sorting of growth factor and chemokine receptors destined for lysosomal degradation.* Traffic, 2007. **8**(11): p. 1617-29.

45. Slagsvold, T., et al., *Endosomal and non-endosomal functions of ESCRT proteins.* Trends Cell Biol, 2006. **16**(6): p. 317-26.

46. Burd, C.G. and S.D. Emr, *Phosphatidylinositol(3)-phosphate signaling mediated by specific binding to RING FYVE domains.* Mol Cell, 1998. **2**(1): p. 157-62.

47. Misra, S. and J.H. Hurley, *Crystal structure of a phosphatidylinositol 3-phosphate-specific membrane-targeting motif, the FYVE domain of Vps27p.* Cell, 1999. **97**(5): p. 657-66.

48. Raiborg, C., et al., *FYVE and coiled-coil domains determine the specific localisation of Hrs to early endosomes.* J Cell Sci, 2001. **114**(Pt 12): p. 2255-63.

49. Katzmann, D.J., et al., *Vps27 recruits ESCRT machinery to endosomes during MVB sorting.* J Cell Biol, 2003. **162**(3): p. 413-23.

50. Luhtala, N. and G. Odorizzi, *Bro1 coordinates deubiquitination in the multivesicular body pathway by recruiting Doa4 to endosomes.* J Cell Biol, 2004. **166**(5): p. 717-29.

51. Odorizzi, G., et al., *Bro1 is an endosome-associated protein that functions in the MVB pathway in Saccharomyces cerevisiae.* J Cell Sci, 2003. **116**(Pt 10): p. 1893-903.

52. Babst, M., et al., *The Vps4p AAA ATPase regulates membrane association of a Vps protein complex required for normal endosome function.* Embo J, 1998. **17**(11): p. 2982-93.

53. Bishop, N. and P. Woodman, *ATPase-defective mammalian VPS4 localizes to aberrant endosomes and impairs cholesterol trafficking.* Mol Biol Cell, 2000. **11**(1): p. 227-39.

54. Kobayashi, T., et al., *Late endosomal membranes rich in lysobisphosphatidic acid regulate cholesterol transport.* Nat Cell Biol, 1999. **1**(2): p. 113-8.

55. Kobayashi, T., et al., *A lipid associated with the antiphospholipid syndrome regulates endosome structure and function.* Nature, 1998. **392**(6672): p. 193-7.

56. Bache, K.G., et al., *The ESCRT-III subunit hVps24 is required for degradation but not silencing of the epidermal growth factor receptor.* Mol Biol Cell, 2006. **17**(6): p. 2513-23.

57. Nickerson, D.P., M.R. Russell, and G. Odorizzi, *A concentric circle model of multivesicular body cargo sorting.* EMBO Rep, 2007. **8**(7): p. 644-50.

58. Amerik, A.Y., et al., *The Doa4 deubiquitinating enzyme is functionally linked to the vacuolar protein-sorting and endocytic pathways.* Mol Biol Cell, 2000. **11**(10): p. 3365-80.

59. Swaminathan, S., A.Y. Amerik, and M. Hochstrasser, *The Doa4 deubiquitinating enzyme is required for ubiquitin homeostasis in yeast.* Mol Biol Cell, 1999. **10**(8): p. 2583-94.

60. Ikonomov, O.C., et al., *Functional dissection of lipid and protein kinase signals of PIKfyve reveals the role of PtdIns 3,5-P2 production for endomembrane integrity.* J Biol Chem, 2002. **277**(11): p. 9206-11.

61. Odorizzi, G., M. Babst, and S.D. Emr, *Fab1p PtdIns(3)P 5-kinase function essential for protein sorting in the multivesicular body.* Cell, 1998. **95**(6): p. 847-58.

62. Shaw, J.D., et al., *PtdIns(3,5)P2 is required for delivery of endocytic cargo into the multivesicular body.* Traffic, 2003. **4**(7): p. 479-90.

63. Roth, M.G., *Phosphoinositides in constitutive membrane traffic.* Physiol Rev, 2004. **84**(3): p. 699-730.

64. Sasaki, T., et al., *The physiology of phosphoinositides.* Biol Pharm Bull, 2007. **30**(9): p. 1599-604.

65. Hurley, J.H. and S.D. Emr, *The ESCRT complexes: structure and mechanism of a membrane-trafficking network.* Annu Rev Biophys Biomol Struct, 2006. **35**: p. 277-98.

66. Diraviyam, K., et al., *Computer modeling of the membrane interaction of FYVE domains.* J Mol Biol, 2003. **328**(3): p. 721-36.

67. Dove, S.K. and Z.E. Johnson, *Our FABulous VACation: a decade of phosphatidylinositol 3,5-bisphosphate.* Biochem Soc Symp, 2007(74): p. 129-39.

68. Efe, J.A., R.J. Botelho, and S.D. Emr, *The Fab1 phosphatidylinositol kinase pathway in the regulation of vacuole morphology.* Curr Opin Cell Biol, 2005. **17**(4): p. 402-8.

69. Gary, J.D., et al., *Regulation of Fab1 phosphatidylinositol 3-phosphate 5-kinase pathway by Vac7 protein and Fig4, a polyphosphoinositide phosphatase family member.* Mol Biol Cell, 2002. **13**(4): p. 1238-51.

70. Ikonomov, O.C., D. Sbrissa, and A. Shisheva, *Mammalian cell morphology and endocytic membrane homeostasis require enzymatically active phosphoinositide 5-kinase PIKfyve.* J Biol Chem, 2001. **276**(28): p. 26141-7.

71. Whitley, P., et al., *Identification of mammalian Vps24p as an effector of phosphatidylinositol 3,5-bisphosphate-dependent endosome compartmentalization.* J Biol Chem, 2003. **278**(40): p. 38786-95.

72. Cooke, F.T., *Phosphatidylinositol 3,5-bisphosphate: metabolism and function.* Arch Biochem Biophys, 2002. **407**(2): p. 143-51.

73. Howard, T.L., et al., *CHMP1 functions as a member of a newly defined family of vesicle trafficking proteins.* J Cell Sci, 2001. **114**(Pt 13): p. 2395-404.

74. Peck, J.W., E.T. Bowden, and P.D. Burbelo, *Structure and function of human Vps20 and Snf7 proteins.* Biochem J, 2004. **377**(Pt 3): p. 693-700.

75. Williams, R.L. and S. Urbe, *The emerging shape of the ESCRT machinery.* Nat Rev Mol Cell Biol, 2007. **8**(5): p. 355-68.

76. Horii, M., et al., *CHMP7, a novel ESCRT-III-related protein, associates with CHMP4b and functions in the endosomal sorting pathway.* Biochem J, 2006. **400**(1): p. 23-32.

77. Shim, S., L.A. Kimpler, and P.I. Hanson, *Structure/function analysis of four core ESCRT-III proteins reveals common regulatory role for extreme C-terminal domain.* Traffic, 2007. **8**(8): p. 1068-79.

78. Zamborlini, A., et al., *Release of autoinhibition converts ESCRT-III components into potent inhibitors of HIV-1 budding.* Proc Natl Acad Sci U S A, 2006. **103**(50): p. 19140-5.

79. Azmi, I.F., et al., *ESCRT-III Family Members Stimulate Vps4 ATPase Activity Directly or via Vta1.* Dev Cell, 2008. **14**(1): p. 50-61.

80. Babst, M., et al., *Endosomal transport function in yeast requires a novel AAA-type ATPase, Vps4p.* Embo J, 1997. **16**(8): p. 1820-31.

81. Sbrissa, D., O.C. Ikonomov, and A. Shisheva, *Phosphatidylinositol 3-phosphate-interacting domains in PIKfyve. Binding specificity and role in PIKfyve. Endomenbrane localization.* J Biol Chem, 2002. **277**(8): p. 6073-9.

82. Shisheva, A., *PIKfyve: the road to PtdIns 5-P and PtdIns 3,5-P(2).* Cell Biol Int, 2001. **25**(12): p. 1201-6.

83. Ikonomov, O.C., et al., *PIKfyve Kinase and SKD1 AAA ATPase define distinct endocytic compartments. Only PIKfyve expression inhibits the cell-vacoulating activity of Helicobacter pylori VacA toxin.* J Biol Chem, 2002. **277**(48): p. 46785-90.

84. Rusten, T.E., et al., *Fab1 phosphatidylinositol 3-phosphate 5-kinase controls trafficking but not silencing of endocytosed receptors.* Mol Biol Cell, 2006. **17**(9): p. 3989-4001.

85. Cabezas, A., K. Pattni, and H. Stenmark, *Cloning and subcellular localization of a human phosphatidylinositol 3-phosphate 5-kinase, PIKfyve/Fab1.* Gene, 2006. **371**(1): p. 34-41.

86. Rutherford, A.C., et al., *The mammalian phosphatidylinositol 3-phosphate 5-kinase (PIKfyve) regulates endosome-to-TGN retrograde transport.* J Cell Sci, 2006. **119**(Pt 19): p. 3944-57.

87. Kim, J., et al., *The phosphoinositide kinase PIKfyve mediates epidermal growth factor receptor trafficking to the nucleus.* Cancer Res, 2007. **67**(19): p. 9229-37.

88. Nicot, A.S., et al., *The phosphoinositide kinase PIKfyve/Fab1p regulates terminal lysosome maturation in Caenorhabditis elegans.* Mol Biol Cell, 2006. **17**(7): p. 3062-74.

89. Stuchell-Brereton, M.D., et al., *ESCRT-III recognition by VPS4 ATPases.* Nature, 2007. **449**(7163): p. 740-4.

90. Obita, T., et al., *Structural basis for selective recognition of ESCRT-III by the AAA ATPase Vps4.* Nature, 2007. **449**(7163): p. 735-9.

91. Xiao, J., et al., *Structural characterization of the ATPase reaction cycle of endosomal AAA protein Vps4.* J Mol Biol, 2007. **374**(3): p. 655-70.

92. Barriere, H., et al., *Plasticity of polyubiquitin recognition as lysosomal targeting signals by the endosomal sorting machinery.* Mol Biol Cell, 2007. **18**(10): p. 3952-65.

93. Urbe, S., *Ubiquitin and endocytic protein sorting.* Essays Biochem, 2005. **41**: p. 81-98.

94. Clague, M.J. and S. Urbe, *Endocytosis: the DUB version.* Trends Cell Biol, 2006. **16**(11): p. 551-9.

95. Clague, M.J. and S. Urbe, *Hrs function: viruses provide the clue.* Trends Cell Biol, 2003. **13**(12): p. 603-6.

96. Bouamr, F., et al., *The C-terminal portion of the Hrs protein interacts with Tsg101 and interferes with human immunodeficiency virus type 1 Gag particle production.* J Virol, 2007. **81**(6): p. 2909-22.

97. Eastman, S.W., et al., *Identification of human VPS37C, a component of endosomal sorting complex required for transport-I important for viral budding.* J Biol Chem, 2005. **280**(1): p. 628-36.

98. Jager, S., E. Gottwein, and H.G. Krausslich, *Ubiquitination of human immunodeficiency virus type 1 Gag is highly dependent on Gag membrane association.* J Virol, 2007. **81**(17): p. 9193-201.

99. Johnson, M.C., et al., *The C-terminal half of TSG101 blocks Rous sarcoma virus budding and sequesters Gag into unique nonendosomal structures.* J Virol, 2005. **79**(6): p. 3775-86.

100. Martin-Serrano, J., T. Zang, and P.D. Bieniasz, *Role of ESCRT-I in retroviral budding.* J Virol, 2003. **77**(8): p. 4794-804.

101. Medina, G., et al., *The functionally exchangeable L domains in RSV and HIV-1 Gag direct particle release through pathways linked by Tsg101.* Traffic, 2005. **6**(10): p. 880-94.

102. Stuchell, M.D., et al., *The human endosomal sorting complex required for transport (ESCRT-I) and its role in HIV-1 budding.* J Biol Chem, 2004. **279**(34): p. 36059-71.

103. Usami, Y., S. Popov, and H.G. Gottlinger, *Potent rescue of human immunodeficiency virus type 1 late domain mutants by ALIX/AIP1 depends on its CHMP4 binding site.* J Virol, 2007. **81**(12): p. 6614-22.

104. Morita, E., et al., *Human ESCRT and ALIX proteins interact with proteins of the midbody and function in cytokinesis.* Embo J, 2007. **26**(19): p. 4215-27.

105. Carlton, J.G. and J. Martin-Serrano, *Parallels between cytokinesis and retroviral budding: a role for the ESCRT machinery.* Science, 2007. **316**(5833): p. 1908-12.

106. Zhao, W.M., A. Seki, and G. Fang, *Cep55, a microtubule-bundling protein, associates with centralspindlin to control the midbody integrity and cell abscission during cytokinesis.* Mol Biol Cell, 2006. **17**(9): p. 3881-96.

107. Barr, F.A. and U. Gruneberg, *Cytokinesis: placing and making the final cut.* Cell, 2007. **131**(5): p. 847-60.

108. Burgess, D.R. and F. Chang, *Site selection for the cleavage furrow at cytokinesis.* Trends Cell Biol, 2005. **15**(3): p. 156-62.

109. Glotzer, M., *The molecular requirements for cytokinesis.* Science, 2005. **307**(5716): p. 1735-9.

110. Yu, X., R. Prekeris, and G.W. Gould, *Role of endosomal Rab GTPases in cytokinesis.* Eur J Cell Biol, 2007. **86**(1): p. 25-35.

111. Ullrich, O., et al., *Rab11 regulates recycling through the pericentriolar recycling endosome.* J Cell Biol, 1996. **135**(4): p. 913-24.

112. Urbe, S., et al., *Rab11, a small GTPase associated with both constitutive and regulated secretory pathways in PC12 cells.* FEBS Lett, 1993. **334**(2): p. 175-82.

113. Wilcke, M., et al., *Rab11 regulates the compartmentalization of early endosomes required for efficient transport from early*

endosomes to the trans-golgi network. J Cell Biol, 2000. **151**(6): p. 1207-20.

114. Lee, J.A., et al., *ESCRT-III dysfunction causes autophagosome accumulation and neurodegeneration.* Curr Biol, 2007. **17**(18): p. 1561-7.

115. Rusten, T.E., et al., *ESCRTs and Fab1 regulate distinct steps of autophagy.* Curr Biol, 2007. **17**(20): p. 1817-25.

116. Shiels, A., et al., *CHMP4B, a novel gene for autosomal dominant cataracts linked to chromosome 20q.* Am J Hum Genet, 2007. **81**(3): p. 596-606.

117. Laemmli, U.K., *Cleavage of structural proteins during the assembly of the head of bacteriophage T4.* Nature, 1970. **227**(5259): p. 680-5.

118. Jones, B.D. and S. Falkow, *Salmonellosis: host immune responses and bacterial virulence determinants.* Annu Rev Immunol, 1996. **14**: p. 533-61.

119. Knodler, L.A. and O. Steele-Mortimer, *Taking possession: biogenesis of the Salmonella-containing vacuole.* Traffic, 2003. **4**(9): p. 587-99.

120. Steele-Mortimer, O., et al., *Biogenesis of Salmonella typhimurium-containing vacuoles in epithelial cells involves interactions with the early endocytic pathway.* Cell Microbiol, 1999. **1**(1): p. 33-49.

121. Steele-Mortimer, O., et al., *The invasion-associated type III secretion system of Salmonella enterica serovar Typhimurium is*

necessary for intracellular proliferation and vacuole biogenesis in epithelial cells. Cell Microbiol, 2002. **4**(1): p. 43-54.

122. Friebel, A., et al., *SopE and SopE2 from Salmonella typhimurium activate different sets of RhoGTPases of the host cell.* J Biol Chem, 2001. **276**(36): p. 34035-40.

123. Hardt, W.D., et al., *S. typhimurium encodes an activator of Rho GTPases that induces membrane ruffling and nuclear responses in host cells.* Cell, 1998. **93**(5): p. 815-26.

124. Galyov, E.E., et al., *A secreted effector protein of Salmonella dublin is translocated into eukaryotic cells and mediates inflammation and fluid secretion in infected ileal mucosa.* Mol Microbiol, 1997. **25**(5): p. 903-12.

125. Marcus, S.L., et al., *A synaptojanin-homologous region of Salmonella typhimurium SigD is essential for inositol phosphatase activity and Akt activation.* FEBS Lett, 2001. **494**(3): p. 201-7.

126. Norris, F.A., et al., *SopB, a protein required for virulence of Salmonella dublin, is an inositol phosphate phosphatase.* Proc Natl Acad Sci U S A, 1998. **95**(24): p. 14057-9.

127. Zhou, D., et al., *A Salmonella inositol polyphosphatase acts in conjunction with other bacterial effectors to promote host cell actin cytoskeleton rearrangements and bacterial internalization.* Mol Microbiol, 2001. **39**(2): p. 248-59.

128. Hernandez, L.D., et al., *Salmonella modulates vesicular traffic by altering phosphoinositide metabolism.* Science, 2004. **304**(5678): p. 1805-7.

129. Bertelsen, L.S., et al., *Modulation of chloride secretory responses and barrier function of intestinal epithelial cells by the Salmonella effector protein SigD.* Am J Physiol Cell Physiol, 2004. **287**(4): p. C939-48.

130. Knodler, L.A., B.B. Finlay, and O. Steele-Mortimer, *The Salmonella effector protein SopB protects epithelial cells from apoptosis by sustained activation of Akt.* J Biol Chem, 2005. **280**(10): p. 9058-64.

131. Ikonomov, O.C., D. Sbrissa, and A. Shisheva, *Localized PtdIns 3,5-P2 synthesis to regulate early endosome dynamics and fusion.* Am J Physiol Cell Physiol, 2006. **291**(2): p. C393-404.

132. Marcus, S.L., L.A. Knodler, and B.B. Finlay, *Salmonella enterica serovar Typhimurium effector SigD/SopB is membrane-associated and ubiquitinated inside host cells.* Cell Microbiol, 2002. **4**(7): p. 435-46.

133. Ridley, S.H., et al., *FENS-1 and DFCP1 are FYVE domain-containing proteins with distinct functions in the endosomal and Golgi compartments.* J Cell Sci, 2001. **114**(Pt 22): p. 3991-4000.

134. Cain, R.J., R.D. Hayward, and V. Koronakis, *The target cell plasma membrane is a critical interface for Salmonella cell entry effector-host interplay.* Mol Microbiol, 2004. **54**(4): p. 887-904.

135. Yoshimori, T., et al., *The mouse SKD1, a homologue of yeast Vps4p, is required for normal endosomal trafficking and morphology in mammalian cells.* Mol Biol Cell, 2000. **11**(2): p. 747-63.

136. Ikonomov, O.C., et al., *PIKfyve controls fluid phase endocytosis but not recycling/degradation of endocytosed receptors or sorting of procathepsin D by regulating multivesicular body morphogenesis.* Mol Biol Cell, 2003. **14**(11): p. 4581-91.

137. Tsujita, K., et al., *Myotubularin regulates the function of the late endosome through the gram domain-phosphatidylinositol 3,5-bisphosphate interaction.* J Biol Chem, 2004. **279**(14): p. 13817-24.

138. Jefferies, H.B., et al., *A selective PIKfyve inhibitor blocks PtdIns(3,5)P(2) production and disrupts endomembrane transport and retroviral budding.* EMBO Rep, 2008.

139. Yamamoto, A., et al., *Novel PI(4)P 5-kinase homologue, Fab1p, essential for normal vacuole function and morphology in yeast.* Mol Biol Cell, 1995. **6**(5): p. 525-39.

140. Sbrissa, D., O.C. Ikonomov, and A. Shisheva, *PIKfyve, a mammalian ortholog of yeast Fab1p lipid kinase, synthesizes 5-phosphoinositides. Effect of insulin.* J Biol Chem, 1999. **274**(31): p. 21589-97.

141. Watson, R.T. and J.E. Pessin, *Bridging the GAP between insulin signaling and GLUT4 translocation.* Trends Biochem Sci, 2006. **31**(4): p. 215-22.

142. Shisheva, A., et al., *Localization and insulin-regulated relocation of phosphoinositide 5-kinase PIKfyve in 3T3-L1 adipocytes.* J Biol Chem, 2001. **276**(15): p. 11859-69.

143. Kyte, J. and R.F. Doolittle, *A simple method for displaying the hydropathic character of a protein.* J Mol Biol, 1982. **157**(1): p. 105-32.

144. Chu, T., et al., *New component of ESCRT-I regulates endosomal sorting complex assembly.* J Cell Biol, 2006. **175**(5): p. 815-23.

145. Curtiss, M., C. Jones, and M. Babst, *Efficient cargo sorting by ESCRT-I and the subsequent release of ESCRT-I from multivesicular bodies requires the subunit Mvb12.* Mol Biol Cell, 2007. **18**(2): p. 636-45.

146. Oestreich, A.J., et al., *Mvb12 is a novel member of ESCRT-I involved in cargo selection by the multivesicular body pathway.* Mol Biol Cell, 2007. **18**(2): p. 646-57.

147. Fujita, H., et al., *Mammalian class E Vps proteins, SBP1 and mVps2/CHMP2A, interact with and regulate the function of an AAA-ATPase SKD1/Vps4B.* J Cell Sci, 2004. **117**(Pt 14): p. 2997-3009.

148. Blackwood, R.A., et al., *Development of an aqueous-space mixing assay for fusion of granules and plasma membranes from human neutrophils.* Biochem J, 1996. **314 (Pt 2)**: p. 469-75.

149. Boesze-Battaglia, K., et al., *Fusion between retinal rod outer segment membranes and model membranes: a role for photoreceptor peripherin/rds.* Biochemistry, 1998. **37**(26): p. 9477-87.

150. Hata, T. and M. Nakayama, *Rapid single-tube method for small-scale affinity purification of polyclonal antibodies using HaloTag Technology.* J Biochem Biophys Methods, 2007. **70**(4): p. 679-82.

151. Lang, C., et al., *HaloTag: a new versatile reporter gene system in plant cells.* J Exp Bot, 2006. **57**(12): p. 2985-92.

152. Reck-Peterson, S.L., et al., *Single-molecule analysis of dynein processivity and stepping behavior.* Cell, 2006. **126**(2): p. 335-48.

153. Zhang, Y., et al., *HaloTag protein-mediated site-specific conjugation of bioluminescent proteins to quantum dots.* Angew Chem Int Ed Engl, 2006. **45**(30): p. 4936-40.

154. Spitzer, C., et al., *The Arabidopsis elch mutant reveals functions of an ESCRT component in cytokinesis.* Development, 2006. **133**(23): p. 4679-89.

155. Albertson, R., B. Riggs, and W. Sullivan, *Membrane traffic: a driving force in cytokinesis.* Trends Cell Biol, 2005. **15**(2): p. 92-101.

156. Dhonukshe, P., et al., *A unifying new model of cytokinesis for the dividing plant and animal cells.* Bioessays, 2007. **29**(4): p. 371-81.

157. Gromley, A., et al., *Centriolin anchoring of exocyst and SNARE complexes at the midbody is required for secretory-vesicle-mediated abscission.* Cell, 2005. **123**(1): p. 75-87.

158. Otegui, M.S., K.J. Verbrugghe, and A.R. Skop, *Midbodies and phragmoplasts: analogous structures involved in cytokinesis.* Trends Cell Biol, 2005. **15**(8): p. 404-13.

159. Muziol, T., et al., *Structural basis for budding by the ESCRT-III factor CHMP3.* Dev Cell, 2006. **10**(6): p. 821-30.

160. Lin, Y., et al., *Interaction of the mammalian endosomal sorting complex required for transport (ESCRT) III protein hSnf7-1 with itself, membranes, and the AAA+ ATPase SKD1.* J Biol Chem, 2005. **280**(13): p. 12799-809.

161. King, I.C. and A.C. Sartorelli, *The relationship between epidermal growth factor receptors and the terminal differentiation of A431 carcinoma cells.* Biochem Biophys Res Commun, 1986. **140**(3): p. 837-43.

162. Prekeris, R., *Rabs, Rips, FIPs, and endocytic membrane traffic.* ScientificWorldJournal, 2003. **3**: p. 870-80.

163. Wilson, G.M., et al., *The FIP3-Rab11 protein complex regulates recycling endosome targeting to the cleavage furrow during late cytokinesis.* Mol Biol Cell, 2005. **16**(2): p. 849-60.

164. Pelissier, A., J.P. Chauvin, and T. Lecuit, *Trafficking through Rab11 endosomes is required for cellularization during Drosophila embryogenesis.* Curr Biol, 2003. **13**(21): p. 1848-57.

165. Skop, A.R., et al., *Dissection of the mammalian midbody proteome reveals conserved cytokinesis mechanisms.* Science, 2004. **305**(5680): p. 61-6.

166. Jones, M.C., P.T. Caswell, and J.C. Norman, *Endocytic recycling pathways: emerging regulators of cell migration.* Curr Opin Cell Biol, 2006. **18**(5): p. 549-57.

167. Strickland, L.I. and D.R. Burgess, *Pathways for membrane trafficking during cytokinesis.* Trends Cell Biol, 2004. **14**(3): p. 115-8.

168. Saksena, S., et al., *ESCRTing proteins in the endocytic pathway.* Trends Biochem Sci, 2007. **32**(12): p. 561-73.

169. Scott, A., et al., *Structural and mechanistic studies of VPS4 proteins.* Embo J, 2005. **24**(20): p. 3658-69.